https://ntrs.nasa.gov/search.jsp?R=19860004802 2020-03-20T16:32:32+00:00Z

General Disclaimer

One or more of the Following Statements may affect this Document

- This document has been reproduced from the best copy furnished by the organizational source. It is being released in the interest of making available as much information as possible.

- This document may contain data, which exceeds the sheet parameters. It was furnished in this condition by the organizational source and is the best copy available.

- This document may contain tone-on-tone or color graphs, charts and/or pictures, which have been reproduced in black and white.

- This document is paginated as submitted by the original source.

- Portions of this document are not fully legible due to the historical nature of some of the material. However, it is the best reproduction available from the original submission.

Produced by the NASA Center for Aerospace Information (CASI)

DAM / LEWIS

CR-174878
PWA-5823-14

PRELIMINARY DESIGN OF A SUPERSONIC CRUISE AIRCRAFT HIGH-PRESSURE TURBINE

Final Report

(NASA-CR-174878) PRELIMINARY DESIGN OF A SUPERSONIC CRUISE AIRCRAFT HIGH-PRESSURE TURBINE Final Report (Pratt and Whitney Aircraft) 128 p HC A07/MF A01 CSCL 21E

N86-14272

Unclas
G3/07 15677

Contract NAS3-23057

November 2, 1983

NASA

1. REPORT NO. CR-174878	2. GOVERNMENT AGENCY	3. RECIPIENT'S CATALOG NO.
4. TITLE AND SUBTITLE PRELIMINARY DESIGN OF A SUPERSONIC CRUISE AIRCRAFT HIGH-PRESSURE TURBINE		5. REPORT DATE November 2, 1983 6. PERFORMING ORG. CODE
7. AUTHOR(S) L. D. Aceto, J. C. Calderbank		8. PERFORMING ORG. REPT. NO. PWA-5923-14
9. PERFORMING ORG. NAME AND ADDRESS UNITED TECHNOLOGIES CORPORATION Pratt & Whitney Engineering Division		10. WORK UNIT NO. 11. CONTRACT OR GRANT NO. NAS3-20357
12. SPONSORING AGENCY NAME AND ADDRESS National Aeronautics and Space Administration Lewis Research Center 21000 Brookpark Road, Cleveland, Ohio 44135		13. TYPE REPT./PERIOD COVERED Final Report 14. SPONSORING AGENCY CODE 533-04-12

15. SUPPLEMENTARY NOTES
Final Report, Project Manager: Frederick C. Yeh, Internal Fluid Mechanics Division, NASA Lewis Research Center, Cleveland, Ohio 44135

16. ABSTRACT

Development of the supersonic cruise aircraft engine continued in this National Aeronautics and Space Administration (NASA) sponsored Pratt & Whitney program for the Preliminary Design of an Advanced High-Pressure Turbine. Airfoil cooling concepts and the technology required to implement these concepts received particular emphasis. Previous supersonic cruise aircraft mission studies were reviewed and the Variable Stream Control Engine (VSCE) was chosen as the candidate for the preliminary turbine design. The design was evaluated for the supersonic cruise mission. The advanced technology to be generated from these designs showed benefits in the supersonic cruise application and subsonic cruise application. The preliminary design incorporates advanced single crystal materials, thermal barrier coatings, and oxidation resistant coatings for both the vane and blade. The 1990 technology vane and blade designs have cooled turbine efficiency of 92.3 percent, 8.05 percent Wae cooling and a 10,000 hour life. An alternate design with 1986 technology has 91.9 percent efficiency and 12.43 percent Wae cooling at the same life. To achieve these performance and life results, technology programs must be pursued to provide the 1990's technology assumed for this study.

17. KEY WORDS (SUGGESTED BY AUTHOR(S))	18. DISTRIBUTION STATEMENT
Supersonic Cruise Aircraft High-Pressure Turbine	General

19. SECURITY CLASS THIS (REPT)	20. SECURITY CLASS THIS (PAGE)	21. NO. PGS	22. PRICE *
UNCLASSIFIED	UNCLASSIFIED	120	

* For sale by the National Technical Information Service, Springfield, VA 22161

TABLE OF CONTENTS

LIST OF ILLUSTRATIONS

LIST OF ILLUSTRATIONS (continued)

LIST OF ILLUSTRATIONS (continued)

LIST OF ILLUSTRATIONS (continued)

LIST OF TABLES

SECTION 1.0

SUMMARY

Development of the supersonic cruise aircraft engine continued in this National Aeronautics and Space Administration (NASA) sponsored Pratt & Whitney contract for the preliminary design of an advanced high-pressure turbine. This program was specifically directed toward executing a preliminary design of the high-pressure turbine, with particular emphasis upon airfoil cooling concepts. Technology was assumed for 1986 and 1990 time frames to implement these concepts. The preliminary design demonstrated that the high-pressure turbine required for the 1990's supersonic cruise engine is feasible, assuming the availability of the advanced technologies that are required. In order for these technologies to be available in a timely manner, specific high temperature turbine programs should be initiated. In addition, a detailed turbine design should be initiated to confirm and identify more fully the high-pressure turbine requirements. The technologies that need to be developed would also benefit both commercial subsonic and military engines.

Previous supersonic cruise aircraft studies (ref's. 1 through 4) were reviewed as part of the current contract, and the Variable Stream Control Engine (VSCE) was chosen as a candidate for the preliminary turbine design. Other engines considered in previous studies (Low Bypass Engine, Inverted Flow Engine, and Variable Cycle Engine) differ in concept and performance, but their turbines have the same technology requirements as the VSCE. Hence, the results of the current study apply in general to the other engine turbines. The supersonic cruise mission defined in the ref. 2 was chosen for this study, but the resulting airfoil design was also evaluated in a comparable military mission and a commercial subsonic application. The advanced technologies required in these airfoils were so fundamental that benefits were shown in all applications.

The VSCE turbine defined the geometric size, temperatures, pressures, speed, cooling air requirements, and component life for the preliminary design criteria. The resulting single-stage turbine has a nominal pressure ratio of 2.0. Its design extends the airfoil stress levels to an AN^2 value of 38.7 x 10^{10} cm^2/min^2 (6.0 x 10^{10} in^2/min^2) while setting aerodynamics at technology levels assumed to be available for the 1990's applications.

The vane design has two separate internal chambers, and relies on efficient internal cooling and external film cooling. A leading edge insert provides an effective distribution of cooling air which exits via showerhead and film holes with sufficient cooling margin to maintain airfoil life over a large range of adverse conditions. The trailing edge cavity is tapered to provide uniform trailing edge flow into the radial pressure field of the controlled vortex design. The design also allows for future utilization of three-dimensional aerodynamic concepts. The spanwise rib ties the suction and pressure surfaces while separating the trailing and leading edge cooling flows. Skewed trip strips are used on both the pressure and suction side inner walls to augment the heat transfer with the available (supply) pressure.

The blade has a six-cavity design with three separate cooling air feeds to the leading edge, midchord, and trailing edge regions. Tip cooling is provided from the leading edge cavity. This concept distributes the coolest air to the highest heat load areas. As in the vane, skewed trip strips are used. However, the trailing edge utilizes high blockage pedestal cooling with a cast trailing edge. The blade contour is designed to reduce the external heat load while maintaining aerodynamic performance.

Advanced single crystal materials, thermal barrier coatings, and oxidation resistant coatings are used for both the vane and blade. This material technology is expected to be available for a 1990 design start. New component technology is also assumed to be available and will result in improved combustion exit temperature distributions and in increased airfoil cooling capability.

These 1990 vane and blade designs meet the performance and durability goals to provide a cooled turbine efficiency of 92.3 percent, 8.05 percent Wae cooling and a 10,000 hour life. An alternate design with 1986 technology will achieve 91.9 percent efficiency and 12.43 percent Wae cooling at the same life. It is crucial that the advanced aerodynamic, cooling, material, and fabrication technologies identified in this program be developed in the next four or five years if these designs are to become part of a 1990 engine.

The supersonic cruise engine technologies when applied to a typical subsonic engine (266,892 N (60,000 lb) thrust, two-spool, two stage high-pressure turbine) demonstrate substantial potential savings in thrust specific fuel consumption (TSFC). The increased AN^2 and blade material provide a 0.58 percent benefit in TSFC. Airfoil aerodynamics, thermal barrier system, and burner technology advances equally contribute a total of approximately 1.0 percent in TSFC benefit.

Throughout the entire process, the manufacturing feasibility was continually assessed. Trailing edge thickness, wall thickness, airfoil taper, and internal complexity were based upon expected developments in fabrication technology.

The performance and life results indicate that the original goals can be met provided the technology programs are pursued.

SECTION 2.0

INTRODUCTION

Pratt & Whitney participated in a series of programs under the NASA sponsored Supersonic Cruise Aircraft Research (SCAR) and Variable Cycle Engine (VCE) programs with the common objectives of identifying and evaluating key elements in propulsion system technology for the second generation advanced supersonic aircraft. These programs defined four overall engine configurations: the Low Bypass Engine (LBE), the Inverted Flow Engine (IFE), the Variable Stream Control Engine (VSCE) and the Variable Cycle Engine (VCE). The aircraft/engine system requirements for supersonic transport applications and engine performance requirements for the 1990's were defined in these studies. Critical components and the related general technology requirements were identified in these programs.

In the turbines, the previous studies concluded the most critical advanced technology features to be those associated with achieving the required durability without using large quantities of cooling air which would impose a penalty on the engine thermodynamic cycle and turbine efficiency. The reasons that supersonic cruise engines are very sensitive to the hot section durability technology are the very high projected turbine inlet temperatures and cooling air temperatures during long periods of supersonic operation, and the cycle characteristics which cause high stresses in the turbine blades at these high temperature levels. Consequently, the need for very advanced materials, design techniques and cooling schemes was indicated. However, these previous studies did not address the problem of heat transfer analysis and design of the high-pressure turbine, which must withstand the stringent requirements of the supersonic cruise aircraft.

The engine cross sections generated in the previous studies defined the overall turbine requirements of pressure ratio, airflow, speed and physical size. The four selected engine configurations defined a series of highly efficient but similar turbines which basically differed only in size. Similar advanced aerodynamic design goals and effective cooling air use were assumed for each turbine so that high levels of turbine efficiency could be achieved. A high-pressure turbine pressure ratio of approximately 2.3, characteristic of current commercial transport engines, was chosen as a result of optimization studies.

The preliminary design of the Supersonic Cruise Aircraft high-pressure turbine, conducted under the current contract, further investigated the details of advanced cycle engine design requirements. The high-pressure turbine flowpath, airfoils and cooling design features were defined in detail assuming the availability and use of the emerging technologies identified under current research and development work. The cooling configurations and materials selected represent advanced state-of-the-art concepts. Pratt and Whitney's Standard Design System was applied to perform detailed aerodynamic design and heat transfer analyses leading to the selected designs.

P&W's Standard Design System includes a series of computer codes which mathematically describe the physics of aerodynamic and heat transfer phenomena known to apply to turbines. Details currently too difficult to model analytically, or those not yet fully understood, are simulated by experimentally determined empirical correlations. These correlations are updated as new calibration data are developed from rig and engine tests, and as the physical models are expanded to include new findings.

Work under the current contract was performed under three technical tasks:

First, an advanced variable cycle engine and a supersonic flight mission applicable to commercial aircraft were selected on the basis of the previous NASA sponsored program (Section 3). The Variable Stream Control Engine (VSCE) was chosen mainly because of its favorable thrust-to-weight ratio. Other differences between the candidate engines were found to be small.

Second, the aerodynamic and durability designs of the VSCE high-pressure turbine were defined using a series of trade studies (Sections 4 and 5). The aerodynamic design evolved from the original VSCE flowpath, after a blade loading optimization study using mean line analysis was completed. Airfoil cooling schemes were selected with assistance from configurational studies of advanced cooling concepts. The blade airfoil shape was also modified as a result of the configurational studies to reduce heat loads. Feasibility of the selected configurations was demonstrated by completing a preliminary design and detailed heat transfer analysis of the critical span cross section.

Third, technology features which are critical to the development of advanced cooling concepts in this program were identified. Benefits of this technology to advanced subsonic engines were also evaluated (Section 6) to show the overall generic value.

SECTION 3.0

ENGINE AND MISSION SELECTION

The initial task in the high-pressure turbine design was the definition of the engine and overall turbine configuration, and the selection of an operating mission for which the high-pressure turbine airfoils were designed.

A series of previous supersonic cruise engine studies identified several candidate engine configurations. These studies identified operating missions for a supersonic cruise aircraft in commercial use. Results of these studies, which also generated noise, cost, and gross weight trade factors to assess economical commercial usage, were used as the basis for the engine selection for this high-pressure turbine preliminary design. A supersonic operating mission was estimated for military applications based on criteria consistent with the commercial studies.

3.1 Engine Selection

A review was made of the four candidate engine configurations which were studied in the previous NASA sponsored Supersonic Cruise Aircraft Research programs. The candidate configurations are: the Variable Stream Control Engine, the Low Bypass Engine, the Inverted Flow Engine and the Variable Cycle Engine. These engines are briefly summarized in the following paragraphs.

Variable Stream Control Engine (VSCE) Concept

The VSCE is an advanced duct burning turbofan concept that makes extensive use of variable geometry components. A flexible throttle schedule allowed the independent variation of the two coannular exhaust streams. This unique scheduling capability provided the inverse velocity profile needed to take advantage of the inherent jet noise reduction benefit at takeoff, while at subsonic and supersonic flight conditions the exhaust velocities can be matched to provide a flat profile for high propulsive efficiency. The VSCE turbine design incorporates a simple stage high-pressure turbine and a two stage low-pressure turbine. The design definition, performance and operating features of this propulsion concept were discussed in detail in NASA CR-159730 (ref. 2).

Low Bypass Engine (LBE) Concept

The LBE is an advanced, nonaugmented, twin spool turbofan in which the design bypass ratios were in the 0.2 to 0.5 range. In the parametric version of this engine the bypass ratio was chosen to be 0.4, the primary and the bypass streams were partially mixed, and the exhaust gases discharged through a common variable area ejector nozzle. The refined LBE-450A incorporated a high effectiveness forced mixer to provide improved supersonic thrust specific fuel consumption through better mixing of the primary and fan streams. The high-pressure spool of the engine consisted of a variable geometry compressor and an advanced single stage turbine with high temperature capability.

Inverted Flow Engine (IFE) Concept

The IFE is an advanced, nonaugmented, twin spool turbofan in which the design bypass ratios are in the 0.4 to 0.6 range. The engine configuration is similar to the Low Bypass Engine (LBE) except that the fan and core streams were inverted through a flow inverter downstream of the low-pressure turbine and discharged through independent nozzles rather than mixing the streams and exhausting through a common variable area ejector nozzle. Inversion of the two exhaust streams enables the IFE to achieve an inverted velocity profile which provides the potential to attain reduced engine noise levels, similar to that obtained with the VSCE. In the IFE the high velocity outer stream is formed by the turbine exhaust flow, and the inner stream in the nozzle by the fan discharge flow. Maintaining a constant jet velocity ratio and constant corrected total airflow while the engine is being throttled at takeoff requires that the IFE have a variable core stream (outer stream) nozzle area and a variable fan stream nozzle area.

Variable Cycle Engine (VCE) Concept

The VCE has a single spool, two stage turbine design and a turbine bypass system. This concept bypasses part of the compressor air around the burner/turbine and injects it into the nozzle system. The bypass air is modulated with power setting to produce inflight matching benefits. The turbine bypass systems will be inoperative during the subsonic and supersonic cruise segments of the flight cycle.

These engine studies were performed for each engine over a range of thrust size, weight, noise, emissions and fuel burned, and cost trade-off studies were conducted. These studies chose the VSCE concept as being the most promising. Table 3-I shows that the VSCE is the lightest engine for the same flow size. The two stage turbine, single spool VCE, based upon a limited amount of study, proved to be the heaviest by approximately 50 percent.

TABLE 3-I

ENGINE WEIGHT SUMMARY
340 kg/sec (750 lb/sec) Airflow Size

VSCE	-	3915 kg (8630 lb)
IFE	-	4491 kg (9900 lb)
LBE	-	4273 kg (9420 lb)
VCE	-	5481 kg (12280 lb) estimated

A comparison of emissions (Table 3-II) to the Environmental Protection Agency (EPA) rules indicates that no engine concept in this group strictly meets the code. However, the VSCE engine has the most potential to be developed to meet these goals.

The VSCE also had the lowest thrust specific fuel consumption at a representative subsonic cruise thrust (ref. 3).

TABLE 3-II

EMISSIONS COMPARISON

	EPA Parameter (EPAP) 1000g emission/1000 lb fn-hr/cycle	
	NOx	CO
EPA CLASS T_5 RULE	5.0	7.8
VCE	8.9	12.2
IFE	6.9	11.2
LBE	6.9	11.2
VSCE	5.1	14.4

A military engine (STJ-562) was considered for the present study but was rejected since it has a substantially lower AN^2 level. In addition, its size is small and therefore a poor base to extrapolate benefits in the larger supersonic cruise engines.

High-Pressure Turbine Comparison

The high-pressure turbines of the VSCE, LBE, IFE and VCE concepts with the same level of technology are compared in Table 3-III. The three turbines are single stage designs, drive similar compressors, and result in similar expansion ratios. The mean velocity ratio and axial velocity ratio of these turbines are essentially identical due to their comparable technology. The stress levels in terms of AN^2 were set at 36.7×10^{10} cm^2/min^2 (5.7×10^{10} in^2/min^2).

The review of the candidate Supersonic Cruise Aircraft Research (SCAR) engines concluded that the VSCE (Figure 3-1) was the most attractive engine concept in terms of direct operating cost and noise. These results were presented to and approved by the NASA Project Manager.

3.2 Mission Selection

In establishing advanced supersonic engine hot section mission life and durability design requirements for these studies, an assessment was made of the various advanced supersonic transport missions in terms of operating time spent at the most severe temperatures and maximum rotor speeds. Figure 3-2 shows a typical flight profile for an advanced supersonic transport, including reserve operating requirements for cruise to alternate landing sites and hold.

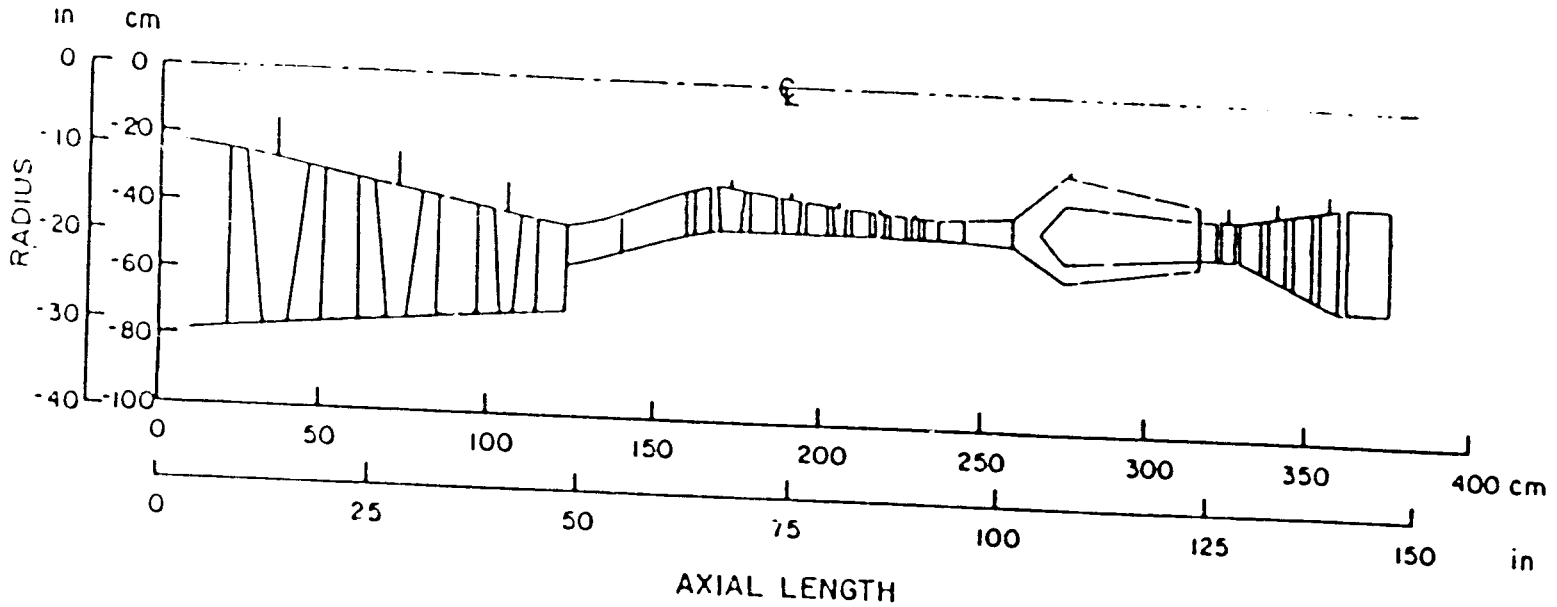

Figure 3-1 Variable Stream Control Engine Flowpath

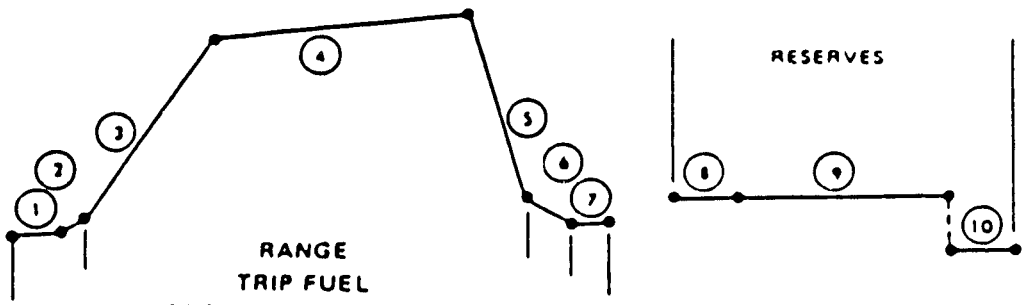

(1)	TAXI	10 MIN, H = 0, GROUND IDLE FUEL FLOW
(2)	TAKEOFF	TO H = 11M (35 FT)
(3)	ACCELERATE AND CLIMB TO BCA*	TO M = CRUISE
(4)	SUPERSONIC CRUISE	CLIMB CRUISE
(5)	DESCEND AND DECELERATE	FLIGHT IDLE FUEL FLOW
(6)	ILS APPROACH	TO TOUCHDOWN
(7)	ALLOWANCE	6% TRIP FUEL
(8)	SUBSONIC CRUISE TO ALTERNATE	M = 0.9, HP = 11521M (37,800 FT), R = 482 KM (260 NMI)
(9)	HOLD	30 MIN HP = 4572M (15,000 FT), M = OPTIONAL
(10)	TAXI	5 MIN, H = 0, GROUND IDLE FUEL FLOW

*BCA = BEST CRUISE ALTITUDE

Figure 3-2 Advanced Supersonic Transport Flight Profile and Reserves

Reference 1 summarizes the time for an entirely supersonic mission and for two mixed missions, which include subsonic legs added to satisfy overland cruise requirements. However, the subsonic elements reduced the compressor temperatures, the combustor temperature, and the high spool speeds. As a result, the severity of the mission is reduced in direct proportion to the length of the subsonic cruise element. It was decided, and approved by NASA, to include a subsonic cruise leg, but to retain the more solid aggressive mission. The mission with the 556 km (300 naut mile) subsonic leg and a block cycle time of 190.6 minutes was selected as being most representative of expected commercial service and used as primary mission for durability design. As indicated in Table 3-IV, more than 50 percent of the operating time is spent at the most severe temperature and stress conditions. Table 3-IV also compares the supersonic mission with a typical subsonic mission and indicates the increased severity of a supersonic cruise application. Based upon a 10,000 hour life, a subsonic engine will accumulate 150 hours at maximum conditions in contrast to 5,000 hours for the supersonic cruise aircraft engine.

TABLE 3-III

HIGH-PRESSURE TURBINE COMPARISON

	VSCE	LBE	IFE	VCE
Number of Stages	1	1	1	2
Pressure Ratio	2.40	2.32	2.25	4.02
Δh, BTU/LB_M	142.00	146.00	142.60	--
Mean Velocity Ratio $U_M/\sqrt{2g\,J\Delta HG}$	0.58	0.578	0.581	0.58
CX/U Axial Velocity Ratio	0.60	0.60	0.60	0.60
Exit Mach No.	0.49	0.53	0.49	--
$AN^2 \times 10^{-9}$ IN^2/MIN^2	57.70	57.90	57.70	58.0
N_1, RPM Rotor Speed	11,190	9451	9305	6144
Inlet Flow Parameter $W\sqrt{T}/PT$	72.70	103.40	108.70	150.2
Exit Swirl Angle	16.60	26.40	17.80	--

TABLE 3-IV

DEFINITION OF SUPERSONIC AND
TYPICAL SUBSONIC FLIGHT MISSIONS

	Supersonic Cruise				Typical Subsonic Mission	
Flight Segment	Altitude m (ft)	Mn	Time (min)	Compressor Exit Temperature K (°F)	Time (min)	Compressor Exit Temperature K (°F)
Taxi	0 (0)	-	10.0		7.5	
Takeoff	335 (1,100)	0.3	0.7	1483 (2210)	1.5	1670+ (2546+)
Subsonic Climb	11,000 (36,089)	0.3-0.9	17.4	1376 (2017)	19.2	1550 (2330)
Subsonic Cruise	11,000 (36,089)	0.9	18.5	1253 (1796)	39.3	1478 (2200)
Supersonic Climb	11,125 (36,500)	1.3	14.7	1500 (2385)	-	-
Supersonic Cruise	16,154 (53,000)	2.3	99.7	1755* (2700*)	-	-
Descent			24.6		15.0	
Taxi	0 (0)	-	5.0		7.5	
Total Time			190.6		89.0	
Designed for 10,000 Hour Life			*5000 Hours at Max Condition		+250 Hours at Max Condition	

Critical mission operating points were selected for consideration in design of the VSCE high-pressure turbine. These operating points and the most significant operating environment for each point were:

1) takeoff, sea level static - high specific thrust, low noise;

2) takeoff, cutback power, 335 m (1,100 ft), 0.3 Mn - low noise;

3) subsonic cruise, 1,100 m (36,089 ft), 0.9 Mn - low thrust, low fuel consumption, inlet flow-matching;

4) subsonic climb, 11,125 m (36,500 ft), 1.3 Mn - high thrust; and

5) supersonic cruise, 16,154 m (53,000 ft), 2.32 Mn - high thrust, low fuel consumption.

A supersonic flight mission for military transport applications also was required for evaluating benefits under this program. On the basis of expected flight routes and supersonic operation restrictions, the military mission was selected to be identical to the commercial mission. Military flights most likely to be made by the supersonic aircraft will be over very long distances on intercontinental routes, similar to the commercial flights. Additionally, for all peace time operation and controlled military conflicts, the noise regulations dictating takeoff and climb conditions and operating routes of commercial aircraft were also applied to military operation.

SECTION 4.0

BASIC TURBINE PARAMETER AND AERODYNAMIC DESIGN DEFINITION

The design of high performance, high-pressure turbines is a complex series of compromises that result from the need to meet both aerodynamic performance and durability goals. Typically, prior to the start of the high-pressure turbine design, turbine goals are set for engine and mission studies to allow early overall evaluation of engine weight, fuel burn and operating cost. Having demonstrated overall engine benefits, preliminary design studies of the turbine are conducted to evaluate the feasibility of meeting assumed goals. Generally, several design iterations are necessary in order to achieve agreement between design goals and the actual design. A natural outcome of the preliminary design iterations is the refining of the goals, the technology required to meet these goals, and the associated trades of performance, weight and cost.

The major elements of the preliminary turbine design process used in the preliminary design of a Supersonic Cruise High-Pressure Turbine Program is shown in Figure 4-1. Input to this process consisted of certain key elements: initial component aerodynamic and mechanical parameters, technology and material projections for the 1990s, engine design tables and the mission definition. Current design systems were used to: verify the performance and life, define the number of airfoils and airfoil contours, flowpath and mechanical speeds, and configure the cooling design of the blade and vane.

Results of the previous Supersonic Cruise Aircraft Research (SCAR) engine studies provided the starting point for the high-pressure turbine preliminary design. The chosen mission cycle and engine cycle established the turbine parameters (Table 4-I) and the initial flowpath. Studies were performed with meanline and streamline analysis to refine the flowpath and to obtain velocity triangles, reaction level, annulus area and wheel speed. Airfoil cross sections for the vane and blade were designed to provide minimum aerodynamic losses and to establish the heat loads on the vane and blade. Internal design of the airfoil was performed and cooling air distributed to obtain the design goals for metal temperatures and life. The cooled aerodynamic loss was then determined for both the vane and blade and the overall turbine efficiency established.

4.1 Aerodynamic Design

Aerodynamic design goals set for the VSCE high-pressure turbine design were maintained for the supersonic transport engine. The goals for the VSCE design, relative to the Energy Efficient Engine design, are: airfoil loading, +17 percent; profile loss, -10 percent; and endwall loss, -15 percent.

The aerodynamic design was started with the selection of the mission profile, the performance requirements, the VSCE turbine, and the above aerodynamic goals. AN^2 equal to 38.7×10^{10} cm^2/min^2 (6.0×10^{10} in^2/min^2), used for both the 1990 and 1986 engines, is an increase from the 36.7×10^{10} cm^2/min^2 (5.7×10^{10} in^2/min^2) used in previous VSCE studies. This increase was decided on before the start of this program.

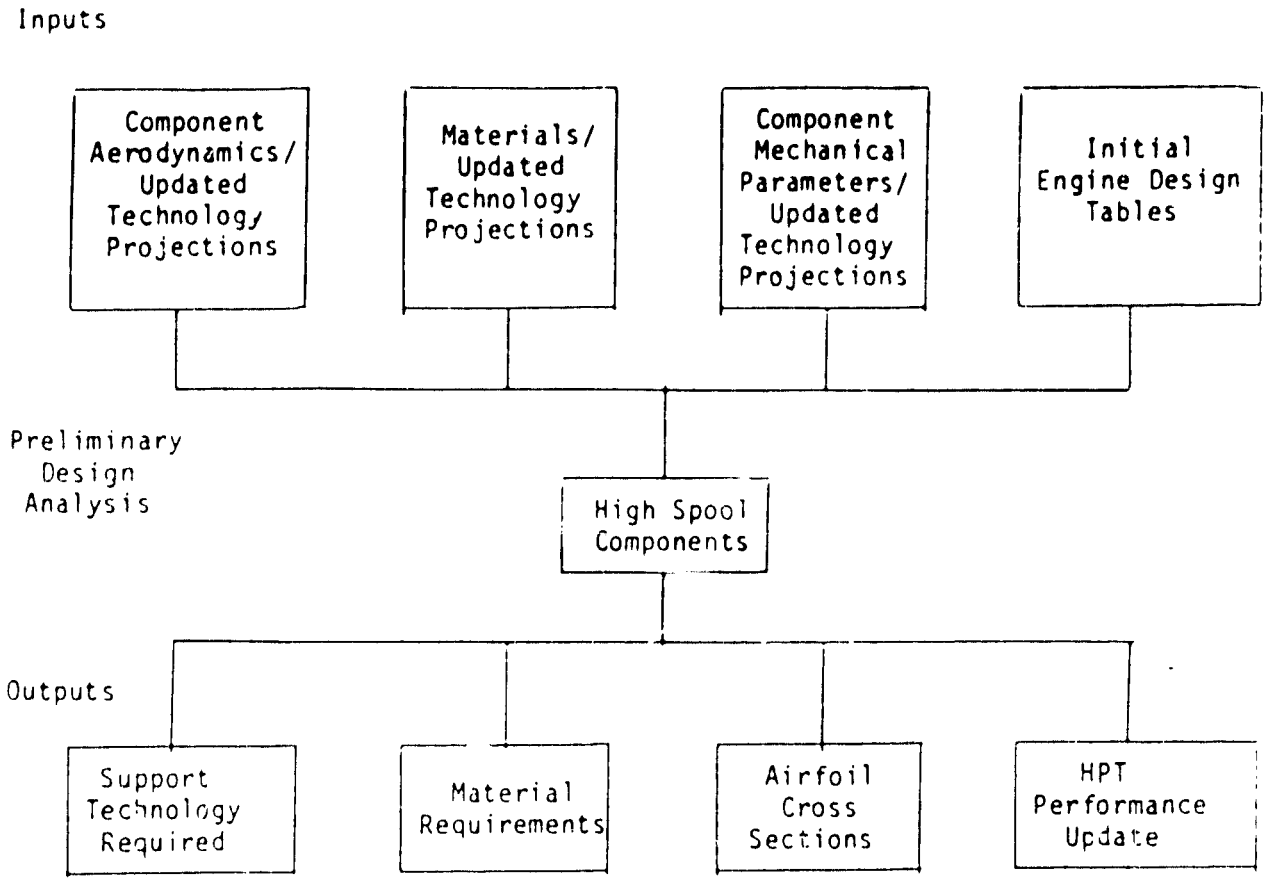

Figure 4-1 Primary Elements of the Preliminary Design Process

TABLE 4-I

TURBINE PARAMETERS FOR 1986 AND 1990 DESIGNS

- o Single Stage
- o Maximum Turbine Inlet Temperature - 1755 K to 1811 K (2700°F to 2800°F)
- o Compressor Discharge Temperature - 922 K (1200°F)
- o High-Pressure Turbine Design Life - 10,000 Hours, 5,000 Hours at Maximum Speed, Maximum Turbine Inlet Temperature, Maximum Compressor Discharge Temperature
- o Velocity Ratio - 0.58
- o Axial Velocity Ratio (C_X/U) - 0.60
- o AN^2 - 38.7×10^{10} cm^2/min^2 (6.0×10^{10} in^2/min^2)

The initial design studies centered on the original VSCE study engine flowpath at conditions modified for the current design program. The predicted pressure distribution on the blade surface is shown in Figure 4-2. The initial study identified an undesirable blade loading distribution which created a 1.35 maximum Mach number on the blade suction surface. The high Mach number lowered turbine efficiency, which in turn increased operating temperatures and prevented meeting durability goals.

Subsequently, a parametric study was conducted to refine the turbine design and to obtain a lower Mach number design but hold the AN^2 to 6.0×10^{10}. Meanline turbine designs were performed over a speed range of ± 10 percent and velocity ratios from 0.4 to 0.8. The mean radius and annulus area of these turbines were varied. This study, graphically summarized in Figure 4-3, provided a 0.5 percent net increase in turbine efficiency using initial cooling loss estimates. The chosen design reduced blade maximum Mach number from 1.35 to 1.1, trailing edge Mach number from 0.93 to 0.86, the axial velocity ratio (C_X/U) from 0.60 to 0.43, and the rotor speed from 11,194 RPM to 10,075 RPM. The reduced speed was acceptable to the VSCE high-pressure spool. The original flowpath and the selected low Mach number flowpath are compared in Figure 4-4. Turbine parameters for the selected engine configuration are presented in Table 4-II. The turbine airfoil geometry is shown in Figures 4-5 and 4-6.

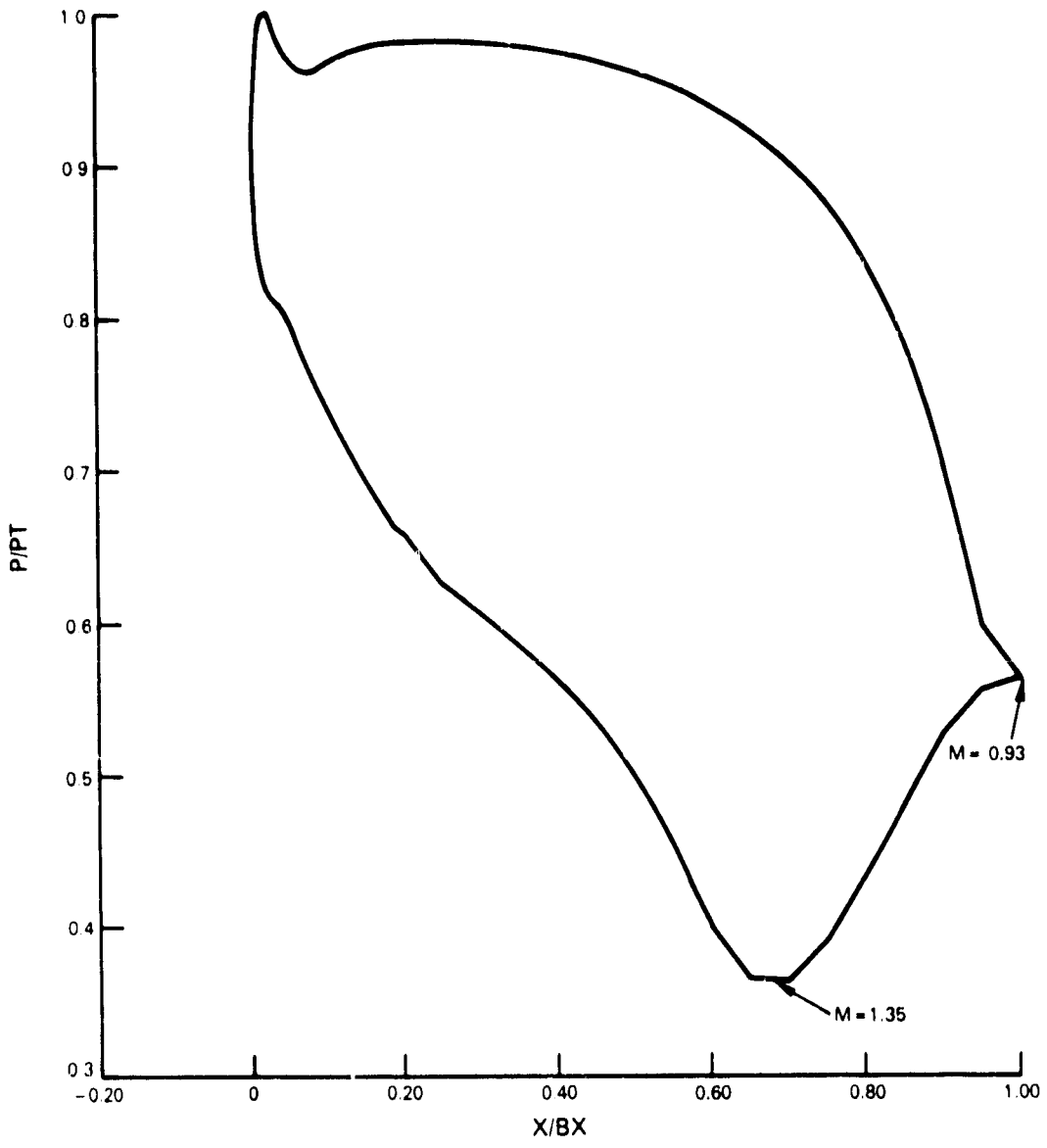

Figure 4-2 Original VSCE Turbine Flowpath High Mach Numbers Required Turbine Redesign

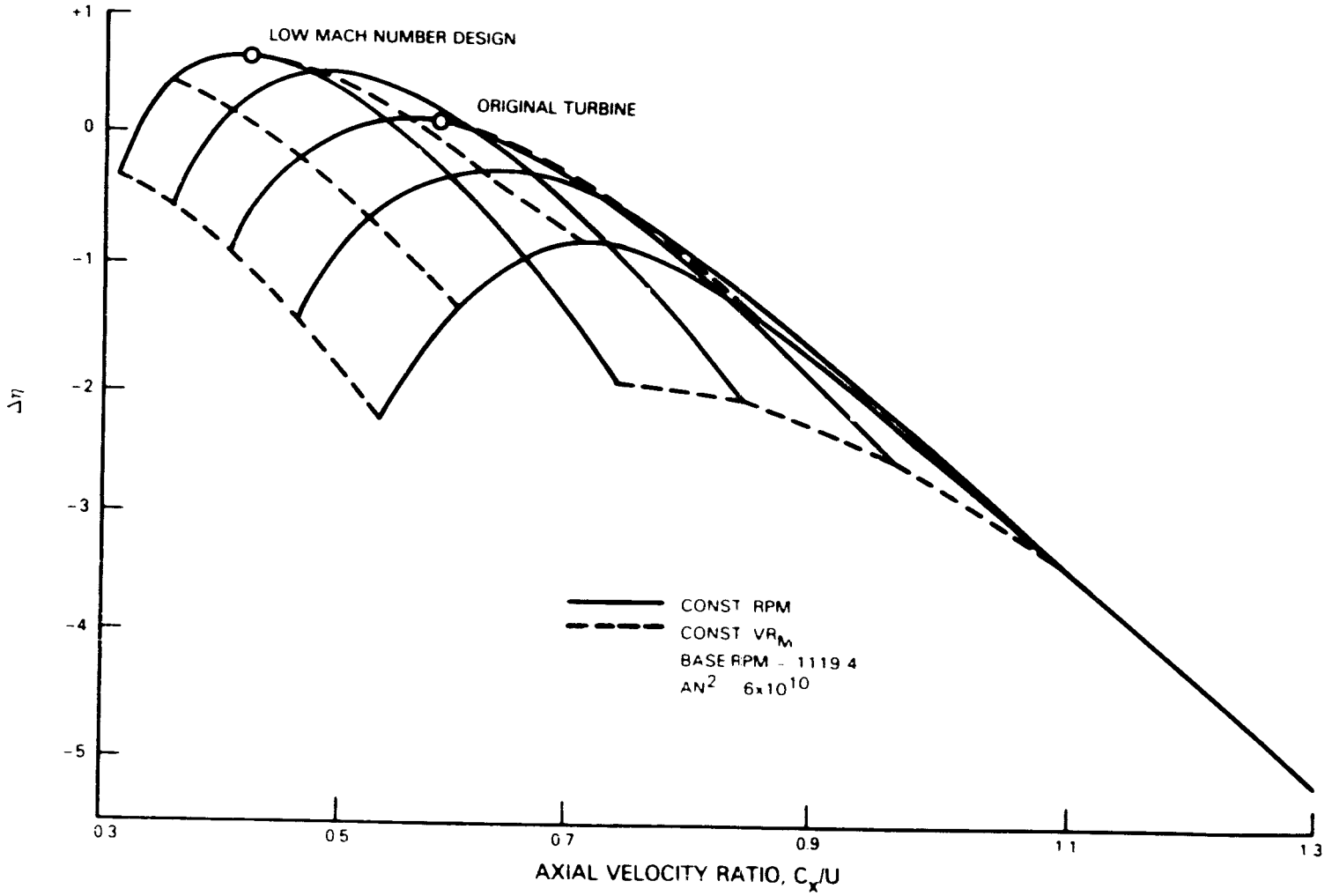

Figure 4-3 High-Pressure Turbine Parametric Study Identified Improved Design

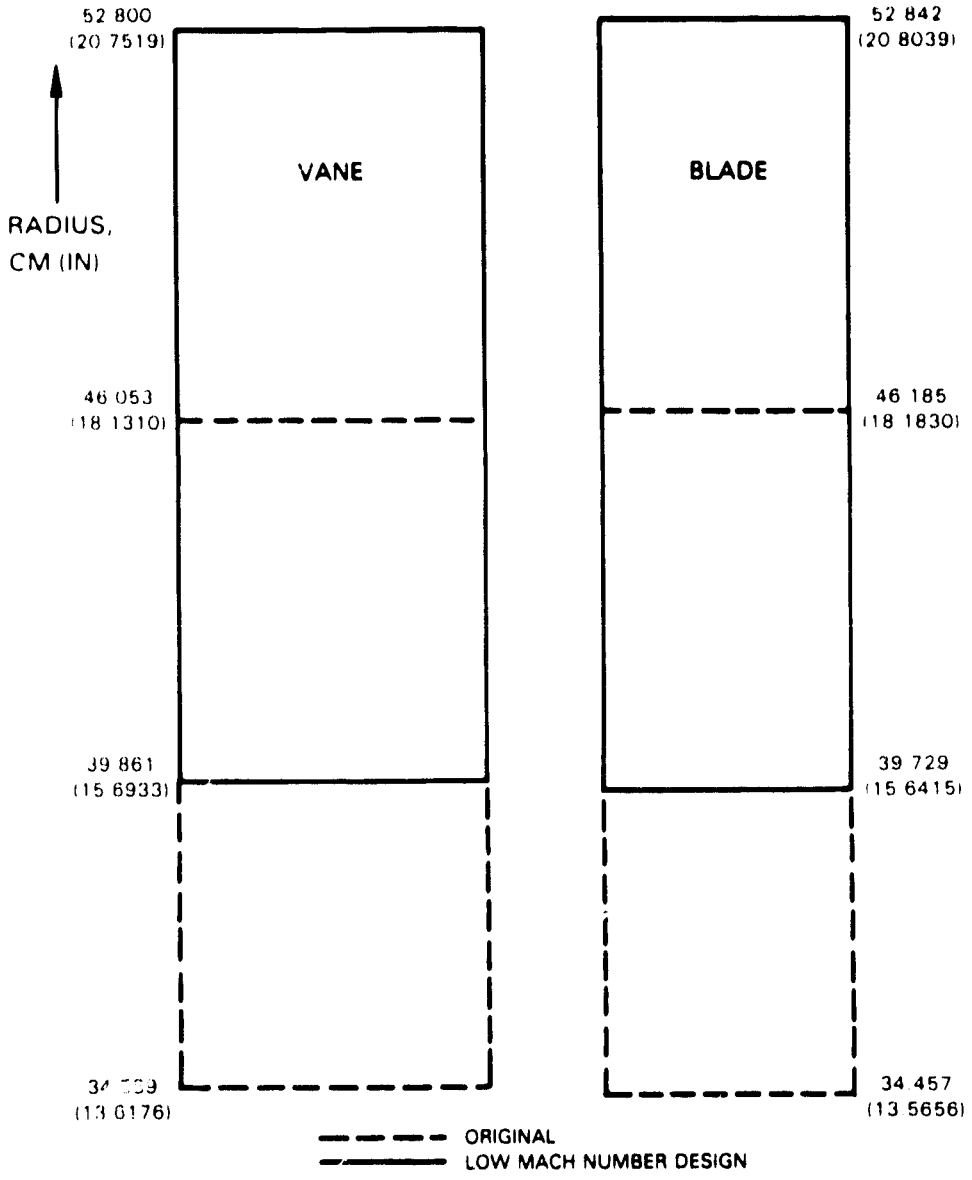

Figure 4-4 Comparison of Original and Final Flowpath

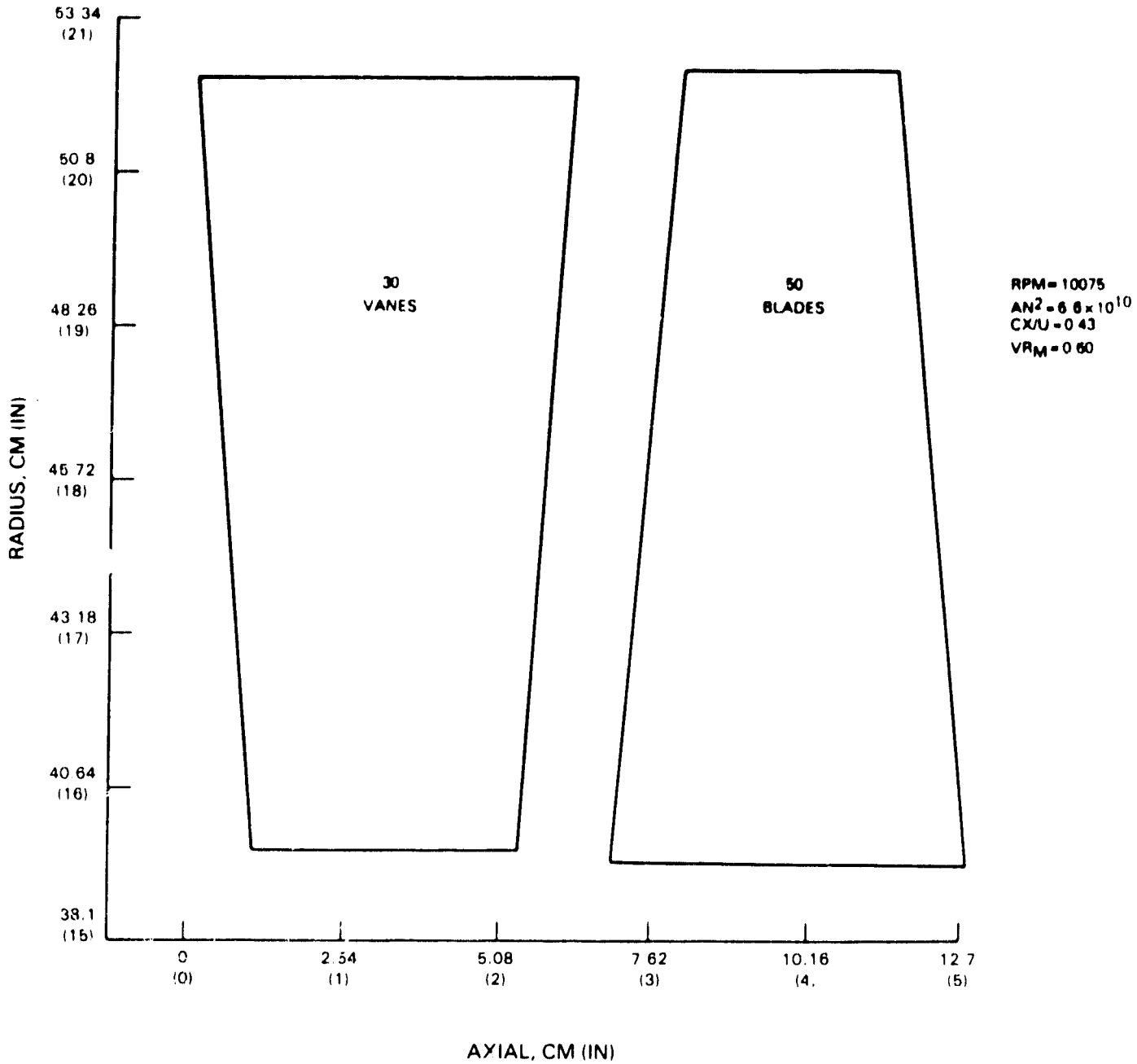

Figure 4-5 Turbine Geometry

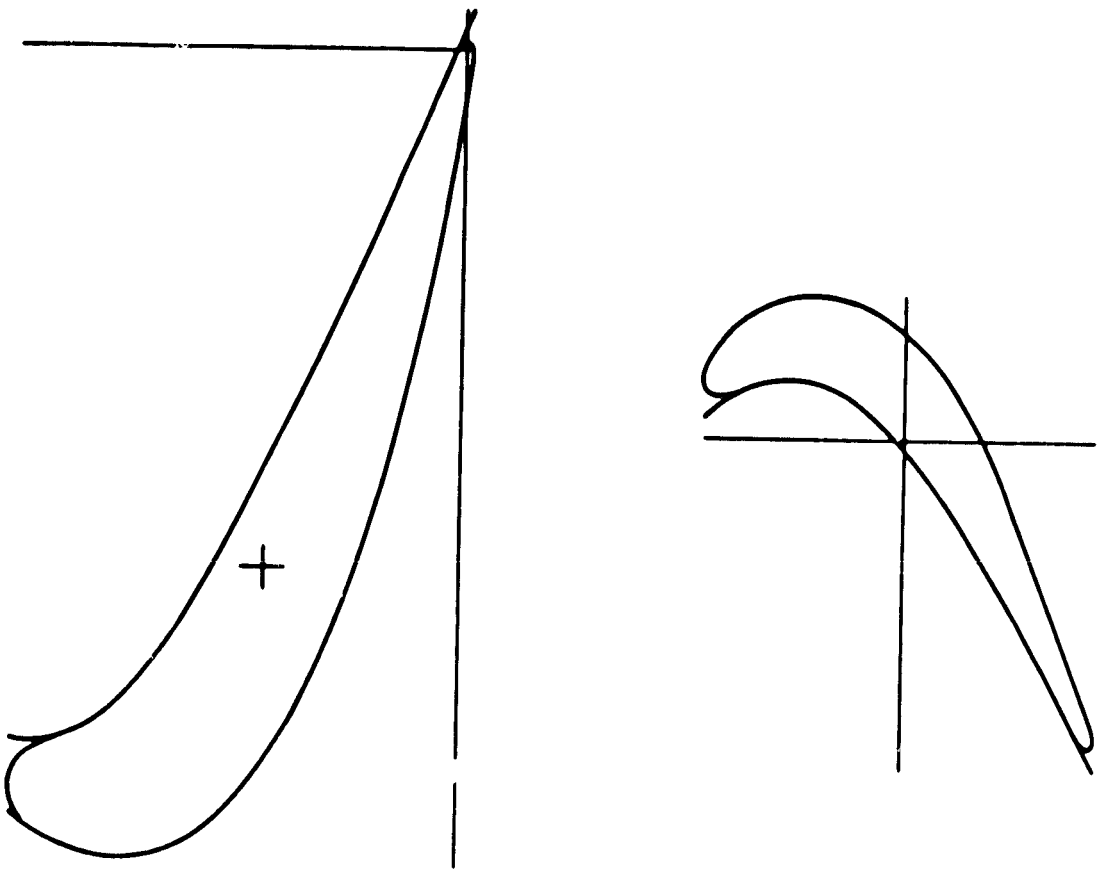

Figure 4-6 Airfoil Geometry

TABLE 4-II

TURBINE PARAMETERS

Airfoil	Section	Radius cm (in)	B_x cm (in)	M_{in}	M_{out}	β_{in} (deg)	β_{out} (deg)
Vane	R	39.85 (15.69)	4.36 (1.72)	0.152	0.965	90.0	15.3
	M	46.28 (18.22)	5.33 (2.10)	0.147	0.832	90.0	15.3
	T	52.71 (20.75)	6.27 (2.47)	0.146	0.737	90.0	15.3
Blade	R	39.73 (15.64)	5.81 (2.29)	0.459	0.811	33.5	22.7
	M	46.28 (18.22)	4.62 (1.82)	0.283	0.862	53.8	22.7
	T	52.83 (20.80)	3.45 (1.36)	0.195	1.01	93.5	22.7

Vane design philosophy has been to select a minimum number of vanes to reduce aerodynamic loss, cooling air requirements and parts cost. However, compensating concerns of controlling platform alignment, and hence leakage, tends to drive the selection toward reduced platform length and increased number of vanes or at least clusters of vanes. The preliminary aerodynamic and structural considerations set the number of vanes at 30.

The trend in advanced turbine rotor designs is to use fewer blades which results in lower parts and maintenance costs, and increased flexibility of the rotor system structural design. Since the number of airfoils along with the chord length also affect aerodynamic performance and blade pull, a separate evaluation was conducted to determine the number of blades that could be used in the VSCE design, consistent with the assumed design goals.

Aerodynamic loss, a sum of the blade profile and secondary (endwall) losses, was evaluated for the range of 50 to 60 blades. The aerodynamic loss and the total loss, including estimated cooling effects, are shown to be relatively insensitive to the number of airfoils. This results from the compensating trends of the profile and endwall losses as illustrated in Table 4-III.

TABLE 4-III

COMPARISON OF LOSSES WITH 50 AND 60 BLADES

Number of Airfoils	50	60
Profile $\Delta P/P$	.0114	.0122
Endwall	.0120	.0104
Cooling	.0118	.0118
Total	.0352	.0344

This loss difference between 50 and 60 blades is considered to be insignificant (2 percent of the loss). Consequently, the number of blades was selected to be 50 in order to take advantage of the potential cost benefits of the smaller number.

The meanline study defined the inlet and exit aerodynamics. The Pratt & Whitney airfoil design system was used to define the airfoil contour. This system defines the inlet and exit aerodynamics, leading edge and trailing edge contours, wedge angle, and overall loading and modifies the chordwise loading distribution to obtain the minimum aerodynamic loss. In configuration studies (Section 5.1.5) this process was extended to include minimizing the external heat load.

Design results for the vane and blade pressure distributions are presented in Figures 4-7 and 4-8. The blade pressure distribution reflects the effects of a reduced exit Mach number. Intra-blade Mach number for mean section is shown in Figure 4-9.

Boundary layer analyses were performed to quantify aerodynamic losses. The airfoil contours and their resulting aerodynamics provided the input for the STAN-5 modeling of the viscid loss calculations. The Pratt & Whitney design system also models the shock losses. Figure 4-10 shows the radial distribution of suction side boundary layer transition from laminar to turbulent and the predicted losses. The aerodynamic losses are shown to be between 1.0 to 1.5 percent, including the shock loss. Based on these results, a preliminary efficiency of 92.3 percent for the high-pressure turbine was obtained as shown on Table 4-IV.

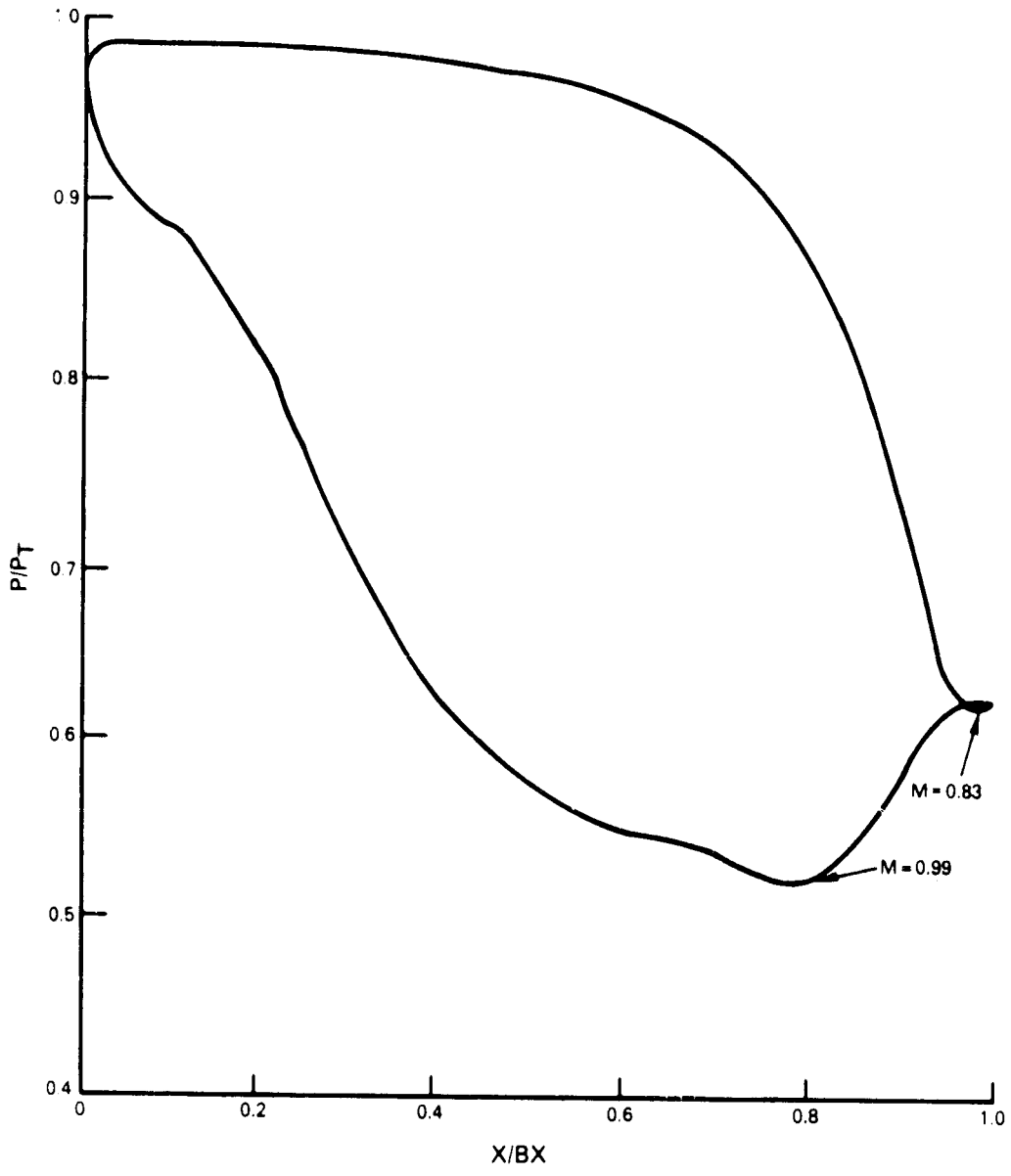

Figure 4-7 Vane (Mean) Pressure Distribution

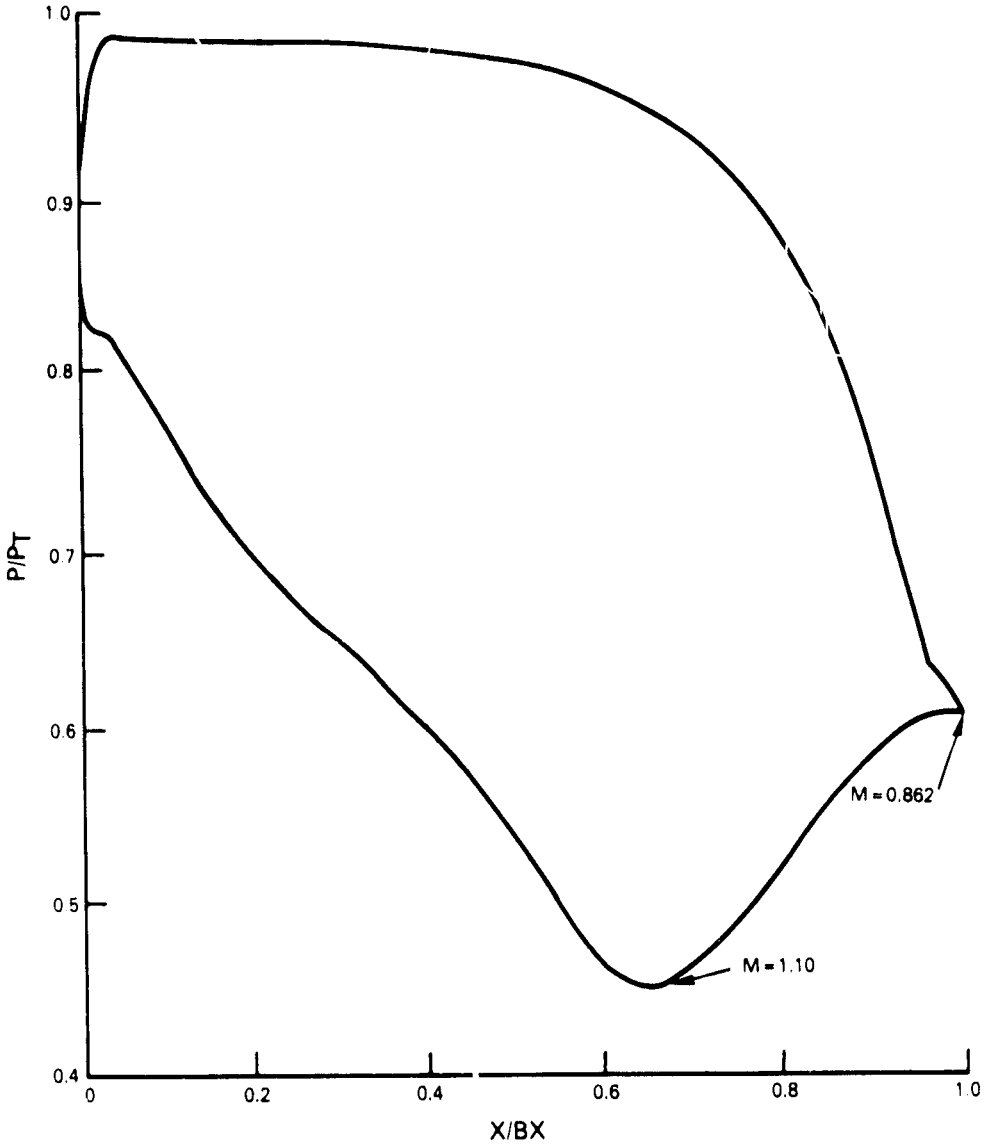

Figure 4-8 Blade (Mean) Pressure Distribution Redesigned Blade Achieved Reduced Mach Numbers

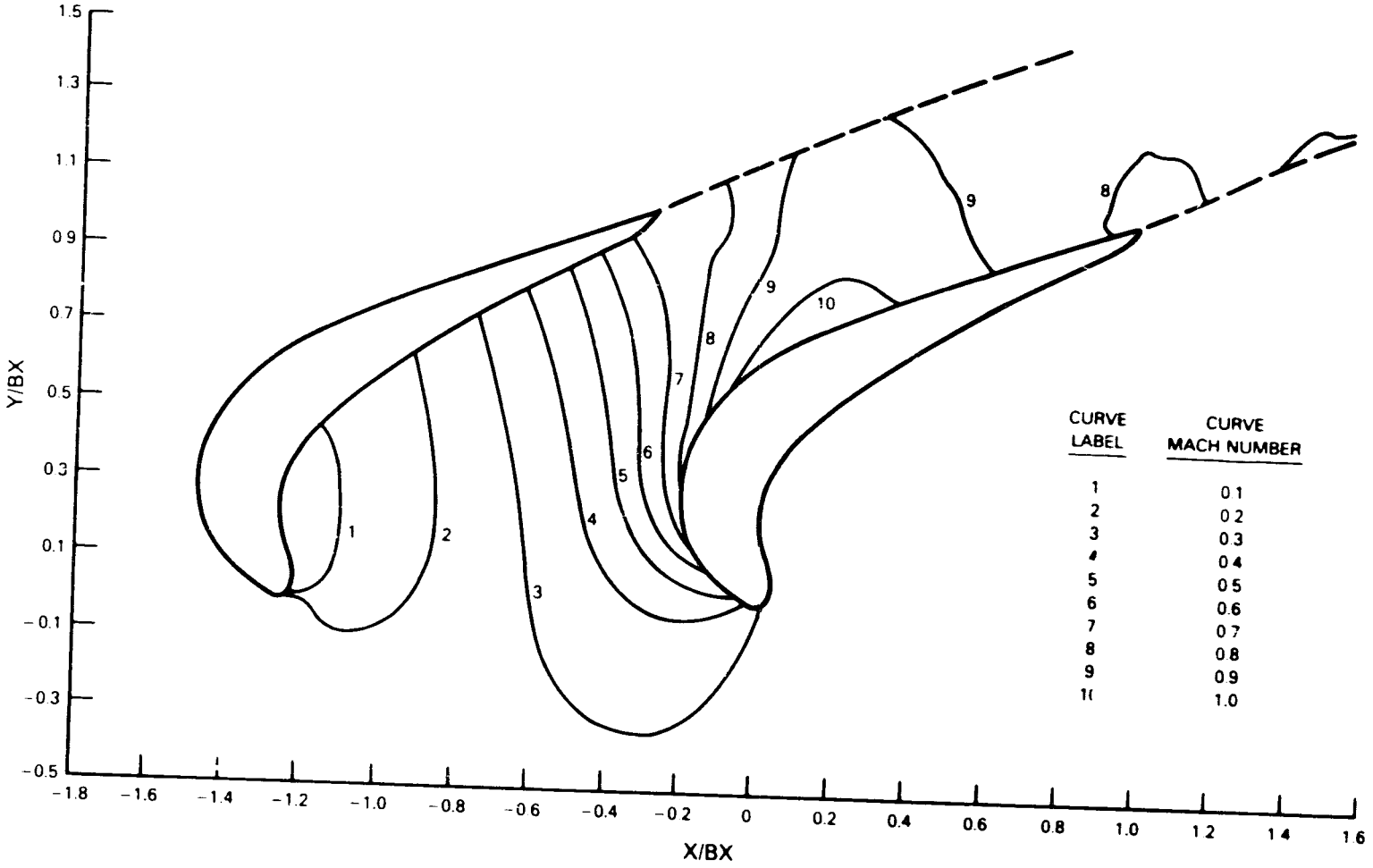

Figure 4-9 Blade Mach Numbers Contour Map

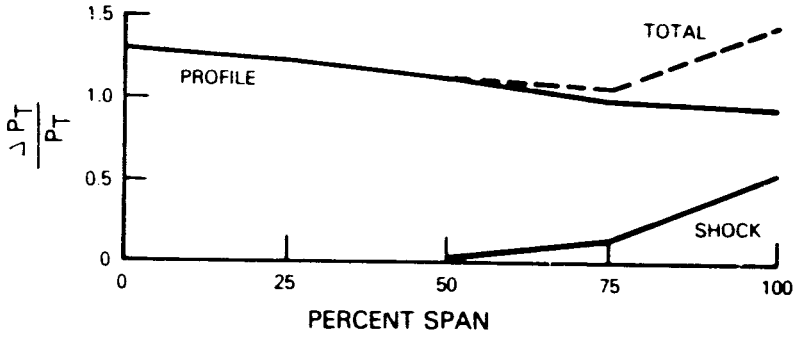

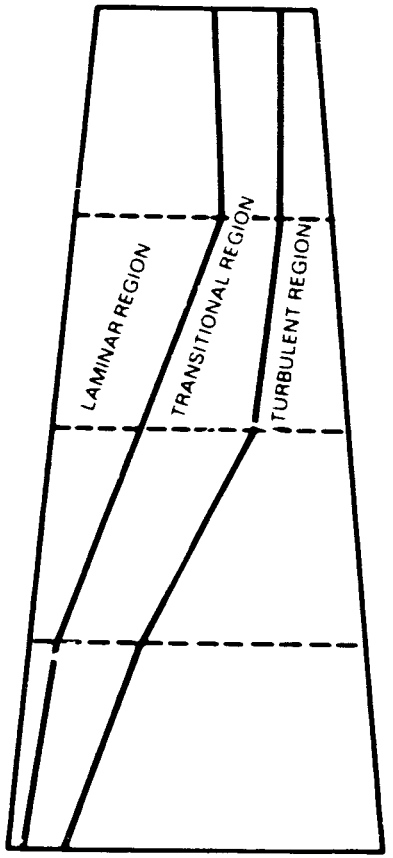

LOSS $\Delta P_T/P_T$	
PROFILE	SHOCK
0.90	0.51
0.96	0.13
1.11	0.01
1.23	0
1.30	0

Figure 4-10 Blade Losses

TABLE 4-IV

EFFICIENCY BREAKDOWN

o Current Technology	91.0%
Including AN^2, Velocity Ratio, Pressure Ratio Effect	
o Advanced Technology	
Profile and Secondary Loss Reductions	+0.6%
Increased Annulus	+0.5
Increased Loading	-0.2
Reduced Cooling Loss	+0.4
	92.3%

4.2 Aerodynamic Conclusions

The high-pressure turbine efficiency estimate based upon the preliminary aerodynamic design is summarized in Table 4-IV. This study identified an increased efficiency of 0.7 percent above that predicted in the original SCAR programs. This 92.3 percent efficiency in the high-pressure turbine was achieved with 10 percent fewer airfoils. It is further concluded that the benefits obtained in this design study are transferable to other advanced aircraft engine designs.

4.3 Mechanical Design Considerations

Blade pulls and stresses were evaluated for the 50 blade design. Included were studies to demonstrate the benefit of axial chord tapering between the airfoil root and tip on blade centrifugal stress. The chord taper ratio (tip chord/root chord) was determined by setting the airfoil tip and root load coefficients at the design goal level (17 percent higher than that in the Energy Efficient Engine). Sections between the tip and root were then assumed to be linear with the radius. The airfoil defined in this manner resulted in blade root centrifugal pull and stress increases of 7 and 5 percent respectively, relative to the Energy Efficient Engine blade. Further reduction of the pull and stresses is possible by more complex tapering of the chord and wall thickness redistribution in the radial direction, which should be considered during a final design program.

SECTION 5.0

DURABILITY DESIGN

The operating requirements of supersonic cruise aircraft engines are unusual in that the maximum turbine temperatures and rotor speeds occur during the long time cruise portion of the mission. At the selected mission and a 10,000 hour total design life, the hot section parts experience the near maximum combustor exit temperature, rotor speed and cooling air temperature for over 5000 hours. In contrast, the hot section parts of a typical subsonic engine would require to withstand only about 150 hours of exposure at these conditions over the same 10,000 hours total life. This difference shifts the major design criteria of the high-pressure turbine life in supersonic applications from takeoff and transient cyclic operation, to creep or oxidation related modes.

Advanced cooling techniques coupled with material improvements are necessary to achieve durability consistent with the engine application goals and the target efficiency. To accomplish this, a three step design approach was used: first, configurational studies for screening durability technologies considered available for the supersonic cruise aircraft engine; second, mission life analysis to establish the design metal temperature limits; and third, preliminary cooling designs of the vane and blade were completed, utilizing the configurational study results and coolant flows determined in earlier studies. Detailed heat transfer analysis was conducted to assure that the combined cooling features satisfy overall durability requirements.

5.1 Configurational Studies

Advanced turbine airfoil cooling designs generally comprise a number of individual local cooling schemes tailored to meet cooling and geometry requirements of each part of the airfoil (leading edge, midchord, and trailing edge). Such individual cooling schemes for the supersonic cruise aircraft engine were selected using configurational studies described in this section. The criteria for inclusion in the subsequent preliminary design was the potential for improving engine performance either by reducing cooling airflows or improving cooling air management.

The following schemes were evaluated:

- Vane coolant precooling to reduce vane coolant flow or reuse the vane coolant in the blade;
- Vane trailing edge cooling configurations and its compatibility with aerodynamic design;
- Blade leading edge configurations;
- Thermal barrier coating with advanced film cooling; and
- Airfoil design for reduced heat load.

5.1.1 Vane Coolant Precooling

The use of a precooler was investigated as a means of reducing the cooling airflow and associated momentum mixing losses for the first stage vane. Two distinct cooling schemes were investigated. The first scheme utilized precooled air to cool the vane leading edge cavity. The precooled air passes between the vane walls and the insert, exiting as film on the suction surface (Figure 5-1). A suction surface exit is required because of the increased pressure drop requirements of internal convection and the precooler relative to a film cooled design. Using a pressure surface (low Mach number) exit would not allow sufficient pressure drop to drive the precooler and additionally provide the required internal convection. As can be seen from Figure 4-7, the pressure surface has surface pressures very nearly equal to the leading edge total pressure in the leading edge cavity region. Utilizing this region as an exit would provide an available pressure ratio for cooling of only 1.09 $((P_{T4}/P_{T3}) / (P_S/P_{T3}))$ not accounting for backflow margin. This pressure ratio is insufficient to drive the precooler as well as to provide sufficient internal cooling.

Flow turbulators were placed on both the insert and vane walls to achieve maximum internal heat transfer augmentation. Internal heat transfer was tailored to maintain a constant interface temperature by varying the insert to vane gap. This gap decreased chordwise from the leading edge towards the rear of the leading edge cavity as the coolant temperature increased. Heat transfer coefficients were limited by the available pressure drop and friction generated by the cooling passages. Maximum available heat transfer coefficients at the critical rear cavity location (maximum $T_{coolant}$) are shown as a function of cooling flow in Figures 5-3 and 5-4 for the suction wall and pressure wall respectively. Wall thicknesses on the vane were thinned to 0.127 cm (0.050 in) to maximize the cooling effectiveness.

The pressure and suction walls were analyzed separately using an idealized one-dimensional heat transfer model to determine the minimum flow required to cool the vane walls.

The idealized model (Figure 5-2) assumed a flat surface at a uniform interface temperature. With these assumptions the required internal heat transfer coefficient could be determined and plotted as a function of coolant flow and the extent of precooling (Figures 5-3 and 5-4). Figures 5-3 and 5-4 also show the attainable heat transfer coefficients using state-of-the-art internal turbulators.

The minimum cooling airflow required to convectively cool the vane leading edge can be less than that required for the film cooled design as shown in Figure 5-5. This convective cooling scheme, although reducing the leading edge cooling airflow, did not reduce the overall momentum mixing losses. Momentum mixing losses are a function of the cooling flow level as well as the ratio of coolant exit velocity to local gas velocity. Increasing the coolant velocity to reduce momentum mixing losses reqires an increasing of the upstream driving static pressure. As can be seen from Figure 5-6, for the leading edge convective cooling this would require increasing the internal static to

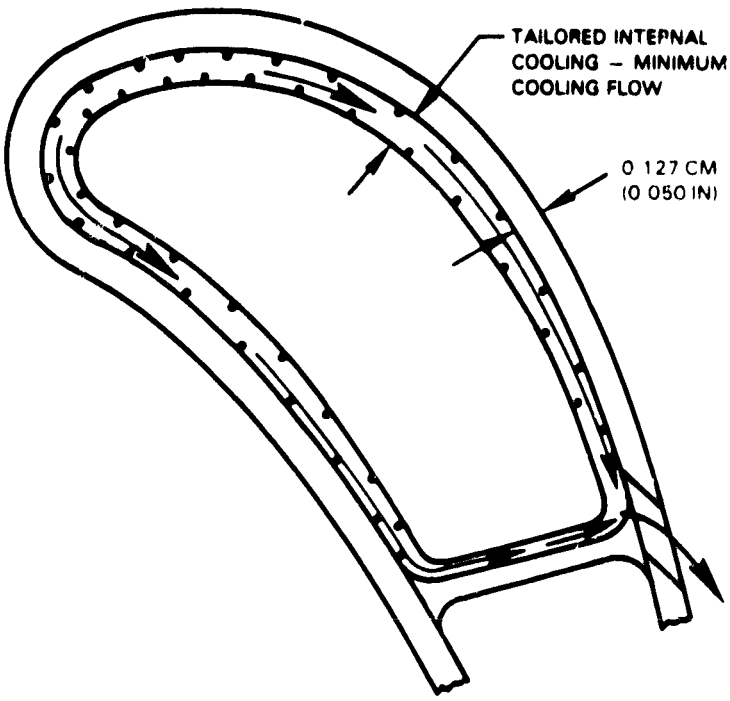

- COOLING TAILORED TO MAINTAIN CONSTANT $T_{INTERFACE}$ TO ATTAIN MINIMUM FLOW REQUIREMENT
- WALL MINIMUM THICKNESS AT 0.127 CM (0.050 IN) TO ATTAIN MAXIMUM INTERFACE COOLING

Figure 5-1 Convectively Cooled Vane Leading Edge

"IDEALIZED" MINIMUM FLOW LEADING EDGE

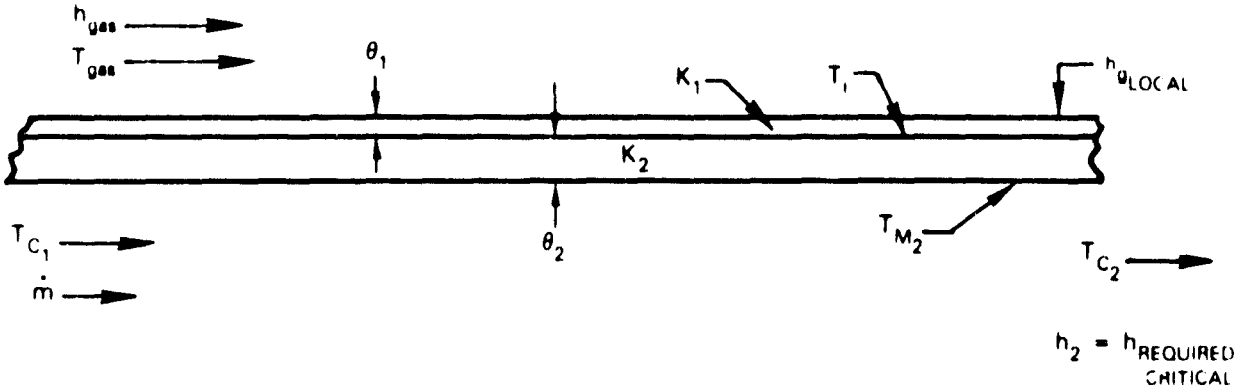

$$\bar{Q} = h_e A_g [T_g - T_1]$$

$$\bar{Q} = \dot{m} C_P [T_{C_2} - T_{C_1}]$$

$$h_e = \frac{1}{\frac{1}{h_g} + \frac{\theta_1}{K_1}}$$

$$Q_L = h_{e_L} A_g [T_g - T_1]$$

$$Q_{L2} = h_2 A_C [T_{M_2} - T_{C_2}]$$

$$h_{e_L} = \frac{1}{\frac{1}{h_{g_{LOCAL}}} + \frac{\theta_1}{K_1}}$$

$$A_g = A_C, \quad T_{M_2} = T_1 - \frac{Q_L \theta_2}{K_2}$$

SOLVING FOR h_2

$$h_2 = \frac{h_{e_L} [T_g - T_1]}{[T_1 (1 + \frac{h_{e_L} \theta_2}{K}) - T_g] - [\frac{h_e A_g}{\dot{m} C_P} (T_g - T_1) + T_{C_1}]}$$

Figure 5-2 Vane Convective Leading Edge Cooling

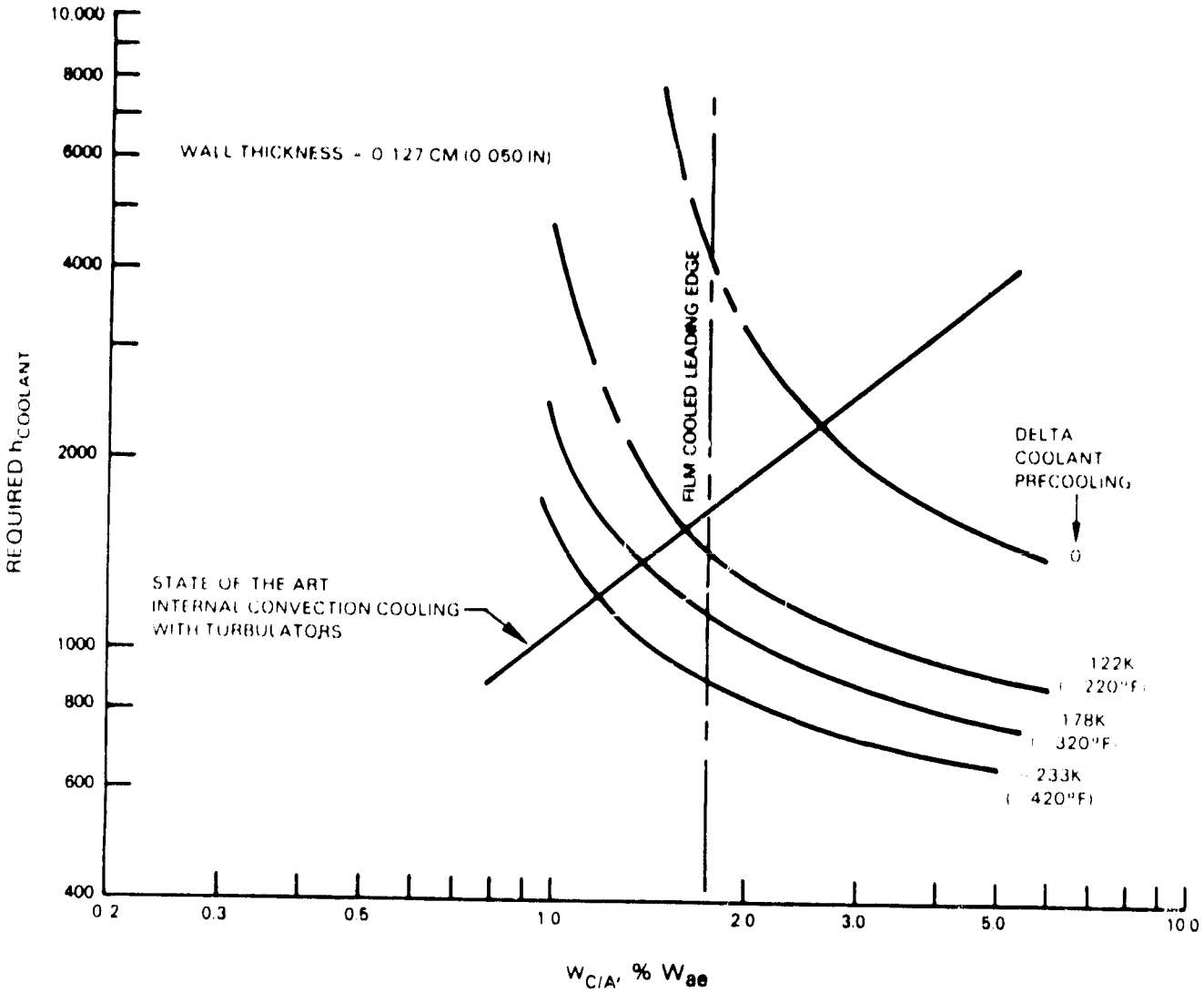

Figure 5-3 Convectively Cooled Vane Leading Edge Using Precooled Air; (Suction Surface)

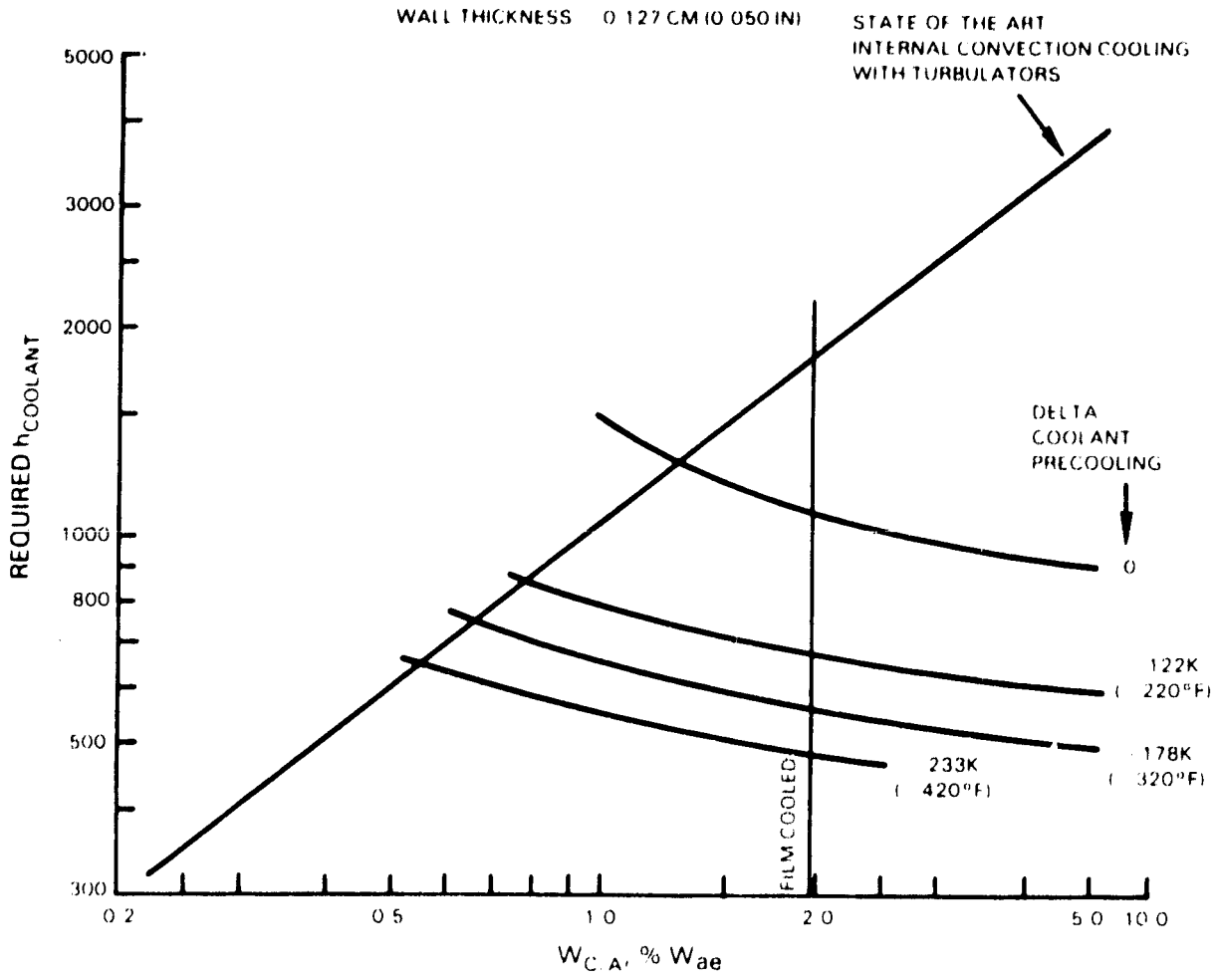

Figure 5-4 Convectively Cooled Vane Leading Edge Using Precooled Air; (Pressure Surface)

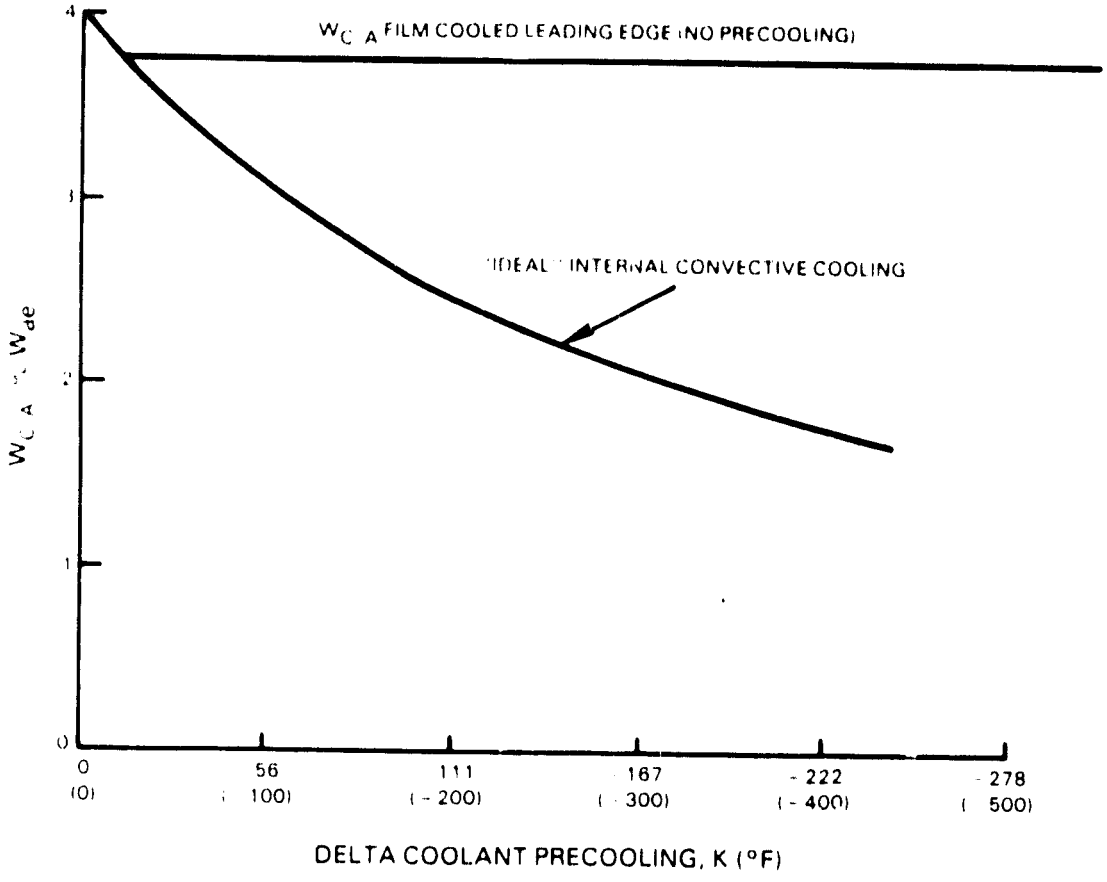

Figure 5-5 Vane Leading Edge Convective Cooling; Effect of Precooling on Coolant Flow

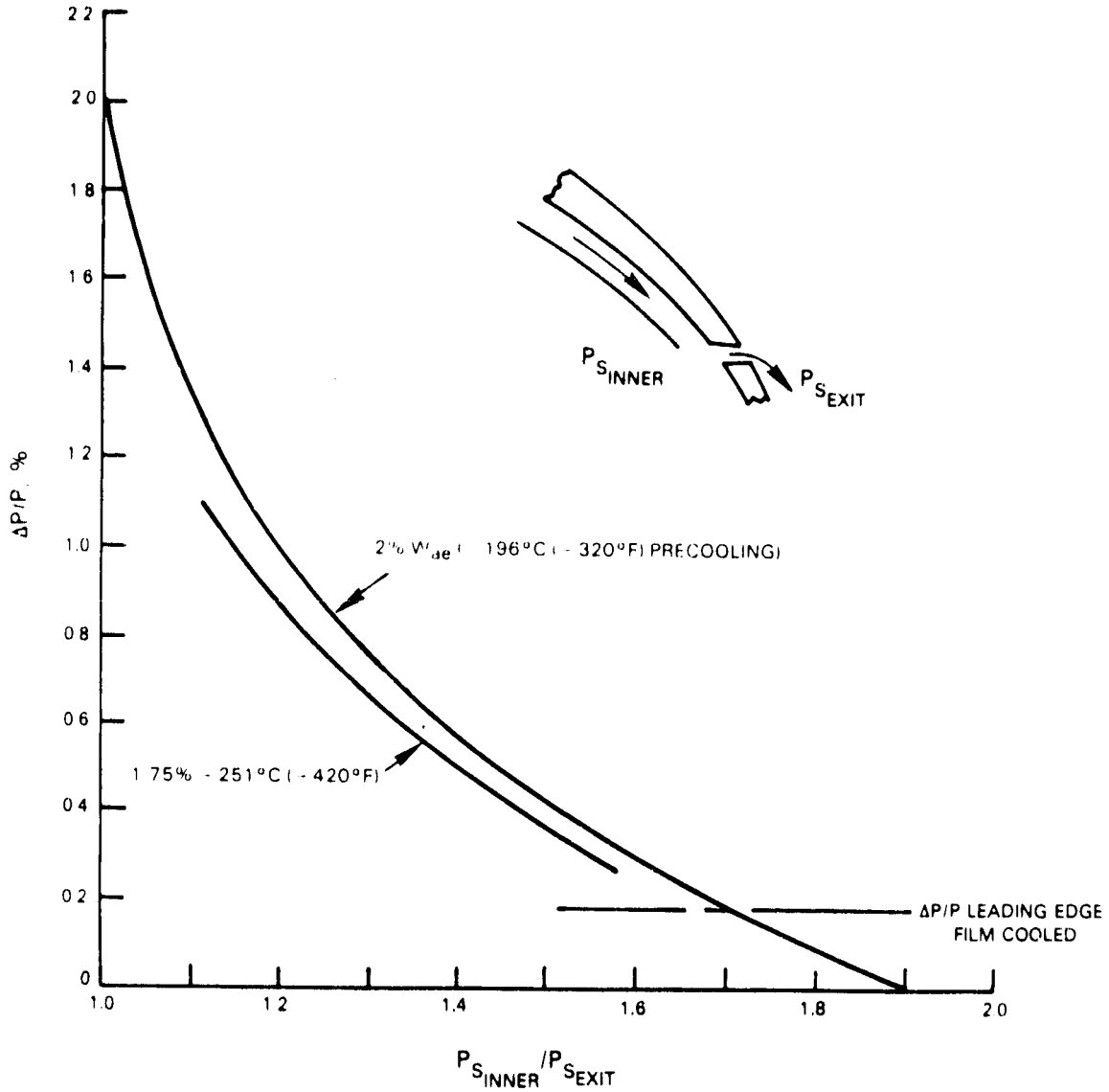

Figure 5-6 Vane Convective Leading Edge; Momentum Mixing vs Exit Pressure Ratio

external static pressure ratio to 1.7 in order to reduce the loss levels to the base film cooled levels of the leading edge. This increase in internal static pressure would reduce the assumed internal convective effectiveness due to the reduced pressure drop available for cooling and require more cooling flow. To maintain momentum mixing losses equal to the base film cooled case, supply pressures in excess of compressor discharge pressure are required. The film cooled base case flow levels, shown for the leading edge in Figures 5-3, 5-4, and 5-5, reflect initial flow level estimates. Total leading edge flow levels were reduced from this initial estimate of approximately 3.8 percent W_{ae} to 3.35 percent W_{ae} when detailed analyses were conducted for the film cooled design.

The vane trailing edge could not utilize the precooler to reduce coolant flow levels and momentum mixing losses. Utilization of a precooler requires elimination of the pressure side film cooling due to the increased pressure drop requirements of the precooler and internal convection. Removal of the pressure side film significantly increases the film temperature at the trailing edge of the vane. This increase in film temperature raises the cooling flow requirement of the trailing edge slot beyond that of the total flow required for the film cooling case even with precooling of 422 K to 477 K (300°F to 400°F). Cooling losses would increase dramatically since the trailing edge is a much higher loss region relative to the pressure wall.

To eliminate the momentum mixing loss of the leading edge cooling air, a second scheme was reviewed in which the vane front cavity was cooled by passing precooled air from the outer diameter to the inner diameter of the vane and using the same air to cool the first stage blade. An optimum or "ideal" cooling scheme was analyzed to determine the maximum potential for reducing the cooling airflow and increase engine performance with this design. Vane cooling configurations were tailored so that the vane cooling airflow and exit temperature matched the blade cooling requirements (Figure 5-7). Precooler pressure, temperature and flow requirements were established over a range of tangential on-board injection (TOBI) pressure ratios (Figure 5-8), and based on the flow characteristics and requirements of the vane and blade. A range of TOBI pressure ratios was presented due to the significant impact of the TOBI on turbine pump work and blade cooling air temperature. The "ideal" system considered does offer an improvement in engine thrust specific fuel consumption (Figure 5-9).

A heat exchanger and its associated plumbing, however, would weigh approximately 54 kg (120 lb) to achieve 477 K (400°F) temperature drop with the allowable pressure drop. This added weight would result in an aircraft thrust specific fuel consumption (TSFC) penalty of 0.23 percent (Table 5-I) bringing the net TSFC benefit down to 0.13 percent at most. This small gain is based on an "ideal" system and the actual benefit, if any, would be significantly less. Because of the extremely small potential of this system coupled with the inherent risk of damage to the blade from ingestion of loose parts, it was not considered as a viable technology option for the supersonic cruise application.

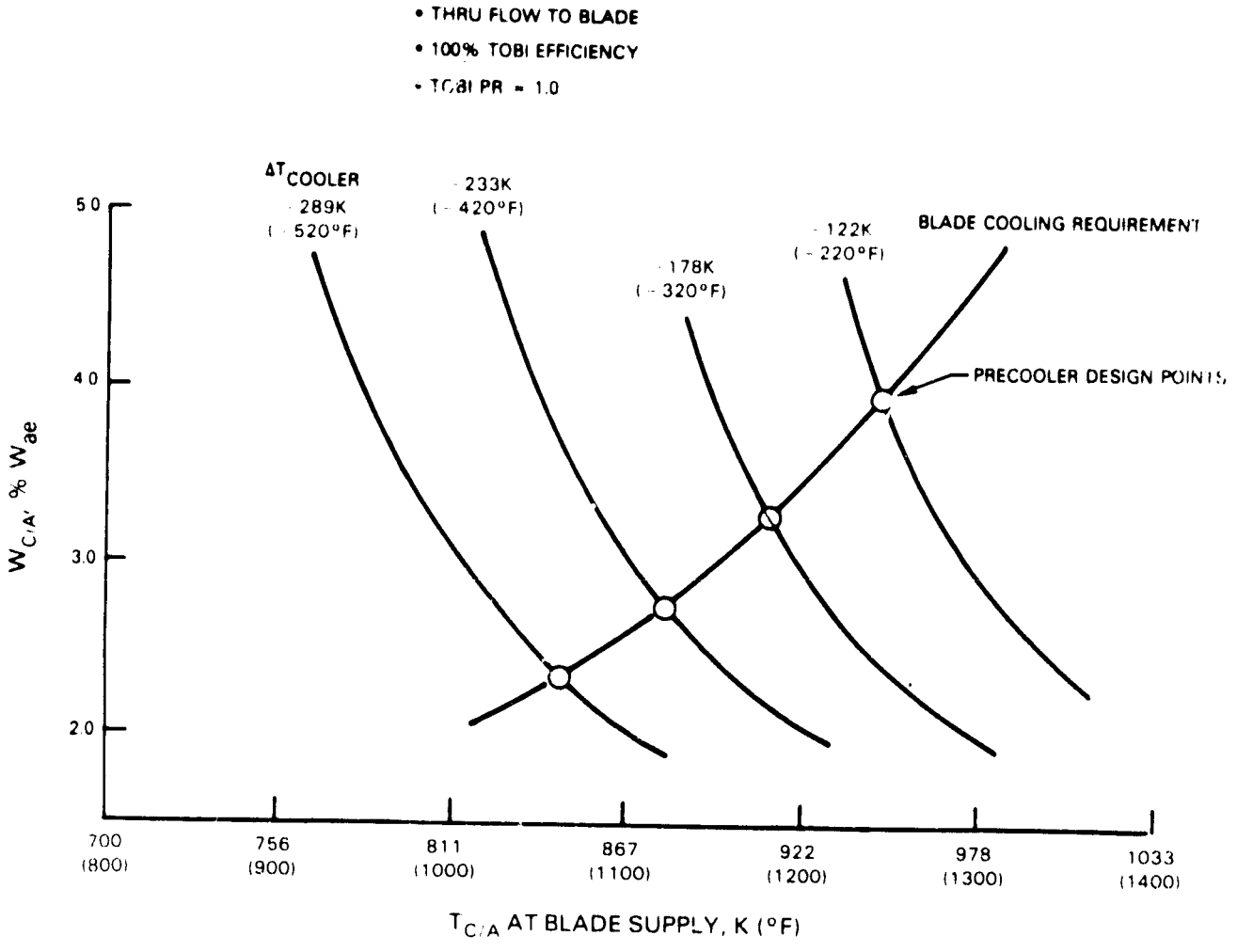

Figure 5-7 Vane Leading Edge Convective Cooling; Coolant Flow vs Temperature

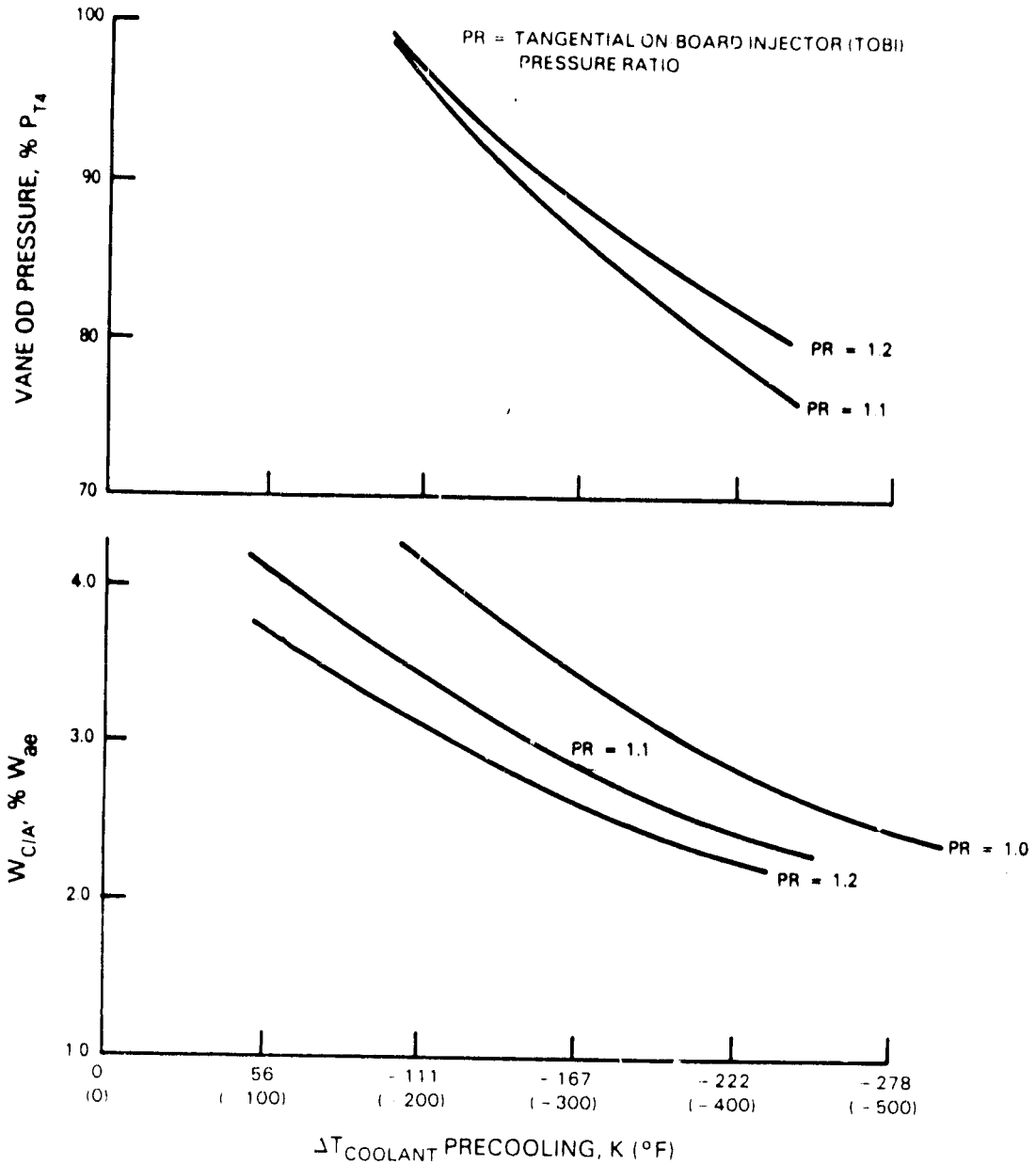

Figure 5-8 Vane Leading Edge Convective Cooling; Coolant Flow vs Precooling

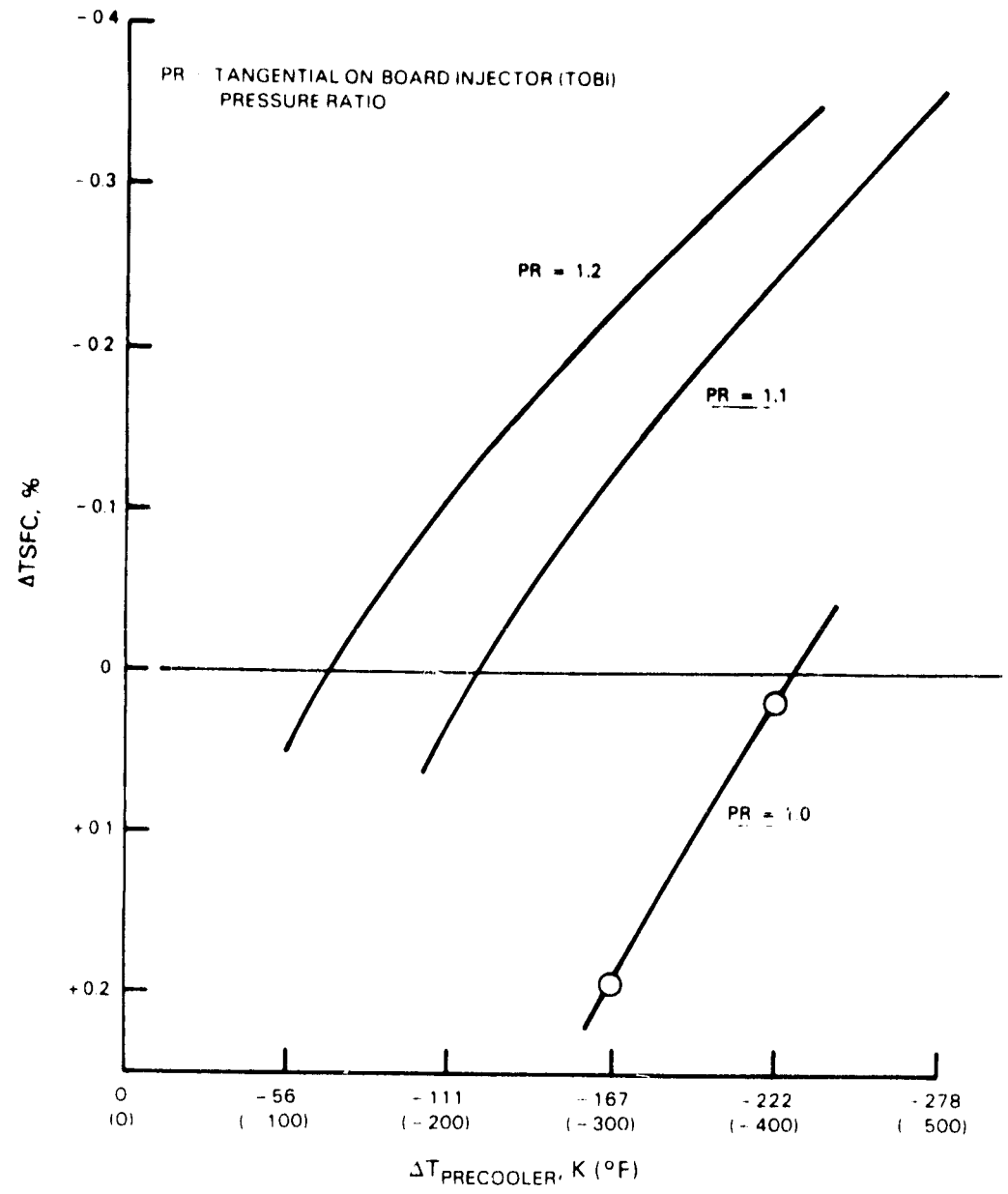

Figure 5-9 Influence on Thrust Specific Fuel Consumption Change of Vane Precooled Airflow from Leading Edge to Blade Cooling With No Weight Penalty

TABLE 5-I

PRECOOLER CONFIGURATION

o Weight - 54 kg (120 lb)minimum	
o Thrust Specific Fuel Consumption Benefit for Precooling	0.36%
o Thrust Specific Fuel Consumption Debit Due to Weight	0.23%
Net Gain	0.13%
+	
Blade Ingestion Risk	
o Conclusion:	
Benefits Do Not Warrant Additional Risk	

5.1.2 Vane Trailing Edge Internal Cooling Geometry

In this study, advanced state-of-the-art cooling schemes for the vane trailing edge were evaluated in terms of cooling effectiveness, required cooling air supply pressure, and compatibility with aerodynamic requirements. Four candidate concepts (Figure 5-10) with either pedestals or trip strips were considered to augment convective heat transfer. These included:

- o a baseline circular pedestal array typical of current trailing edge designs;
- o a ribbed design in which the ribs form rectangular channels for coolant flow passages; these ribs also incorporate trip strips on their surface;
- o a pear shaped pedestal array, and
- o an alternate ribbed design with skewed trip strips on the airfoil pressure and suction side inner walls.

Another fifth scheme, employing a "cut back" pressure wall, was also considered and discarded early because its cooling effectiveness is not currently considered to be competitive with the other candidate schemes. The cut back design becomes more effective in applications having aerodynamic performance more sensitive to airfoil trailing edge thickness than the supersonic cruise aircraft engines high-pressure turbine vane (also see Section 5.2).

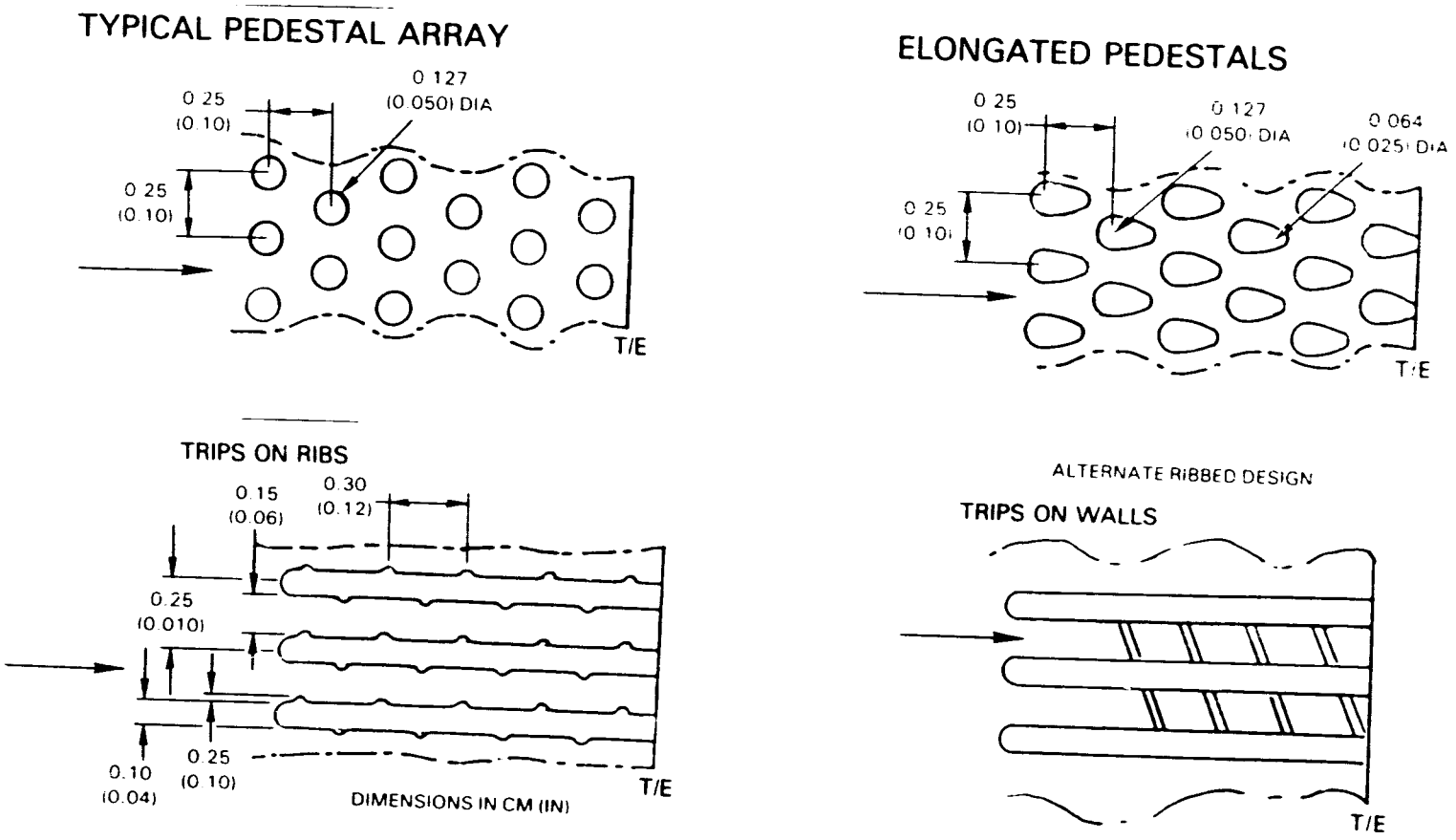

Figure 5-10 Vane Trailing Edge Concepts

Analysis was performed on the trailing edge configurations to determine the coolant flows at available supply pressure, define the corresponding heat transfer coefficients, and calculate the local metal temperatures. For each configuration, the cooling surface and the conduction areas were modeled to reflect the presence of pedestals. Thermal barrier coating was assumed on the airfoil surface for metal temperature calculations.

The study results are presented in Figure 5-11. The results showed that the best trailing edge internal cooling scheme is the alternate ribbed with trips on walls design (skewed). The design with trips on the ribs also achieved high heat transfer coefficients on the ribs but could not generate the necessary side wall heat transfer with the available coolant supply pressure. The reduced flow and smaller exposed coolant surface areas of the pedestal designs resulted in lower cooling effectiveness. Both pedestal designs provided similar heat transfer coefficients but could not adequately cool the trailing edge with the available coolant supply pressure.

5.1.3 Blade Leading Edge Study

Two competitive leading edge cooling concepts (Figure 5-12) suitable for advanced engines were evaluated for the high-pressure turbine blade design. Both were judged to require internal convective cooling supplemented by showerhead film cooling. The evaluation was made on the basis of cooling effectiveness, showerhead back flow margin, and the ability to tolerate local film hole plugging without catastrophic failure. Manufacturability was also considered. Both designs used showerhead film cooling, but one design relied on trip strip augmented channel flow for internal convective cooling while the other used impingement cooling for heat transfer augmentation.

The trip strip augmented convectively cooled design directs cooling air through a radial supply passage from which a portion of the flow passes through showerhead holes and film cools the leading edge. The remainder of the cooling airflow continues radially outward and is subsequently used to cool the blade tip. The impingement cooling design has one additional rib which divides the radial supply passage and the leading edge passage. Coolant flow is ejected through holes cast in this rib onto the leading edge surface to provide impingement cooling and is then ejected through the showerhead holes and additional "gill" holes to provide film cooling. For the impingement cooled leading edge design, tip cooling air must be supplied from separate midchord cooling passages.

Both designs met the operational requirements of the supersonic cruise aircraft engine high-pressure turbine. Coolant flow and heat transfer study results for both the "full-flowing" and the "plugged" showerhead holes are summarized in Table 5-II. These results show that the trip strip augmented channel design supplies about 0.2 percent more cooling airflow to the leading edge feed. However, the impingement design must supply an additional 0.4 percent flow from the midchord supply for tip cooling.

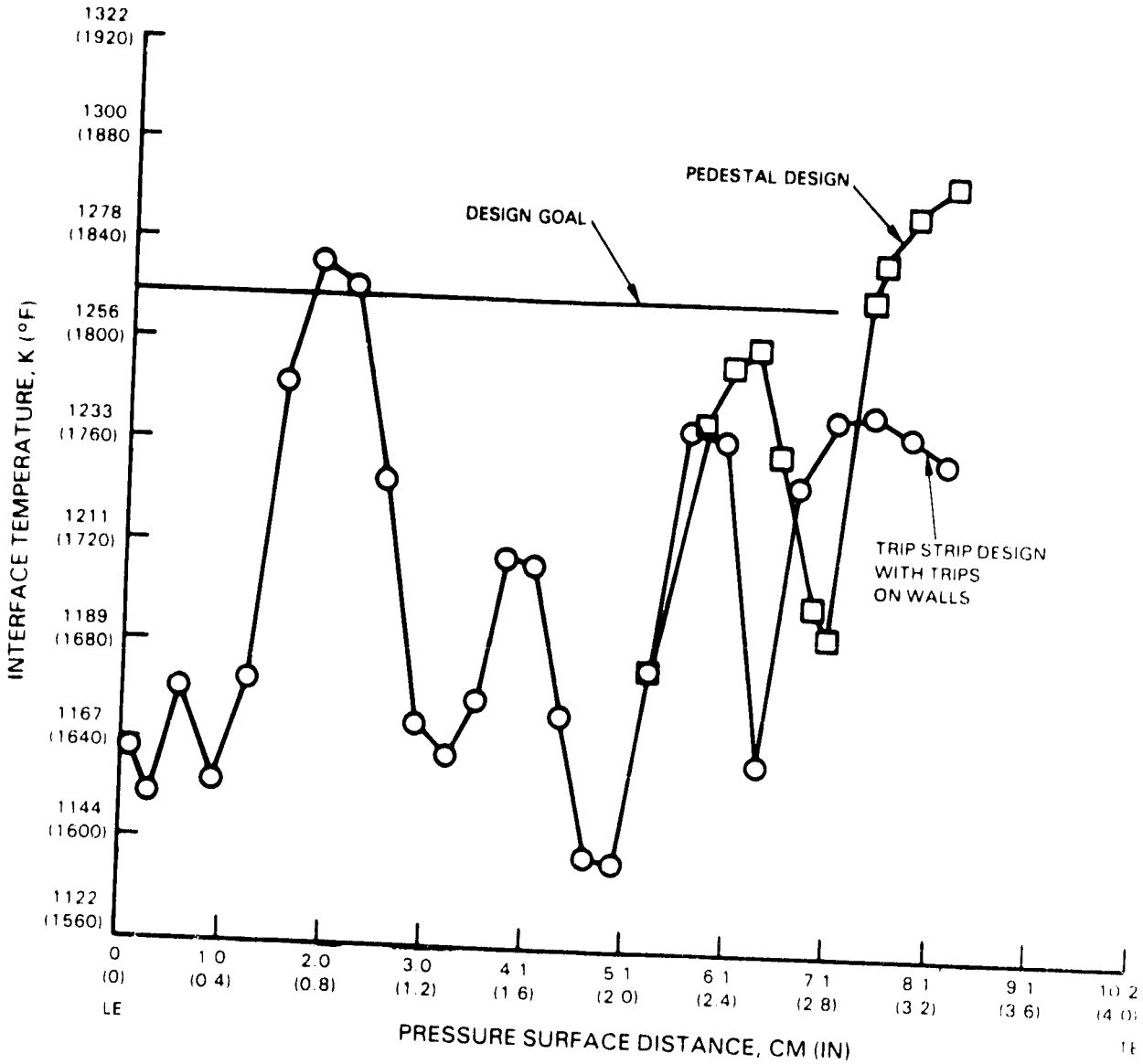

Figure 5-11 Vane Interface Temperature Distributions on Pressure Surface (1990 Technology)

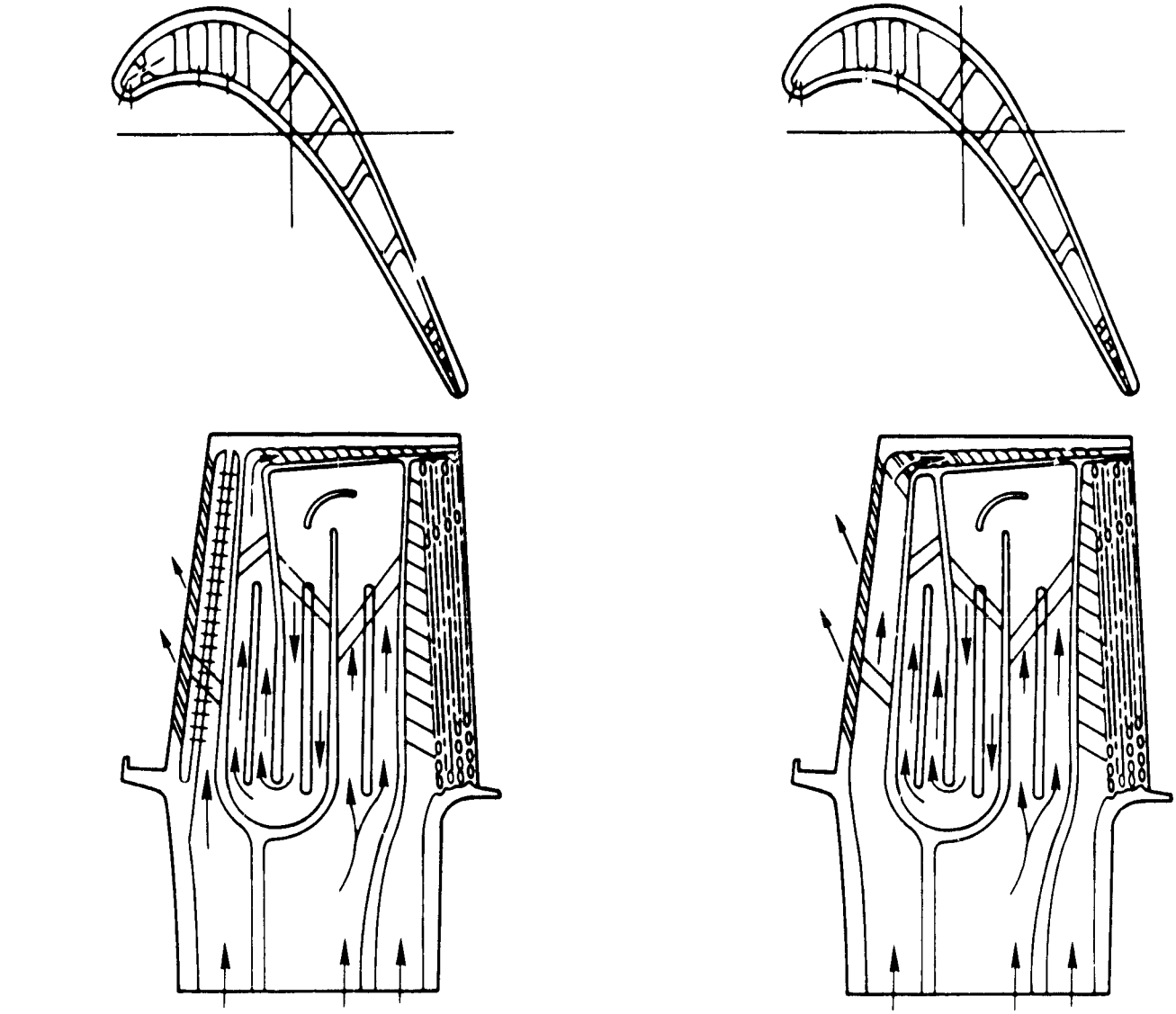

Figure 5-12 Blade Cooling Configurations

Both designs (Table 5-II) still provide more than two-thirds of the full-flowing convective heat transfer coefficient if the showerhead holes are completely plugged. Although local metal temperatures in both designs increase by more than 422 K (300°F) when complete showerhead plugging occurs, rapid failures will not follow as indicated by experience with current showerhead leading edge designs.

The trip strip augmented channel cooled leading edge design was chosen for the supersonic engine high-pressure turbine because of: 1) the slightly lower total coolant flow, 2) successful experience of this design in current engine applications, and 3) projected lower manufacturability risks.

TABLE 5-II

RESULTS OF AUGMENTED CHANNEL AND IMPINGEMENT COOLED SHOWERHEAD LEADING EDGE COMPARISON

	Channel	Impingement
Full Flowing Showerhead		
Coolant Supply (% of Compressor Discharge Pressure)	80%	80%
L. E. Feed Flow (% Wae)	1.41%	1.23%
L. E. Feed and Tip Flow (%Wae)	1.41%	1.63%
S/H Back Flow Margin (Location)	1.065 (90% Span)	1.065 (40% Span)
Tmax	1351 K (1972°F)	1361 K (1991°F)
Fully Plugged Showerhead		
Critical h_c (% of Full Flowing Case) (at critical location)	76% (50% span)	69% (50% span)
T_m max	+450 K (+350°F)	+430 K (+315°F)
Manufacturability		
Castability	Base	More difficult (smaller cores and very small holes)
Showerhead hole drilling	Base	More difficult (smaller target passage)

5.1.4 Thermal Barrier Coating with Film Cooling

Current advanced state-of-the-art airfoil cooling designs employ a combination of convective cooling with film or thermal barrier coating. In this study, the desirability of combining advanced film cooling with thermal barrier coating was considered. The results show that the use of film cooling in combination with thermal barrier coating minimizes the amount of cooling air required in the supersonic cruise aircraft application.

Airfoil cooling effectiveness and the interrelationship between film cooling, convective cooling and thermal barrier coating were investigated by treating the airfoil as a heat exchanger. Utilizing an idealized one-dimensional analysis of the airfoil (Figure 5-13), the overall cooling effectiveness (ϕ) is expressible in terms of film effectiveness (η_f), heat exchanger efficiency (η_c), and heat load parameter (β) as:

$$\phi = \frac{\eta_f + (\beta - \eta_f)_c}{1+(\beta - \eta_f)\eta_c}$$

This expression was utilized to assess the relative merits of one cooling design versus another and to assess the relative level of difficulty associated with a given cooling requirement. Shown in Figure 5-14 is effectiveness level (ϕ) versus heat load parameter (β) for a film effectiveness (η_f) equal to zero. It can be seen for the VSCE blade that:

1) The required average effectiveness of the VSCE blade is significantly higher than the present state-of-the-art turbine blade. The VSCE airfoil requires an average effectiveness of 0.71. Present state-of-the-art blades achieve effectiveness levels of only 0.56 for the most advanced design. Thus, the VSCE blade must achieve an effectiveness level 26 percent higher than present state-of-the-art blades.

2) The required effectiveness levels can be achieved in the VSCE blade using film cooling with flow levels less than that required for convective cooling designs having heat exchanger efficiencies equal to 1. If a convective effectiveness of 1 was attainable, the heat load parameter of the VSCE blade must increase 28 percent to attain the desired effectiveness with no film (as detailed in the following paragraphs). This would represent an increase of approximately 0.8 percent W_{ae} in cooling airflow. The VSCE blade achieves a convective effectiveness level of 0.81. At this level of convective effectiveness the heat load parameter must increase more than 50 percent. This would represent an increase of over 1.4 percent W_{ae} in cooling airflow.

3) From the above observations it is concluded that the VSCE blade must use film in order to achieve the required effectiveness with a minimum of cooling airflow.

• IDEALIZED AIRFOIL (THERMAL CONDUCTIVITY IS INFINITE)

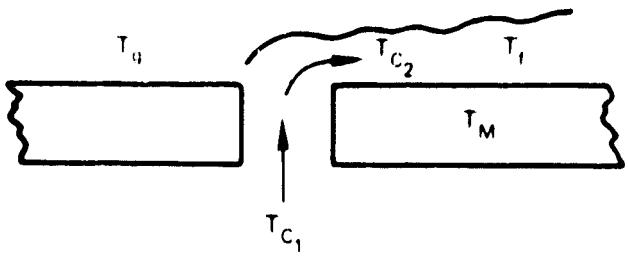

GOVERNING EQUATIONS

• OVERALL EFFECTIVENESS: $\phi = \dfrac{T_g - T_M}{- - T_{C_1}}$

• HEAT EXCHANGER EFFICIENCY: $\eta_C = \dfrac{T_{C_2} - T_{C_1}}{T_M - T_{C_1}}$

• FILM EFFECTIVENESS: $\eta_f = \dfrac{T_g - T_f}{T_g - T_{C_2}}$

• HEAT LOAD PARAMETER: $\beta = \dfrac{\dot{m} C_{P_C}}{h_f A_g} = \dfrac{T_f - T_M}{T_{C_2} - T_{C_1}}$

SOLVING FOR ϕ IN TERMS OF η_f, η_C, β:

$$\phi = \frac{\eta_f + (\beta - \eta_f)\,\eta_C}{1 + (\beta - \eta_f)\,\eta_C}$$

Figure 5-13 Airfoil Cooling Effectiveness One-Dimensional Analysis

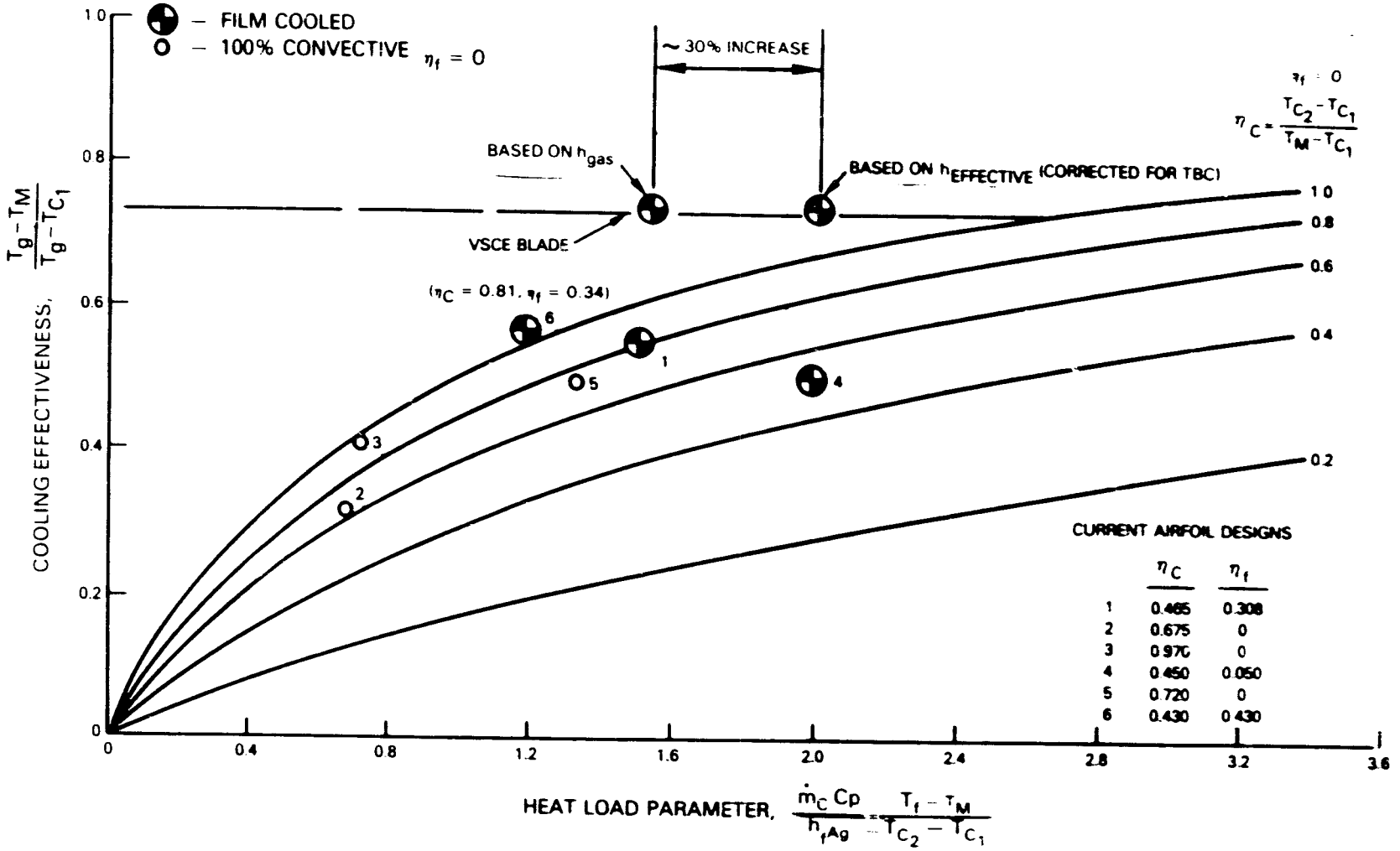

Figure 5-14 Airfoil Cooling Effectiveness Benefits Due to Thermal Barrier Coating

The above advantages of film cooling can be illustrated by looking at the VSCE first stage blade cooling requirements. The VSCE first stage blade cooling requires an effectiveness level of 0.71 to achieve its design creep life. The coolant flow required to achieve this effectiveness is a function of the airfoil heat exchange efficiency and average film effectiveness. This is shown in Figure 5-15, where cooling airflow level is indicated by the heat load parameter (β). If film cooling were completely eliminated ($\eta_f = 0$), and the heat exchange efficiency of unity were achievable, the 100 percent convectively cooled blade would still require 28 percent more cooling airflow than the combined convective and film cooled design.

The utilization of thermal barrier coating serves to effectively reduce the external heat load to the airfoil and, therefore, increase the heat load parameter (β) for a given level of cooling flow:

$$h_{effective} = \frac{1}{\frac{1}{h_g} + \frac{t_{TBC}}{K_{TBC}}}$$

$$\beta = \frac{\dot{m}_c C_p}{h_{effective} A_g}$$

where h_g = gas side heat transfer coefficient

t_{TBC} = thermal barrier thickness

K_{TBC} = thermal barrier conductivity

A_g = gas side convection area

C_p = specific heat of cooling air

$\dot{m}_c$ = cooling air mass flow

The reduction in the external heat load or increase in heat load parameter is independent of the use of film cooling and depends only on the initial heat transfer coefficient and the properties of the thermal barrier coating. The benefits of the thermal barrier coating to the VSCE airfoils are graphically shown in Figure 5-14, where the blade heat load parameters are plotted with and without thermal barrier coating. It is seen that the thermal barrier coating effectively increases the heat load by 30 percent at constant coolant flow.

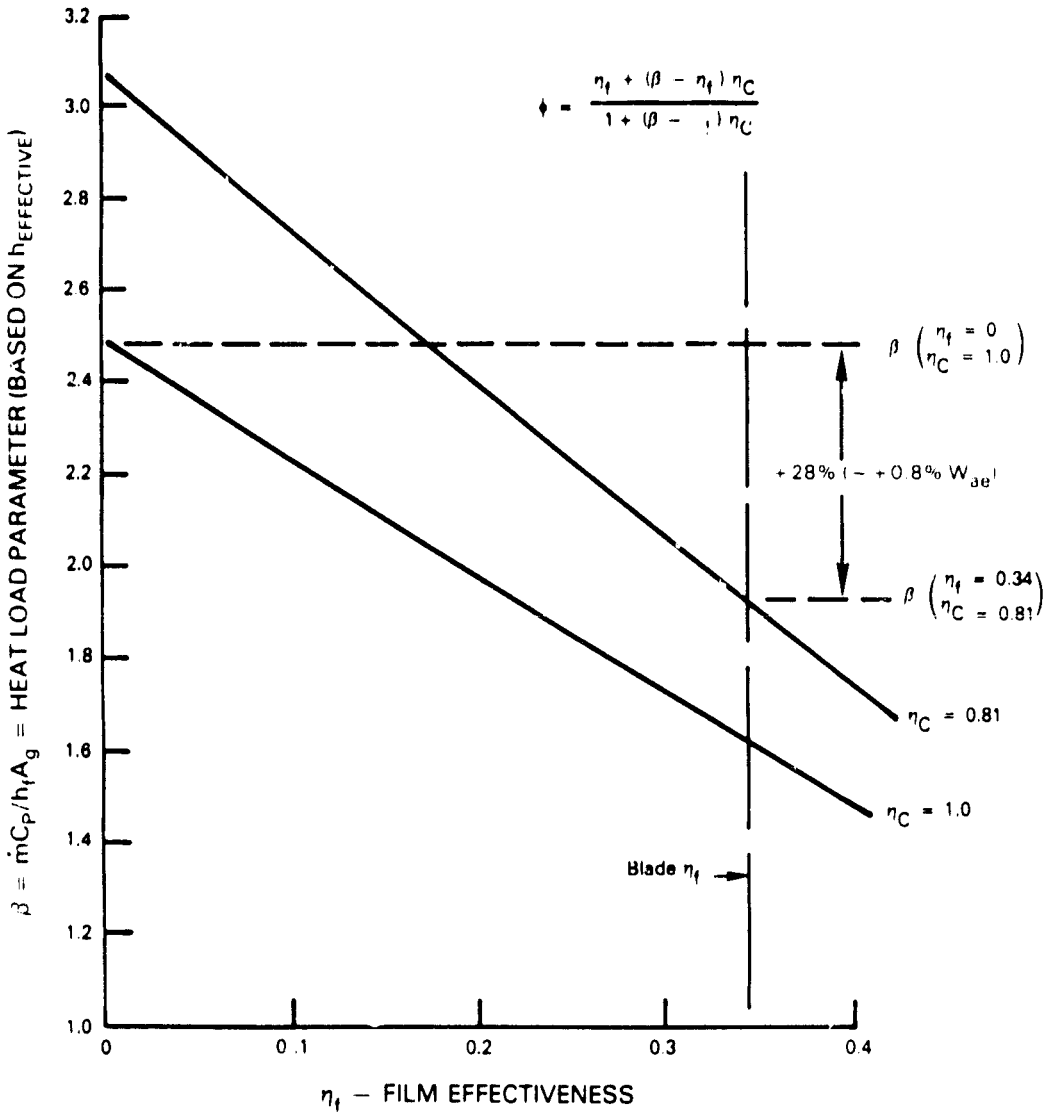

Figure 5-15 Heat Load Parameter vs Film Effectiveness; Blade $\phi = 0.713$, $\eta_f = 0.34$

Increasing airfoil heat exchanger efficiencies as a means of reducing cooling airflow becomes increasingly more difficult as the heat exchanger efficiency approaches unity. Heat exchanger efficiency is given by the expression below and shown in Figure 5-16.

$$\eta_c = \frac{Tc_{out} - Tc_{in}}{T_{metal} - Tc_{in}} = 1 - \exp - \frac{h_c A_c}{\dot{m} C_{pc}}$$

where h_c = cooling side heat transfer coefficient

In the case of the VSCE first stage blade with a heat exchanger efficiency of 0.81, a 10 percent increase in heat exchanger efficiency would require a 32 percent increase in h_c, and a 14 percent increase in heat exchanger efficiency (to 95 percent) would require a 76 percent increase in h_c when compared to the base VSCE design case. Considering the level of effort which would be required to achieve these higher efficiencies and the relatively small decrease in the resulting coolant flow, it does not seem reasonable to pursue further increases in internal cooling complexity. The pursuit of more internal cooling complexity becomes even less attractive when the effects of higher required supply pressure are included in the analysis.

5.1.5 Low Heat Load Design

Historically, the design of airfoils for high-pressure turbines was primarily conducted according to aerodynamic criteria to optimize performance. External heat loads were calculated for aerodynamically optimized airfoils and, subsequently, cooling air requirements were estimated to achieve the goal in metal temperatures occasionally at the cost of compromises to aerodynamic design.

The initial design of the high-pressure turbine for the supersonic cruise aircraft was conducted by utilizing the airfoil design system which optimized aerodynamic performance. A study was next conducted under the present contract to establish whether the mean section of the rotor and the stator airfoils could be redesigned to reduce heat loads without compromising the aerodynamic performance. A two-dimensional potential flow solver and a differential boundary layer code with a new turbulence model were utilized in the design optimization study. This code, developed at Pratt & Whitney, gives reliable predictions of both momentum and thermal boundary layers on a wide range of turbine airfoil designs and makes possible optimization of turbine airfoils for both aerodynamic and heat load considerations.

Attempts to reduce the heat load on the vane were not successful without compromising the aerodynamic performance. The mean section of the blade was then redesigned by reducing the curvature on the airfoil pressure side. The redesigned blade cross section is compared to the original in Figure 5-17. Comparison of the obtained airfoil pressure distribution is very similar (Figure 5-18). The profile losses calculated for the redesigned airfoils are

DOTTED LINES SHOW LIMITED POTENTIAL FROM CONVECTION COOLING

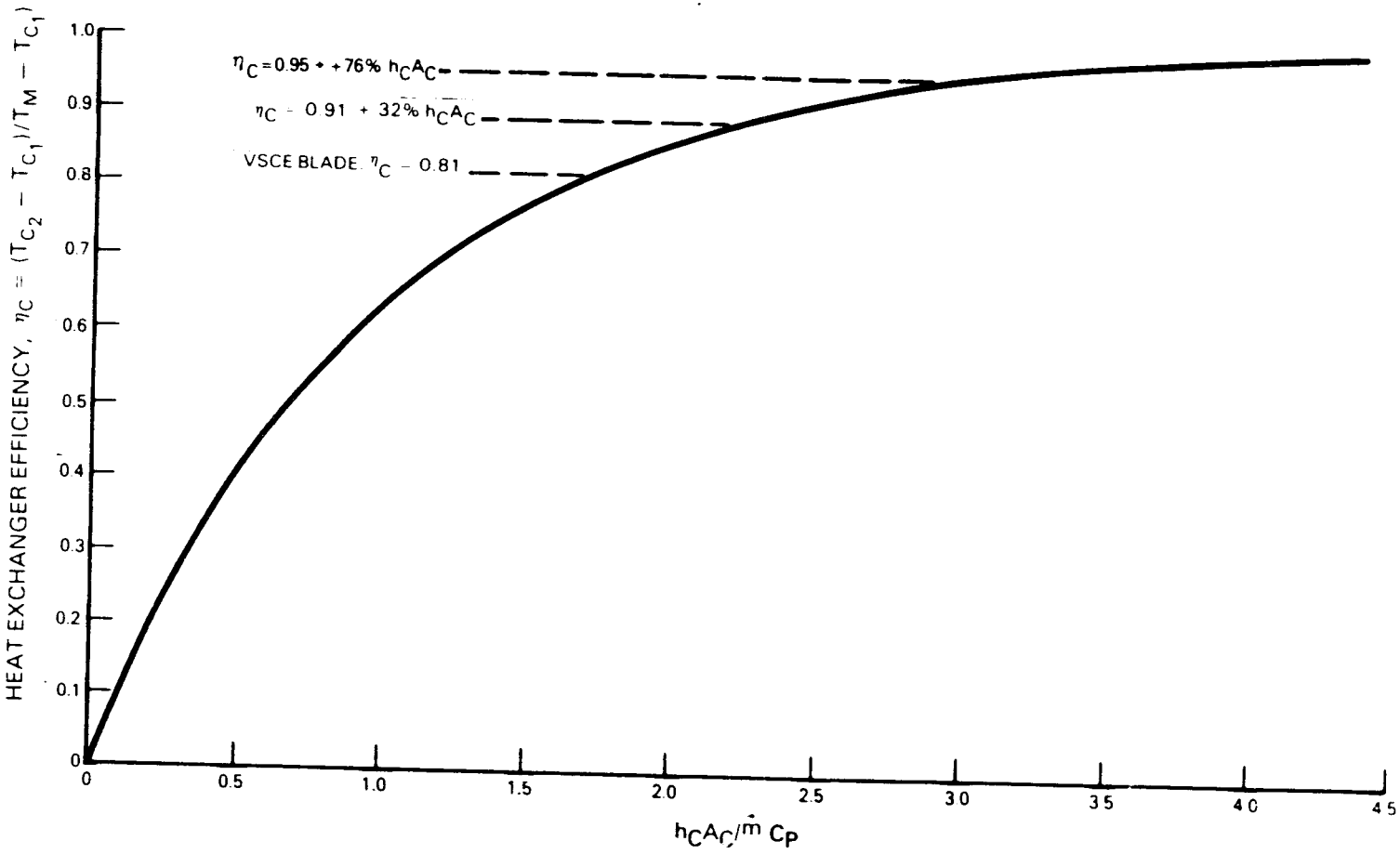

Figure 5-16 Heat Exchanger Efficiency vs Heat Load Parameter (h_C A_C/m C_P)

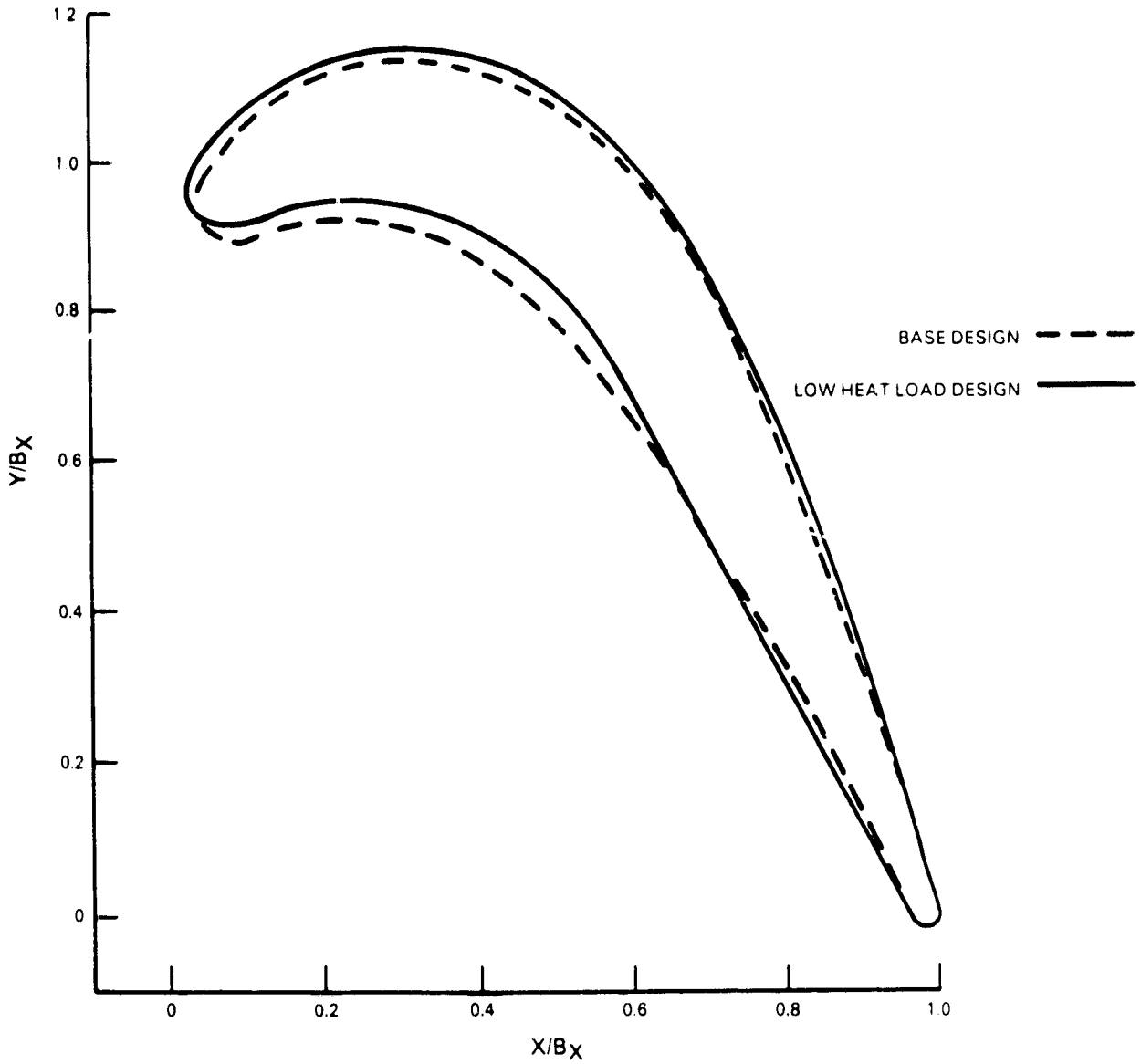

Figure 5-17 Blade Geometry for Low Heat Load Design

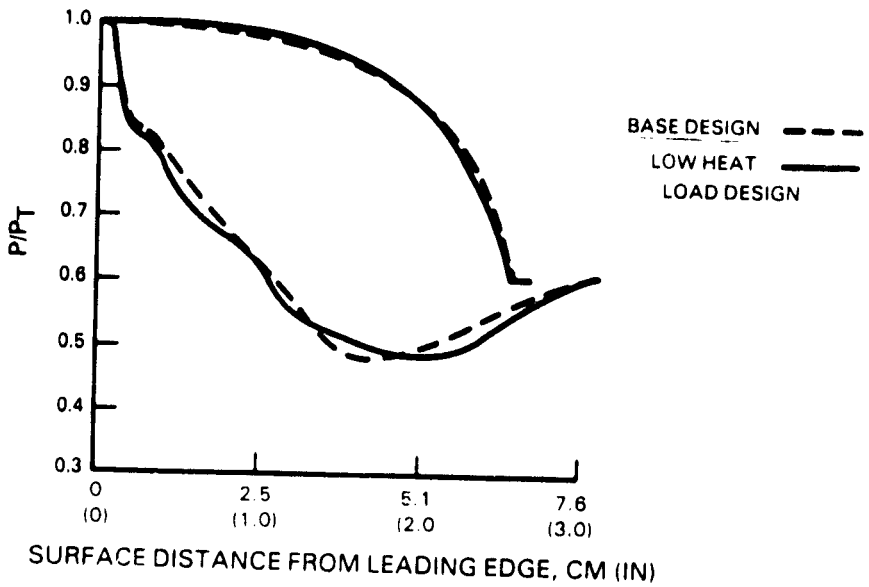

Figure 5-18 Blade Loading for Low Heat Load Design

the same as calculated for the base airfoil indicating that the optimized heat load airfoil has retained the aerodynamic performance of the base design. The redesigned airfoil has lower curvature on the airfoil pressure surface in the trailing edge region.

External heat load to the pressure surface of the blade has been reduced to reflect aerodynamic tailoring near the trailing edge. Analysis indicates that external heat load to an airfoil pressure wall can be lowered by reducing the curvature near the trailing edge. Boundary layer analysis of the VSCE blade predicts nearly a 50 percent reduction in external heat transfer coefficient near the trailing edge (Figure 5-18) for airfoil contour tailoring as shown in Figure 5-19. The level of heat load reduction is based on a surface roughness of approximately 50 to 70 microns. This roughness level should be achievable with polished thermal barrier coating, and data obtained from commercial application indicate that it will be sustainable during operation. Increased roughness levels will only lessen, but do not eliminate the heat load reduction benefit. Cascade tests will be required to verify the actual level of benefit and the sensitivity to contour shape and roughness changes.

Predicted heat transfer coefficients and the metal temperatures for the pressure surfaces of the base and the redesigned airfoils are also shown in Figure 5-19 as a function of surface distances. Reductions in heat load and metal temperature distribution for the redesigned blade were obtained for over 40 percent of the length in the trailing edge regions.

Predicted metal temperatures (Figure 5-20) for the redesigned airfoil are lower than the base design by as much as 340 K (120°F) in the critical trailing edge region of the airfoil. Experience at Pratt & Whitney has indicated that the trailing edge region on the rotor airfoils may have maximum thermal distress problems. The reduction in heat load results in lower metal temperature in this region and allows reduction of coolant flow.

The heat load distribution on the suction surface of the base and the redesigned airfoils was found to be similar and, therefore, not shown in this report.

5.2 Preliminary Design

This section describes the preliminary designs of the high-pressure turbine vane and blade, making use of the aerodynamic design results, configurational studies, and technology assumed to be available for the VSCE in the time period when the VSCE will be in use. The term "preliminary design" in the context of this report refers to complete cooling design definition at the airfoil midspan section, including all necessary iterations and detailed temperature analysis usually included in the final design. However, not included are design iterations which do not affect cooling, detailed manufacturing tolerance definitions, inspection and acceptance criteria, final detailed dimensional drawings, and cost considerations.

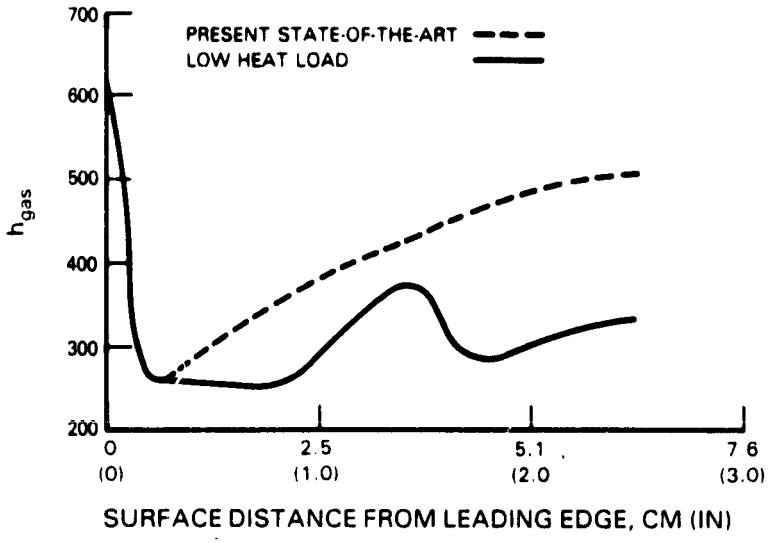

Figure 5-19 Heat Transfer Reduction on Pressure Surface for Low Heat Load Design

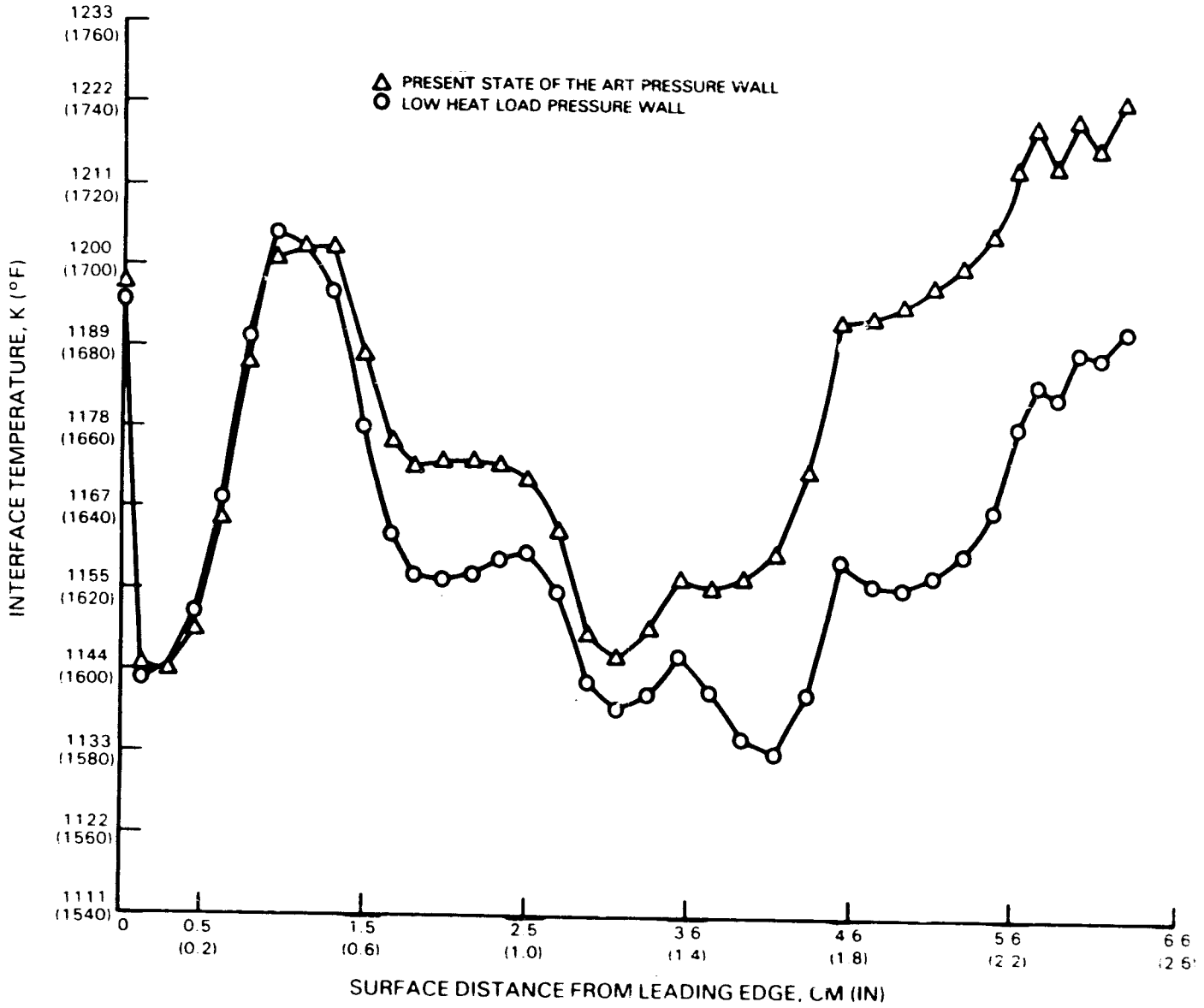

Figure 5-20 Blade Interface Temperature Pressure Wall

Two preliminary designs are provided for both the vane and blade for subsequent technology benefits evaluation: one uses technology assumed to be available in the 1990 time period and the other limited to technology assumed to be available in 1986. These technology projections and detailed design criteria used for the durability design are summarized in Sections 5.2.1 and 5.2.2. Design details and analysis results are presented in Sections 5.2.3 and 5.2 4.

5.2.1 Technology Projections and Design Features

The following component and materials technology was assumed to be available for the supersonic cruise aircraft engine and was used in the durability design. Materials technology predictions for 1986 and 1990 are shown in Table 5-III.

- Advanced combustor design with 1.25 gas temperature pattern factor and 1.10 profile factor (1990) and 1.12 profile factor (1986) at combustor exit.
- Advanced single crystal materials that are 370 K (175°F) and 356 K (150°F) better than that used for the Energy Efficient Engine vane and blade, respectively.
- Advanced casting methods to provide 0.043 cm (0.017 in) nominal thickness walls around 0.043 cm (0.017 in) thick core; trip strips skewed 45° relative to coolant flow direction; and high density ribs and pedestals in vane and blade trailing edges.
- Conical shaped showerhead film cooling holes.
- Advanced thermal barrier coatings for the 1990 airfoils; zirconia based thermal barrier coatings for the 1986 airfoils.
- Diffuser shaped film cooling holes through the thermal barrier coating.
- Advanced oxidation resistant metallic coatings.
- Blade root stress to be 20 percent higher than that used in the Energy Efficient Engine high-pressure turbine blade design.
- Advanced disk materials with a 301 K (50°F) higher temperature capability than the current state-of-the-art materials.

TABLE 5-III

VSCE MATERIALS PROJECTIONS

1986 Tecnnology

First Vane	First Blade
Vane Material: SC1000 (single crystal) Metallic Coating: PWA 286, 0.012 cm (0.005 in) thick	Blade Material: SC3000 (single crystal) Metallic Coating: PWA 286, 0.012 cm (0.005 in) thick
Thermal Barrier Coating (Yttria Stabilized Zirconia) 0.025 cm (0.010 in) thick	
+329 K (+100°F) Interface Temperature Relative to 264/276/PWA647	+301 K (+50°F) oxidation +329 K (+100°F) Creep Strength Relative to PWA 1480

1990 Technology

First Vane	First Blade
Vane Material: SC1000 (single crystal)	Blade Material: SC3000 (single crystal)
Metallic Coating: PS200, 0.012 cm (0.005 in) thick	Metallic Coating: PS200, 0.012 cm (0.005 in) thick
Thermal Barrier Coating (No Zirconia-Somewhat Opaque) 0.038 cm (0.015 in) thick	Thermal Barrier Coating (No Zirconia-Somewhat Opaque) 0.025 cm (0.010 in) thick
+367 K (+170°F) Interface Temperature Relative to 264/276/PWA647	+340 K (+120°F) Interface Temp. Relative to 264/276/PWA647 +329 K (+100°F) Creep Strength Relative to PWA 1480

5.2.2 Design Criteria

The vane and blade cooling levels were set to achieve 10,000 hours operating life in the predicted failure modes of creep, oxidation and thermal cracking. Limiting criteria were considered to be: 2 percent local creep or thermal fatigue cracking of the base metal, loss of metallic coating with 0.012 cm (0.005 in) penetration of base metal, and/or spalling of thermal barrier coating.

The design gas temperature profiles for the vane and blade are shown in Figure 5-21, based on a 1.25 pattern factor (ΔTVR) for the hot spot vane and a 1.10 profile factor for the blade. These temperature profiles reflected expected 1990 combustor technology. The 1986 airfoils were designed to the same pattern factor but with a 1.12 profile factor for the blade, which is representative of the expected 1986 combustor technology. Temperature profiles for the 1986 design shown in Figure 5-22 include the effect of an additional 3.2 percent W_{ae} cooling airflow to account for the reduced technology level in the 1986 engine.

Both Figure 5-21 and 5-22 temperatures reflect nominal engine performance plus design increments explained in Section 5.3.

5.2.3 Mission Life Analysis

Mission life analysis combines mission operational variables and hot section life models in order to predict turbine vane and blade life. The operating variables must include a mission definition, applicable engine ratings, engine performance, ambient environment conditions and deterioration due to tolerances or wear. Life limiting modes applicable to the VSCE hot section were creep and coating oxidation and spalling, based on the temperature and stress conditions determined in Sections 5.2.3 and 5.2.4.

Initial performance levels for the VSCE were assumed to be represented by the performance of the Study Turbofan engine in Reference 1. The corresponding nominal temperatures and rotor speeds applicable to the selected mission (Section 3.2) are summarized in Table 5-IV. The temperatures and speeds seen in a turbine during actual service and subsequently the design temperature levels are higher than reflected by nominal performance. Temperature levels increase relative to nominal performance due to the effects of installation, deterioration during operation between overhauls, and nonrecoverable overhaul losses in the case of a mature engine. Consistent with subsonic commercial design practices increments have been added to the nominal VSCE performance as shown graphically in Figure 5-23 and summarized in Table 5-V. To determine performance for an installed, previously overhauled (mature) engine typical of commercial supersonic operation, increments for installation, nonrecoverable overhaul and deterioration must be applied to the nominal temperatures and speeds as graphically shown in Figure 5-23. Table 5-V summarizes all such increments at the limiting supersonic cruise operating condition, based on present JT9D commercial engine experience, scaled to reflect the supersonic flight time where applicable. In addition, an increment was included to account for performance loss due to vane and blade cooling airflow increase over the reference engine estimates. Cooling flow increases would thermally reduce the temperatures through the turbine before work could be extracted with a resultant loss in thrust. In order to maintain thrust with increased cooling airflows, the combustor exit temperature must be increased. This increase was taken prior to design in order to more realistically account for the temperature levels expected in actual operation. The increase was 5.2 percent for the 1990 engine and affected both combustor exit and rotor inlet temperature. The resulting temperature profiles for 1990 and 1986 technologies are shown in Figures 5-21 and 5-22.

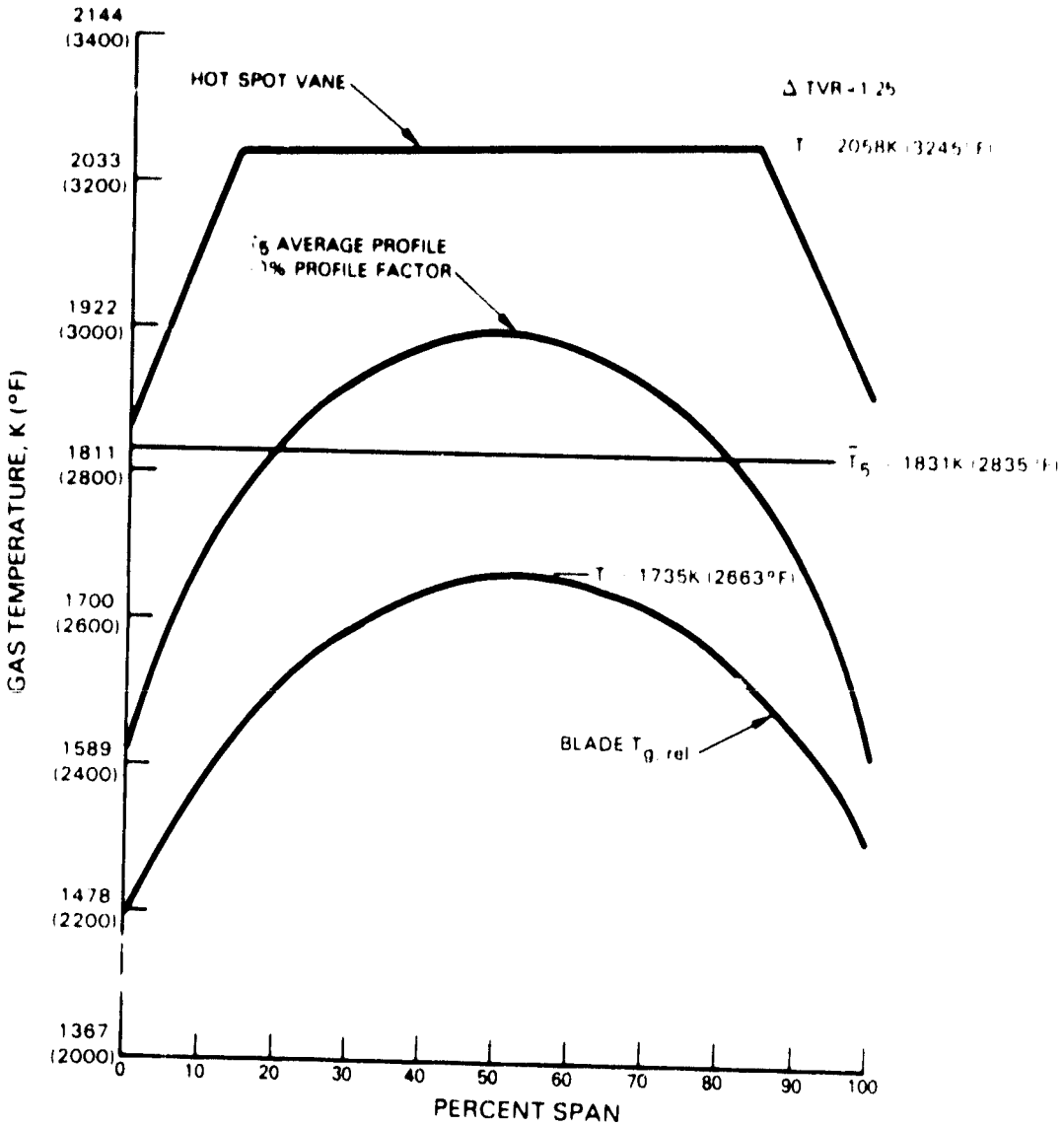

Figure 5-21 Design Gas Temperature Profile = 1990 Technology

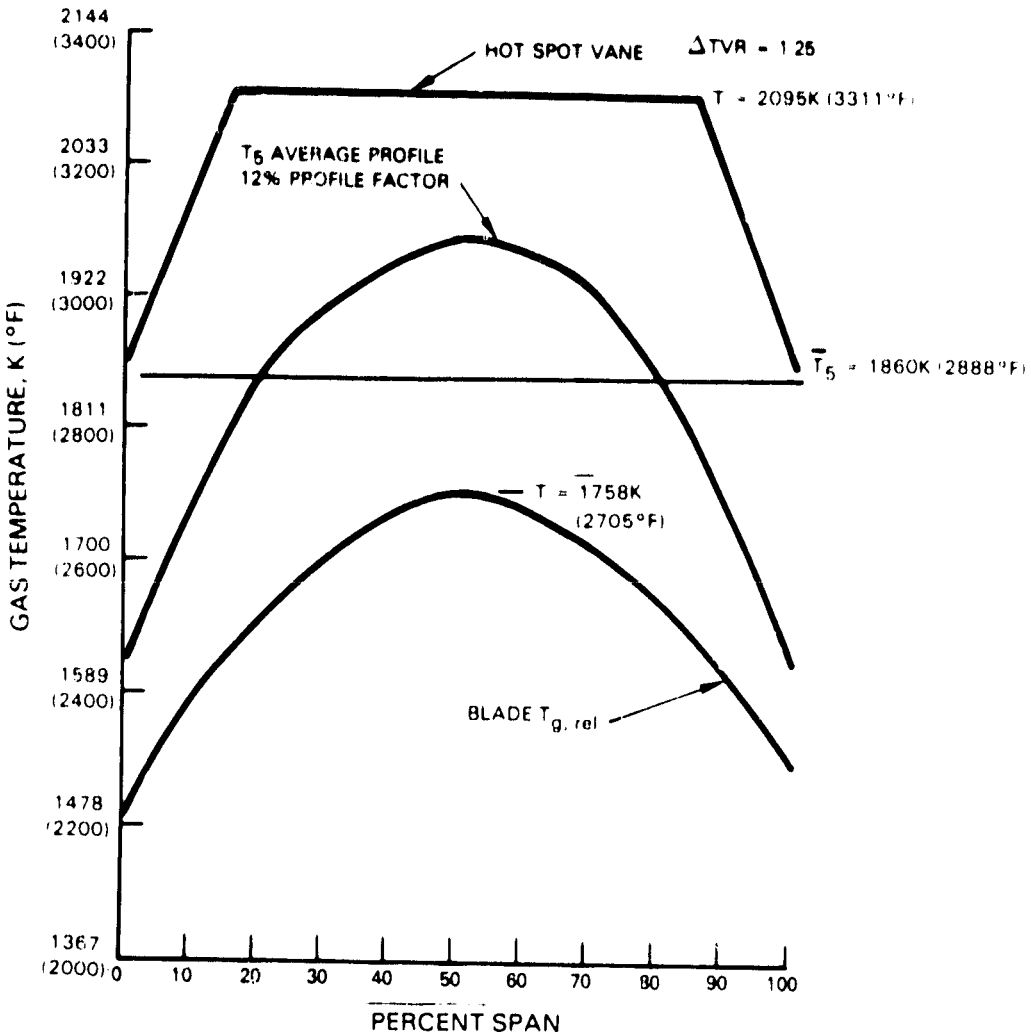

Figure 5-22 Design Gas Temperature Profile - 1986 Technology

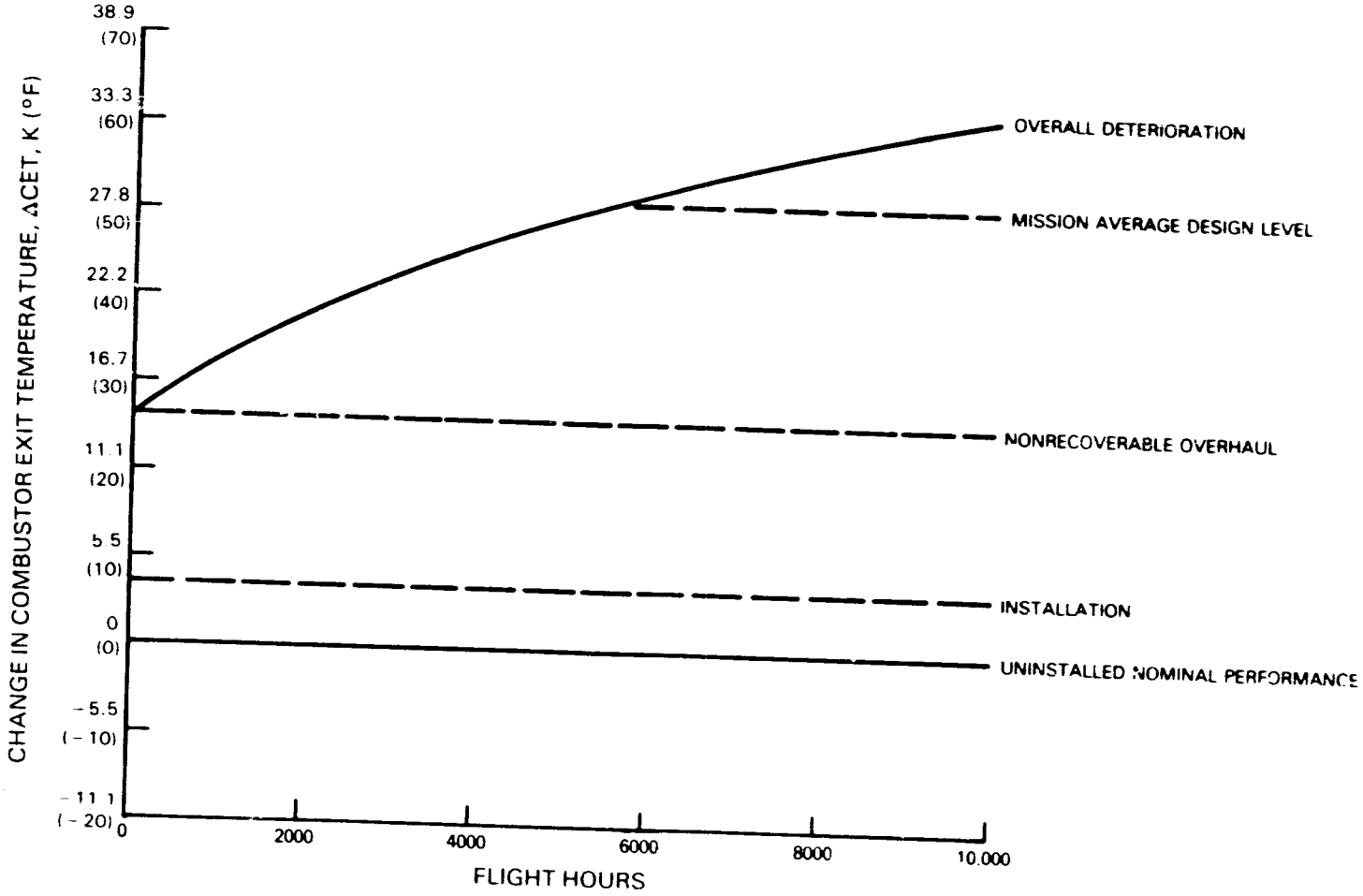

Figure 5-23 Mission Performance Increments

TABLE 5-IV

SUPERSONIC CRUISE AIRCRAFT ENGINE
MISSION LIFE DESIGN PARAMETERS

Flight Segment	Time (min)	T4(1) K (°F)	T5 K (°F)	N2 (RPM)
Taxi (Idle)	10.0	---	---	---
Takeoff	0.7	800 (980)	1483 (2210)	9482
Subsonic Climb	17.4	625 (665)	1376 (2017)	8712
Subsonic Cruise	18.5	603 (626)	1253 (1796)	8235
Supersonic Climb	14.7	719 (835)	1580 (2385)	9435
Supersonic Cruise(2)	99.7	915 (1187)	1754 (2698)	10075
Decent and Approach	24.6	---	---	---
Taxi (Idle)	5.0	---	---	---

Total Block Time = 190.6 minutes
Total Flight Time = 175.6 minutes

DESIGN REQUIREMENT

(1) Temperatures are for a nominal base engine on hot days.

(2) Design Point - Temperatures are not representative of actual design levels.

TABLE 5-V

VSCE DESIGN POINT PERFORMANCE
SUPERSONIC CRUISE

	Study Turbofan Nominal(1)	Installation	Nonrecoverable Overhaul	Average Deterioration	Cooling Air (2)	Design Level
High-Pressure Compressor Exit Temperature K (°F)	915 (1187)	+1.11 (+2)	+1.67 (+3)	+1.67 (+3)	0	919 (1195)
Burner Exit Temperature K (°F)	1754 (2698)	+3.89 (+7)	+10.56 (+19)	+13.89 (+25)	+47.78 (+86)	2130 (2835)
High Rotor Speed - RPM	10075	+7	+28	+36	---	10146

(1) STF515B nominal performance

(2) Temperature increase due to increased cooling flow relative to initial performance table (IV 1.9% to 6%, IB 2.5% to 3.6%)

The existing Pratt & Whitney (P&W) mission analysis data base, reflecting International Standard Atmosphere definition, was used to describe ambient temperature distributions expected for the VSCE. However, since the 16,154 m (53,000 ft) cruise altitude for the supersonic mission exceeds limits of the P&W data base, some extrapolation was necessary. The probable ambient temperature distribution for the 16,154 m (53,000 ft) cruise altitude is shown in Figure 5-24. The average ambient temperature at this altitude is shown to be 216.5 K (-69.7°F) and one standard deviation equal to 8.2°C (14.76°F). The engine was assumed to be flat rated in thrust up to a standard day plus +8 K (14.4°F). The combustor exit temperature response to ambient temperature variation is shown in Figure 5-25.

Airfoil lives were calculated for the vane and blade designs. The limiting damage modes are coating oxidation and/or spalling for both the vane and blade, and creep for the blade. Figure 5-26 shows the predicted limiting lives of the vane as functions of metal temperature for the 1986 and 1990 engines. The metal temperature represents what can be expected in a typical installed, average deteriorated engine in hot day (+8 K, +14.4°F) at supersonic cruise conditions. Figure 5-27 shows the predicted blade creep life as a function of design average metal temperature.

A breakdown of damage due to various flight conditions of the mission (Table 5-VI) shows that cruise is the most severe condition as expected.

TABLE 5-VI

BREAKDOWN OF BLADE AND VANE DAMAGE
AT VARIOUS OPERATING CONDITIONS

	Takeoff (%)	Climb (%)	Cruise (%)
Creep (Blade)	0	0	100
Oxidation (Blade and Vane)	0	1	99

5.2.4 Vane Durability Design

Both the 1986 and 1990 vane cooling designs utilize advanced single crystal material and thermal barrier coatings in order to meet the design life requirements with a minimum amount of cooling airflow. The cooling configurations incorporate two cavities in order to optimize the distribution of cooling airflow and to maintain acceptable levels of bulging stress.

The leading edge cavity cooling is achieved by using impingement and external surface film. Cooling air is fed into the leading edge cavity from both the inside and outside diameters, impinged on the inner wall via an impingement tube, and then vented through the walls as external film obtaining a showerhead pressure ratio equal to 1.02 to prevent backflow. The pressures

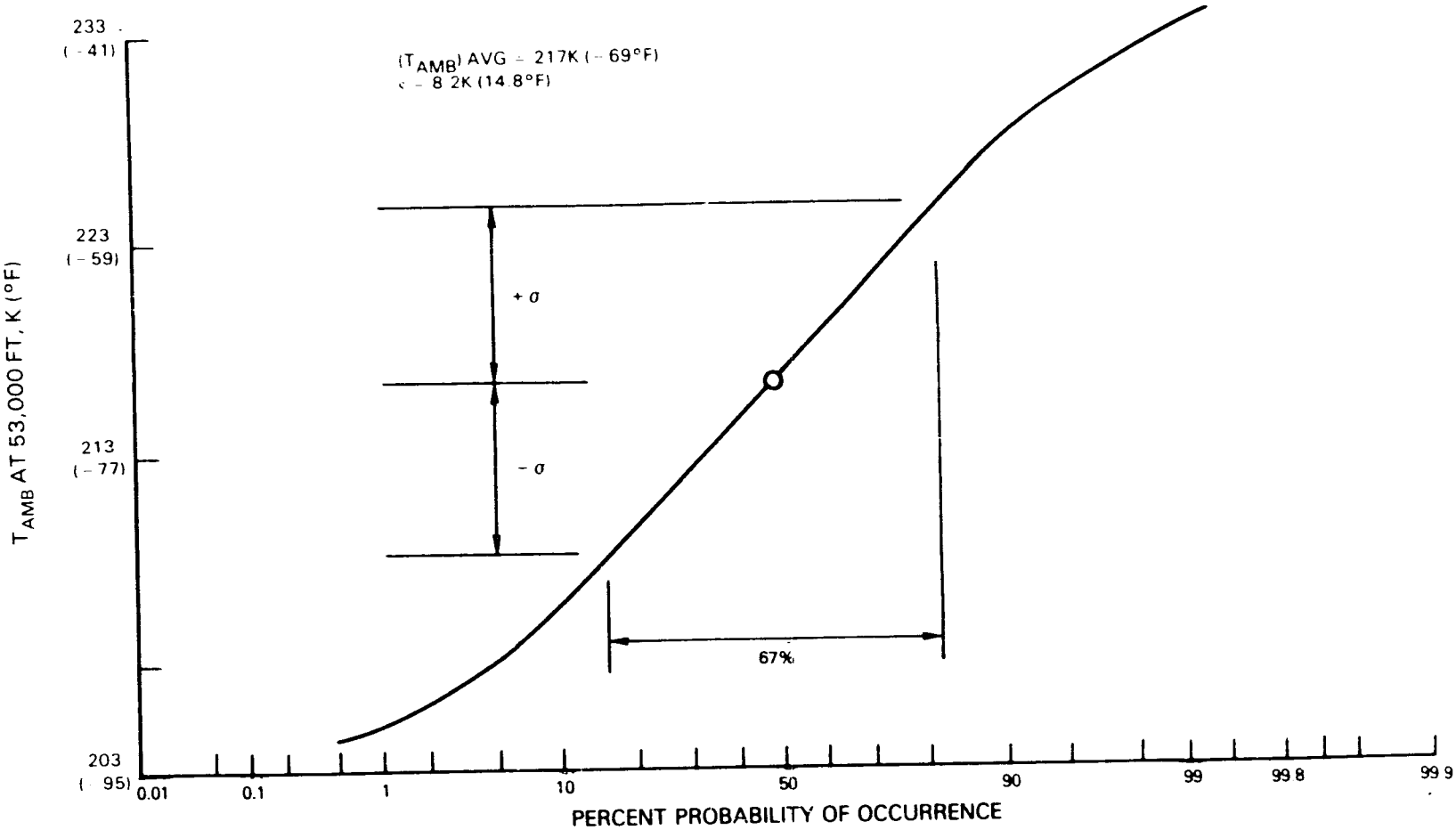

Figure 5-24 Ambient Temperature Probability Distribution at 16,154 m (53,000 ft)

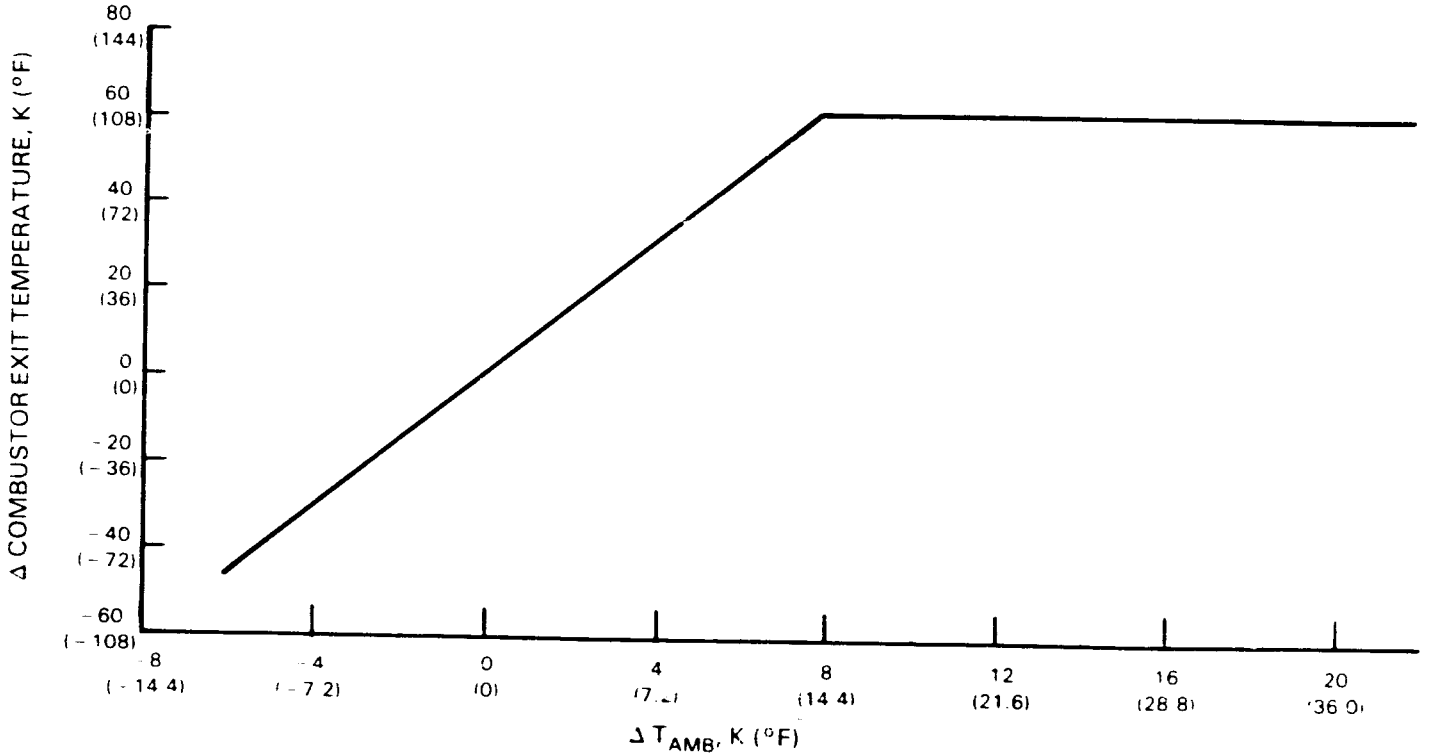

Figure 5-25 Variation of Combustor Exit Temperature as a Function of Variation of the Ambient Temperature

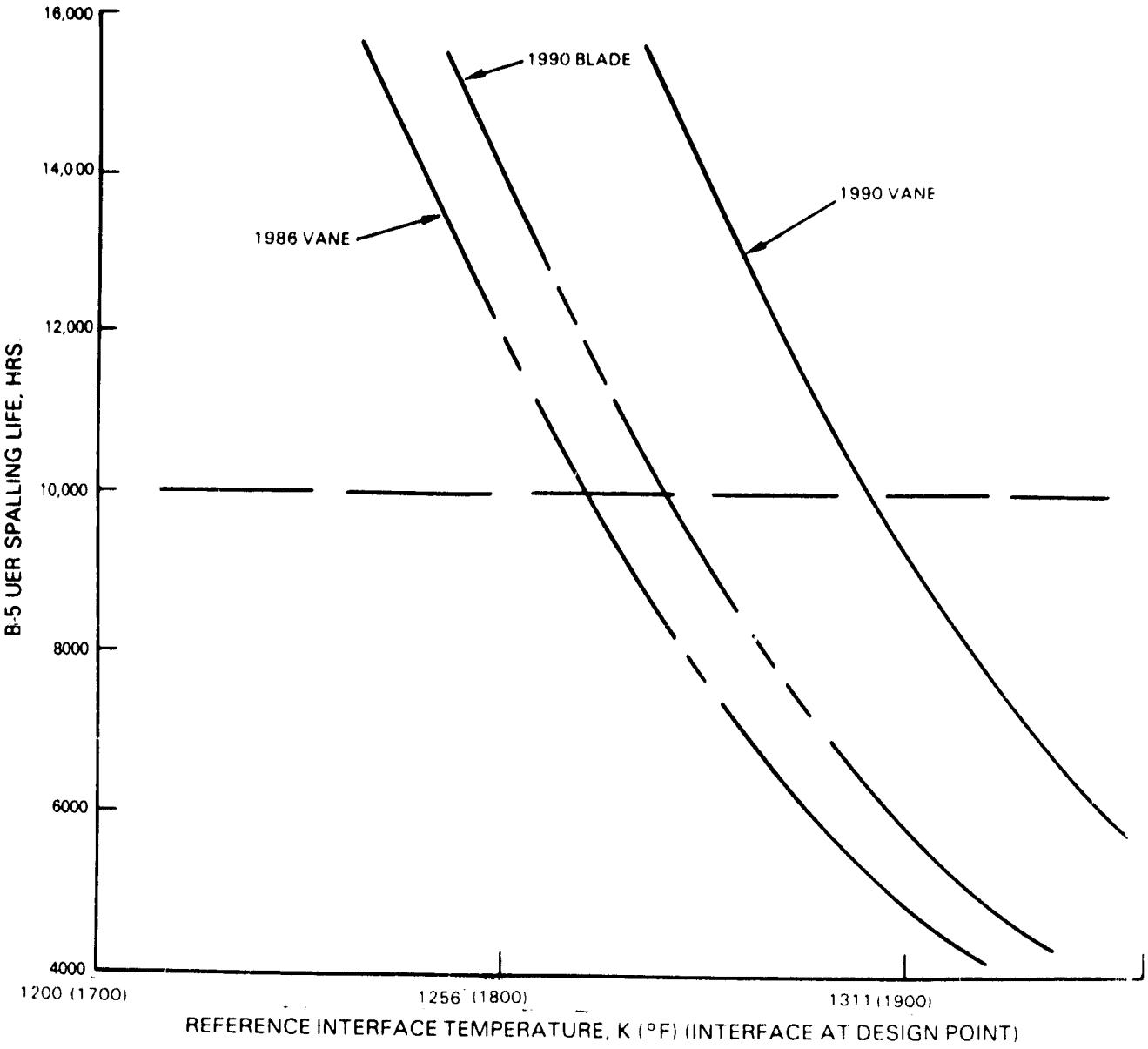

Figure 5-26 Turbine Vane Thermal Barrier Coating Spalling Life vs Design Metal Temperature

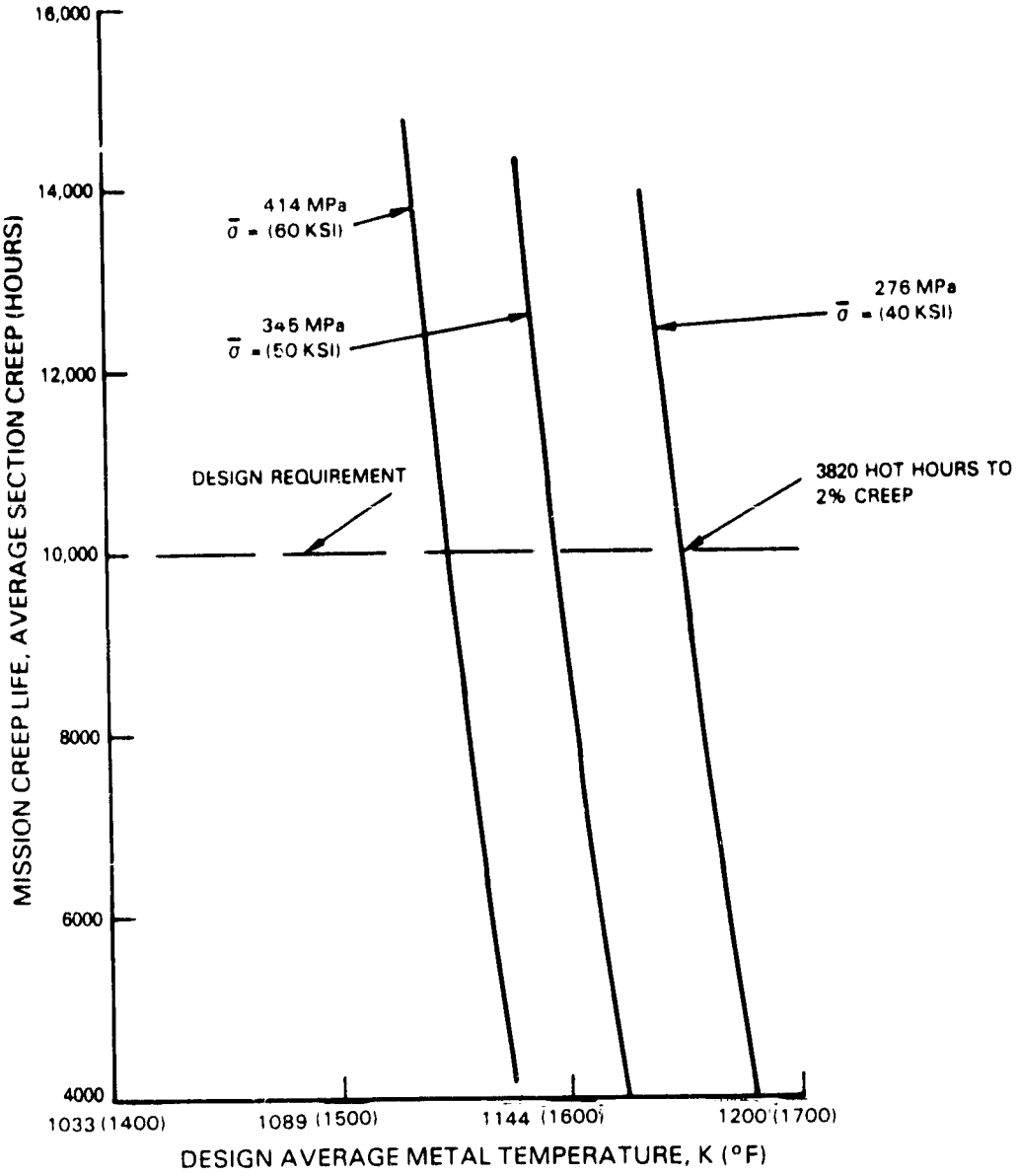

Figure 5-27 Turbine Blade Mission Creep Life vs Average Design Temperature

outside the impingement tube are balanced so that internal dams are not required to distribute the flow. This design configuration produces a much more reliable cooling than configurations relying on internal flow dams to maintain separate cooling regions. Experience with previous vane designs has shown that casting tolerances and impingement tube tolerances combined to result in leakage around the internal flow dams. The internal leakages create cooling maldistribution followed by burning or cracking of the airfoil.

Midchord and trailing edge cooling is achieved by using a tubeless configuration with flow in the midchord region passing radially from the outside to the inside diameters, and then flow chordwise through the multiple channel passages as shown in Figure 5-28. Cooling in both the midchord and the trailing edge regions is augmented with internal flow turbulators and film. A tubeless midchord and trailing edge configuration is utilized because it is anticipated that a three-dimensional aerodynamic airfoil design with bowing and leaning of the airfoil will be used. This would make insertion of a tube into the trailing edge cavity extremely difficult if not impossible. The midchord cavity is tapered as depicted in Figure 5-28 to maintain high internal heat transfer coefficients as flow is bled off in going from the outside to the inside diameter. The degree of taper will be determined during final design of the vane when multiple sections will be analyzed in detail.

The trailing edge chordwise passages contain 0.025 cm (0.010 in) trip strips skewed 45 degrees to the cooling airflow as shown in Figure 5-29. Trip strips are carried as far into the trailing edge as possible until a minimum core thickness (flow channel height minus trip strip height) of 0.050 cm (0.020 in) is reached. This minimum core thickness with trip strips is judged to be near the limit of acceptable castability. Additionally, extending the trips further downstream would serve to significantly increase the pressure losses, thereby reducing the flow capability of the trailing edge.

The uncoated trailing edge diameter is 0.129 cm (0.051 in), consistent with the expected technology levels of 1986 and 1990. The VSCE high-pressure turbine has relatively low levels of aerodynamic trailing edge blockage due to its large size and reduced number of airfoils.

1990 Technology Vane Design

The 1990 technology vane design incorporates an advanced non-zirconia thermal barrier coating and shaped film holes in addition to the features common to both levels of technology. A non-zirconia thermal barrier coating, being somewhat opaque to oxygen, allows a higher design temperature for interface spalling criteria than a current state-of-the-art zirconia based coating.

Additionally, the 1990 coating technology will allow a 0.038 cm (0.015 in) thick coating which is 0.012 cm (0.005 in) thicker than current (1986) state-of-the-art technology. Shaped film holes through thermal barrier coating are assumed to be technically feasible by 1990 and are incorporated into the design.

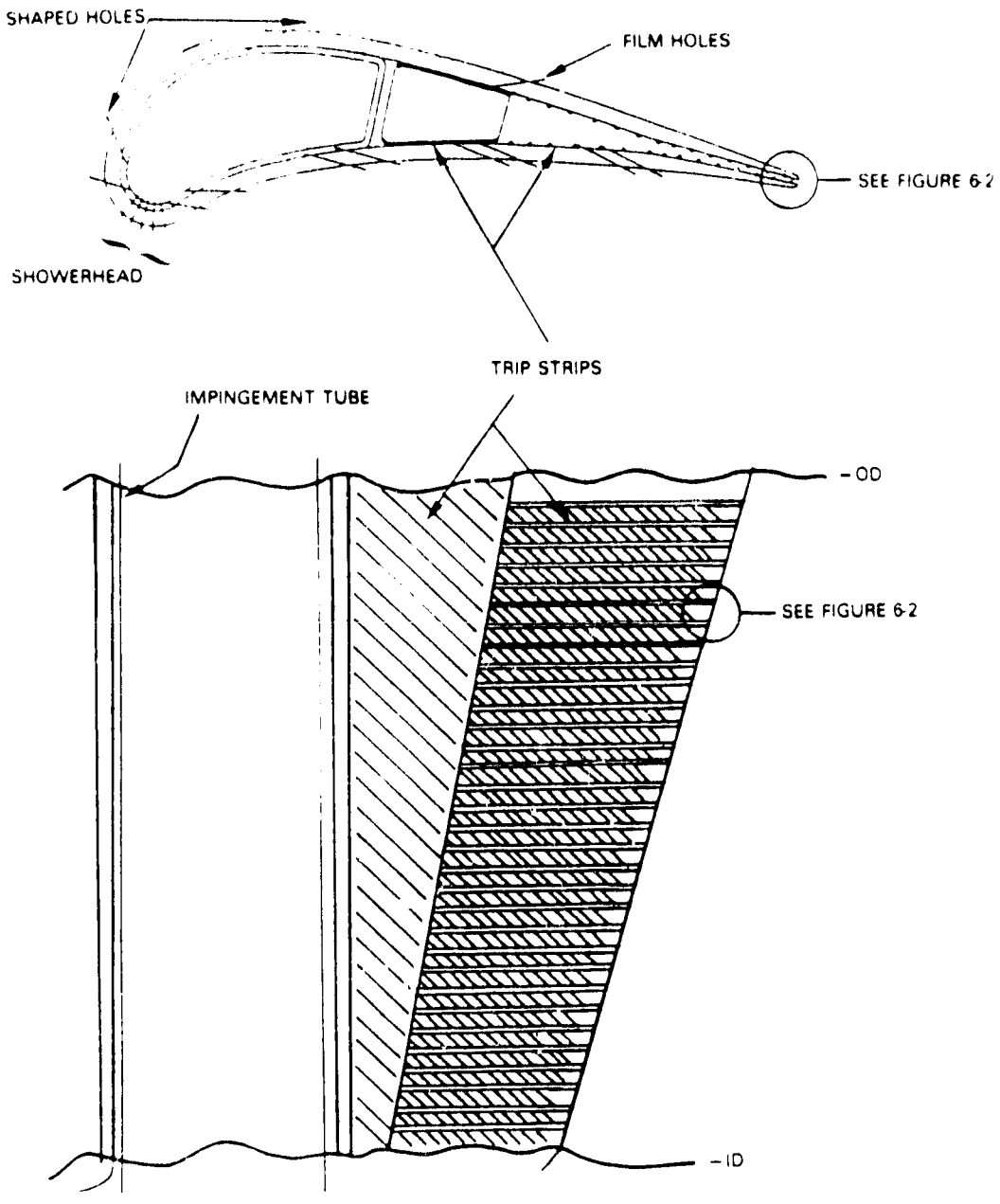

Figure 5-28 vane Cooling Configuration

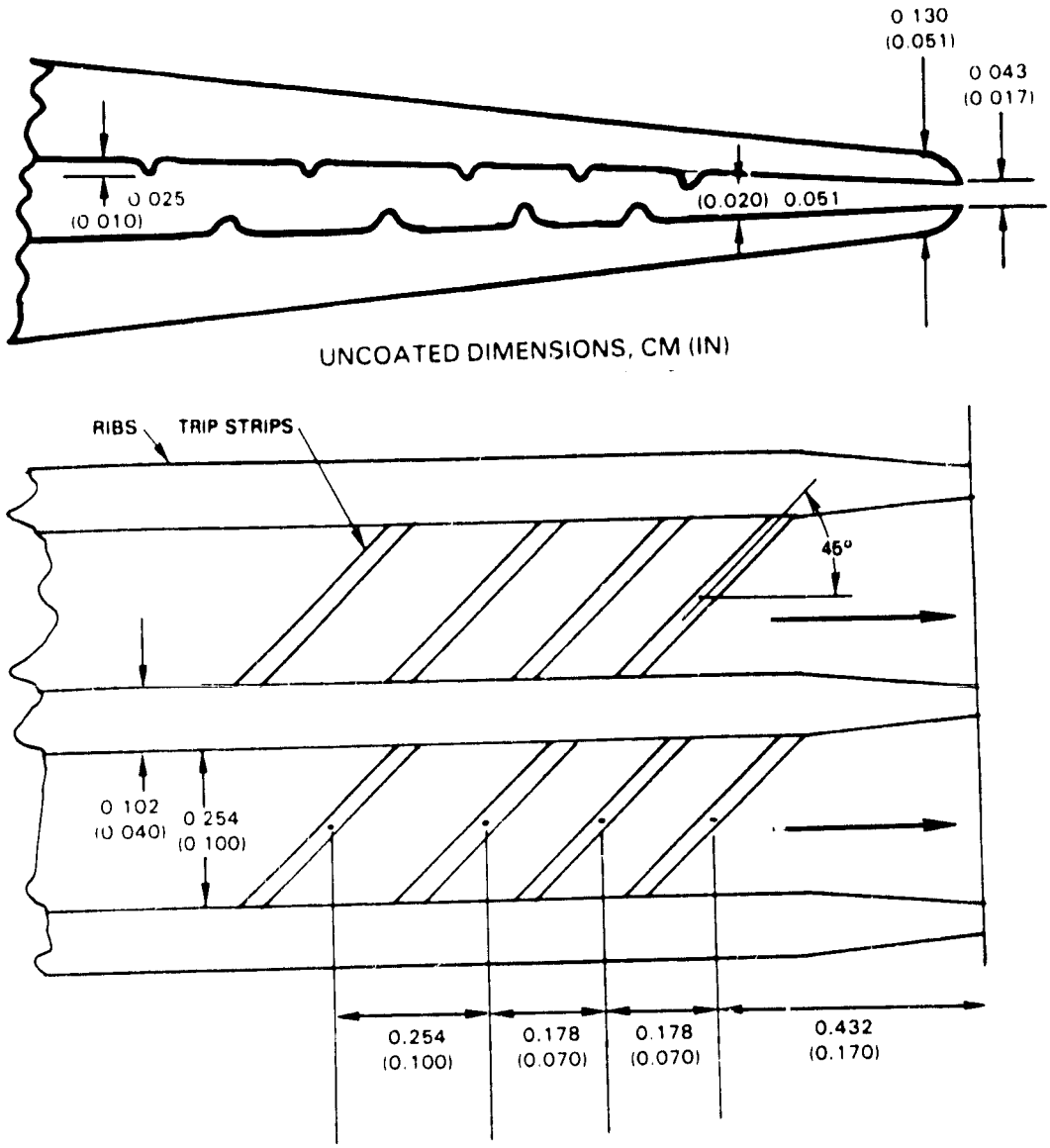

Figure 5-29 Typical Vane Trailing Edge Geometry

Utilizing 1990 technology, the VSCE first-stage vane requires 5.28 percent W_{ae} cooling airflow, distributed as shown in Figure 5-30, to achieve the design B-5 life goal of 10,000 hours unscheduled engine removal (UER). The resulting interface temperature distribution for the pressure surface and suction surface is shown in Figure 5-31 and 5-32, respectively.

Shaped film holes (Figure 5-33) are utilized on the second and third suction side film rows and allow the removal of two rows of suction side film holes and a 0.6 percent W_{ae} reduction in required cooling flow. Film effectiveness for the shaped hole is based on recently obtained data for advanced state-of-the-art film cooled airfoils (Figure 5-34) and represents a significant increase relative to standard cylindrical holes.

The showerhead holes are designed to be conical, tapering from 0.076 cm (0.030 in) on the surface to 0.038 cm (0.015 in) at the inner surface (Figure 5-35). Tapering the showerhead holes produces the same leading edge coverage and film effectiveness at reduced coolant flow levels as closer spaced cylindrical holes would with higher flows, based on an extrapolation of the existing cylindrical showerhead hole data base. Confirmation of the effectiveness level as well as the resistance to plugging needs to be verified through testing. Cooling flow from the conical shaped holes are a function of the internal-to-external hole area ratio and the pressure ratio across the hole, as shown in Figure 5-36. In the VSCE vane design, the conical shaped holes reduce the cooling airflow by about 10 percent (0.6 percent W_{ae}). The flow characteristics of the actual machined hole shapes need to be confirmed by test.

A summary of the initial internal and external hole diameters and spacing is shown in Figure 5-37. This geometry is based on an analysis of the mean section and may vary somewhat when a detailed analysis at multiple sections is undertaken for the final design.

1986 Technology Vane Design

The 1986 technology vane incorporates the 0.025 cm (0.010 in) thick yttria stabilized zirconia thermal barrier coating and casting and manufacturing technologies consistent with the 1986 time range. The zirconia based thermal barrier coating is porous to oxygen so that the allowable interface temperature is 21 K (70°F) lower than that for the 1990 technology. This lower allowable interface temperature coupled with the thinner thermal barrier coating results in a significantly higher cooling requirement in 1986.

Utilizing 1986 technology, the VSCE first-stage vane requires 8.66 percent W_{ae} cooling airflow, distributed as shown in Figure 5-38. The resulting interface temperature distributions for the pressure side and suction side are shown in Figures 5-39 and 5-40, respectively. The internal and external cooling hole geometries based on the 1986 technology are shown in Figure 5-41.

Relative to 1990 technology, the 1986 technology vane requires 3.38 percent more cooling airflow and reduces the turbine efficiency by approximately 0.3 percent.

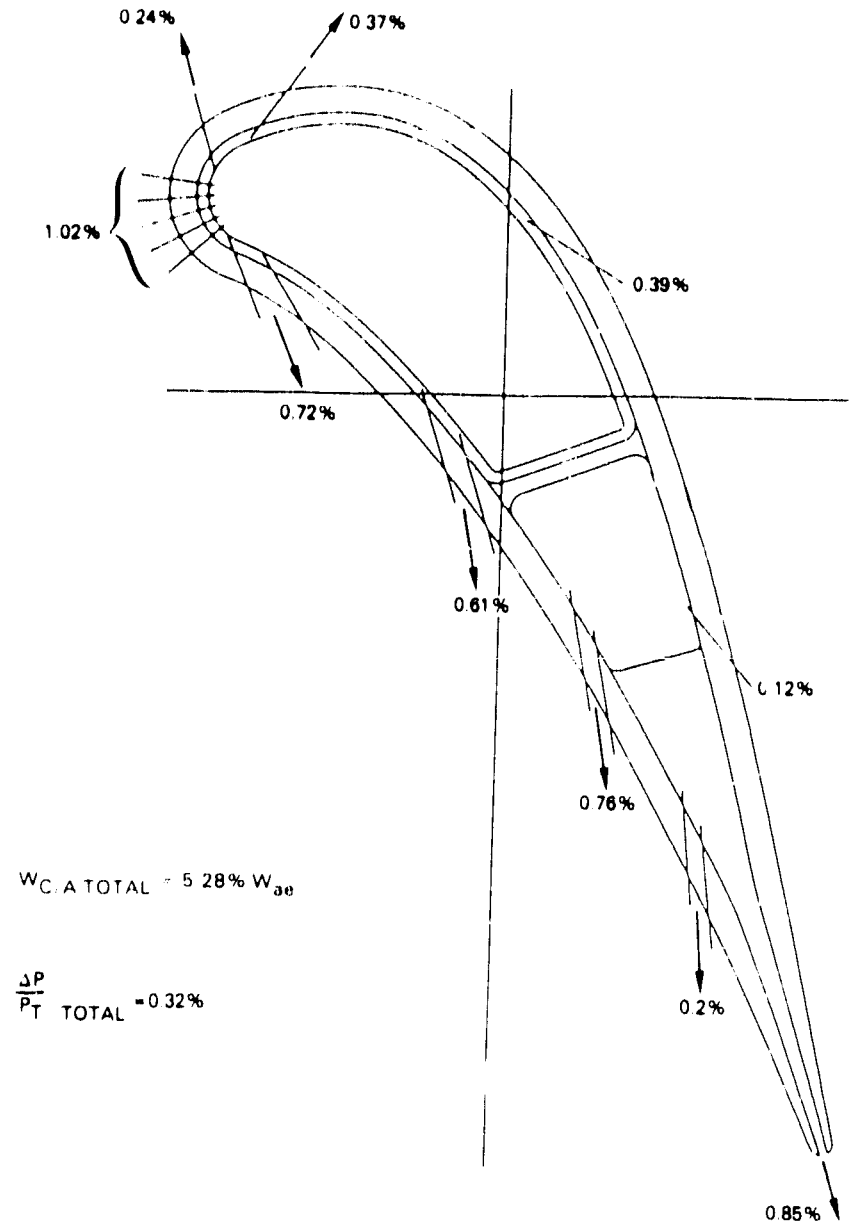

Figure 5-30 Vane Cooling Air Flows (1990 Technology)

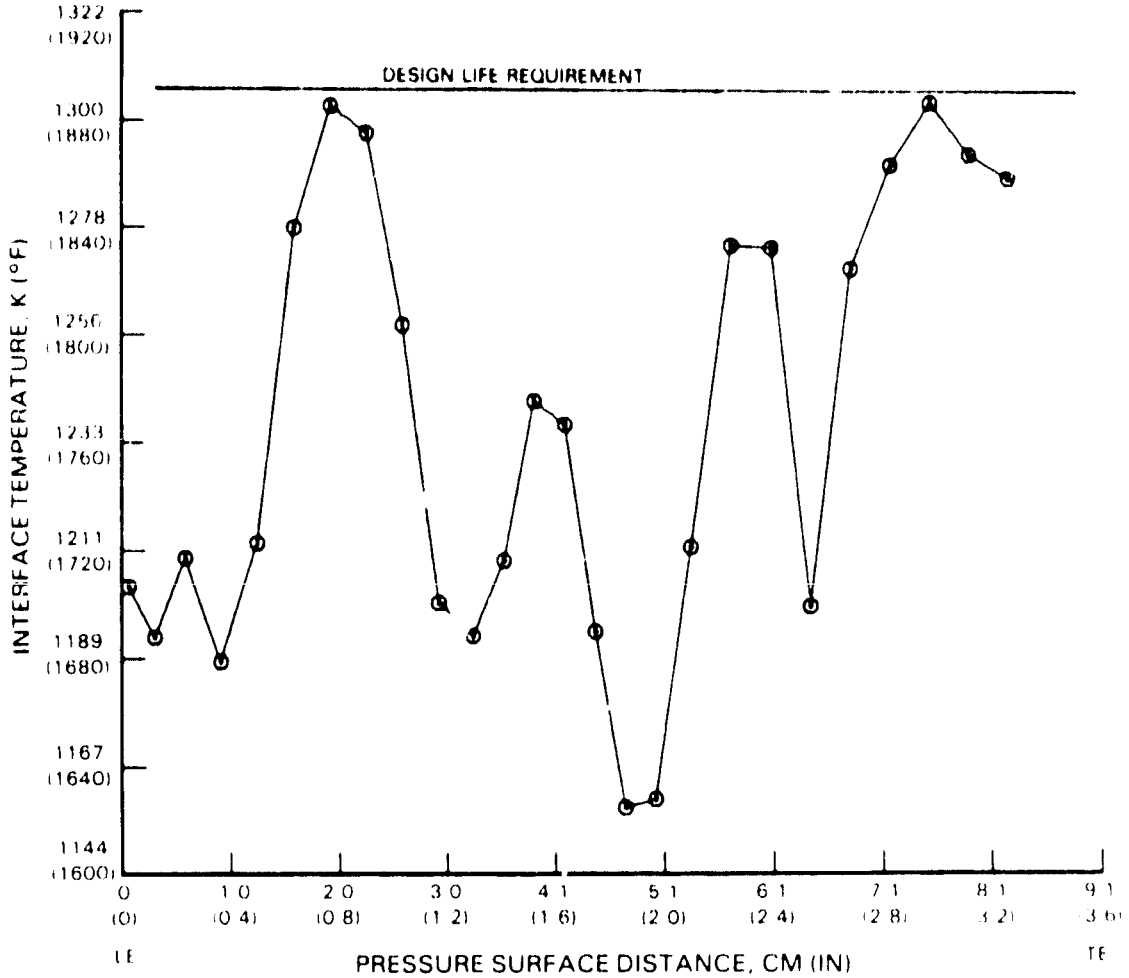

Figure 5-31 Vane Interface Temperature Distribution on Pressure Surface (1990 Technology)

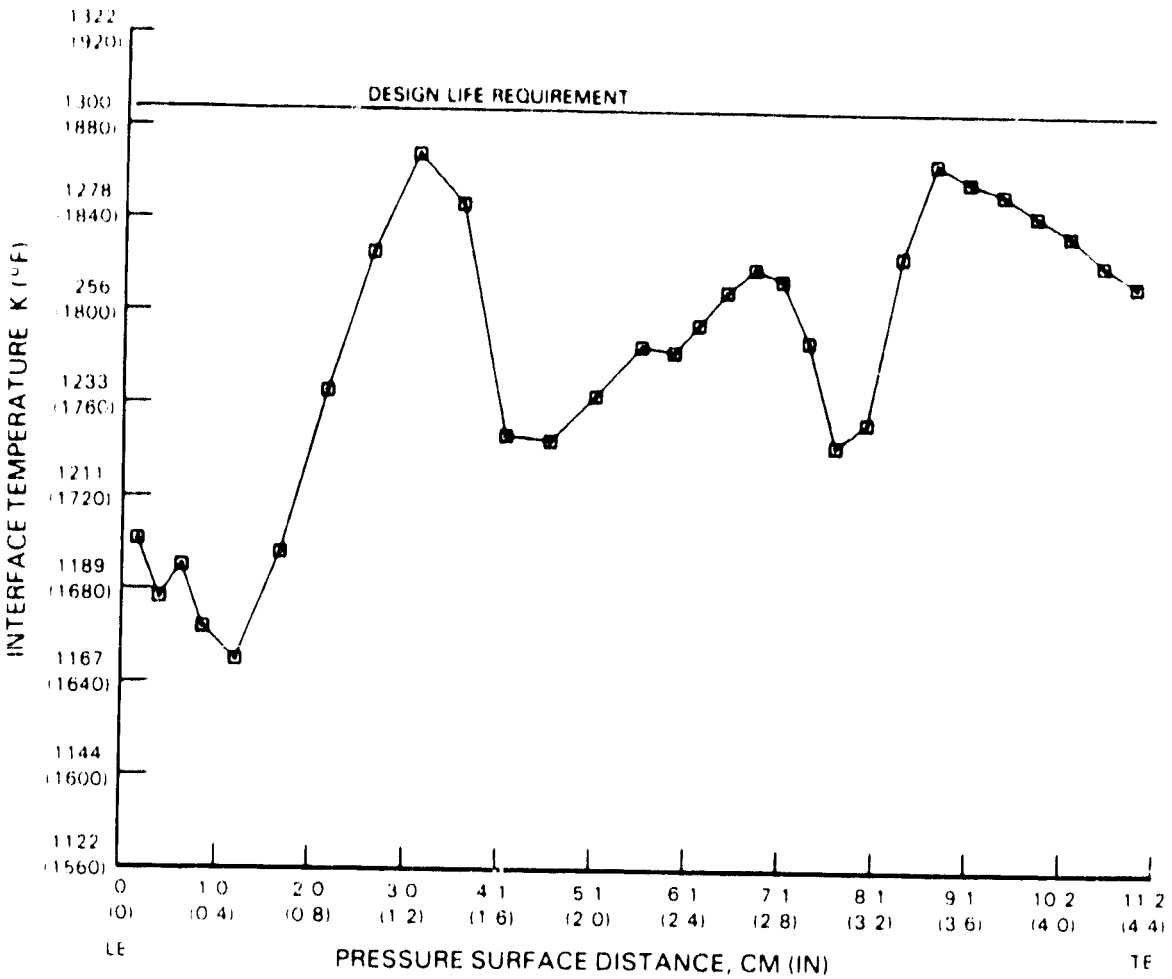

Figure 5-32 Vane Interface Temperature Distribution on Suction Surface (1990 Technology)

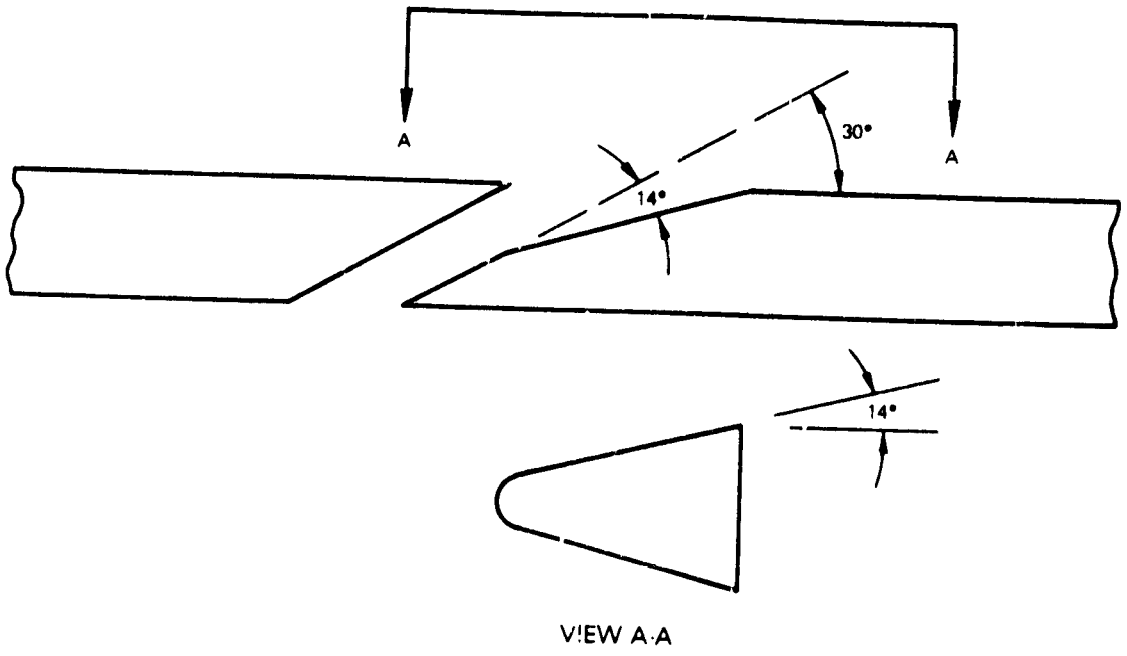

Figure 5-33 Geometry of Suction Surface Shaped Holes

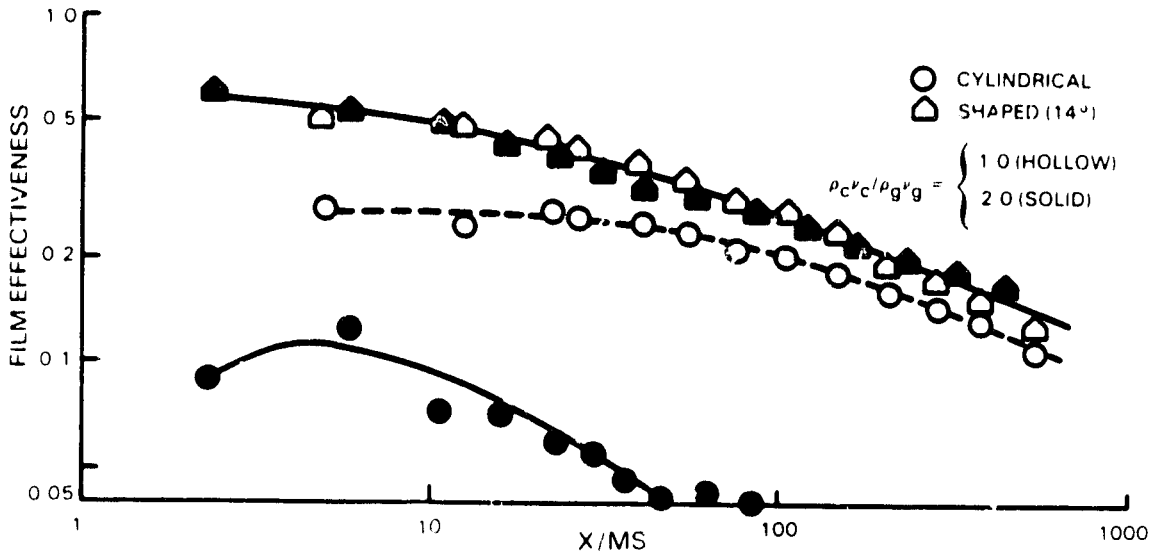

Figure 5-34 Film Effectiveness vs Nondimensional Distance Cylindrical and Shaped Holes

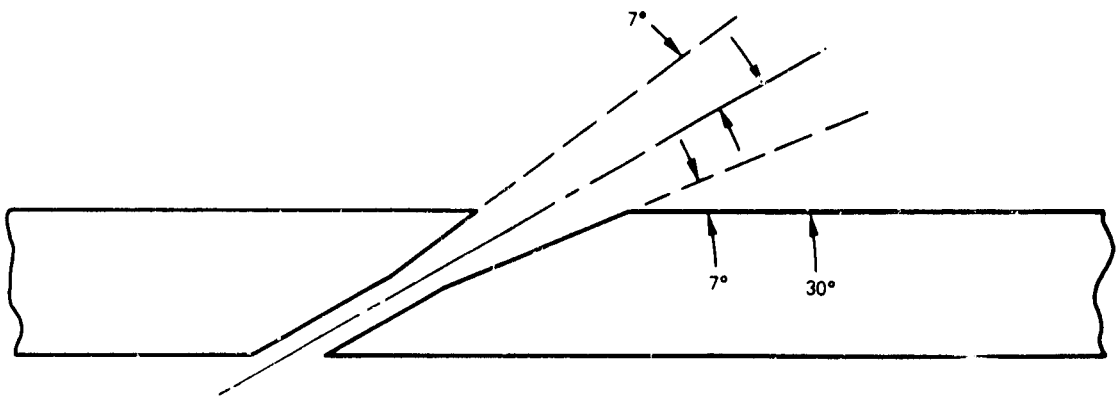

Figure 5-35 Geometry of Conical Showerhead Holes

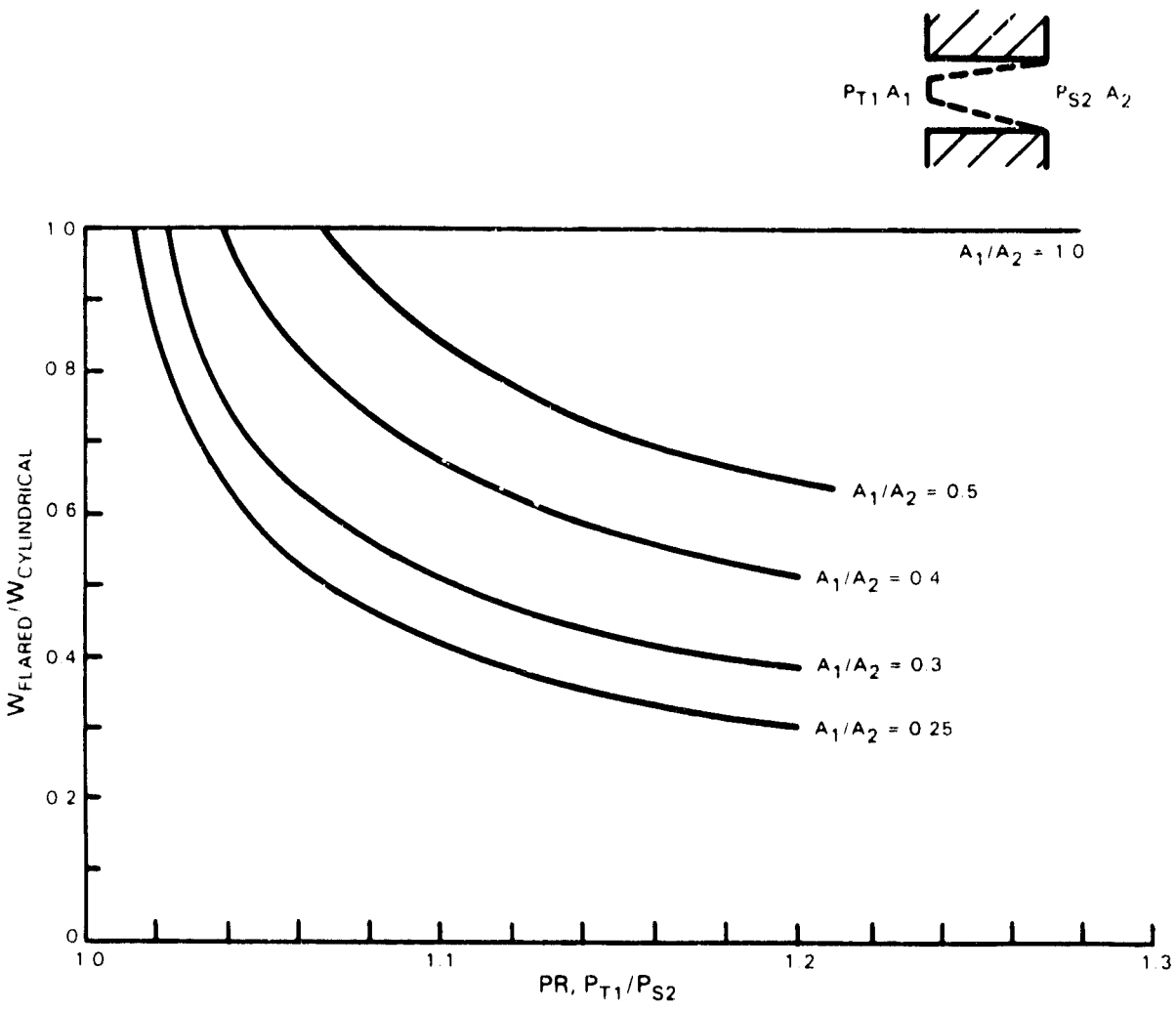

Figure 5-36 Conical Holes Cooling Air Flow Rates

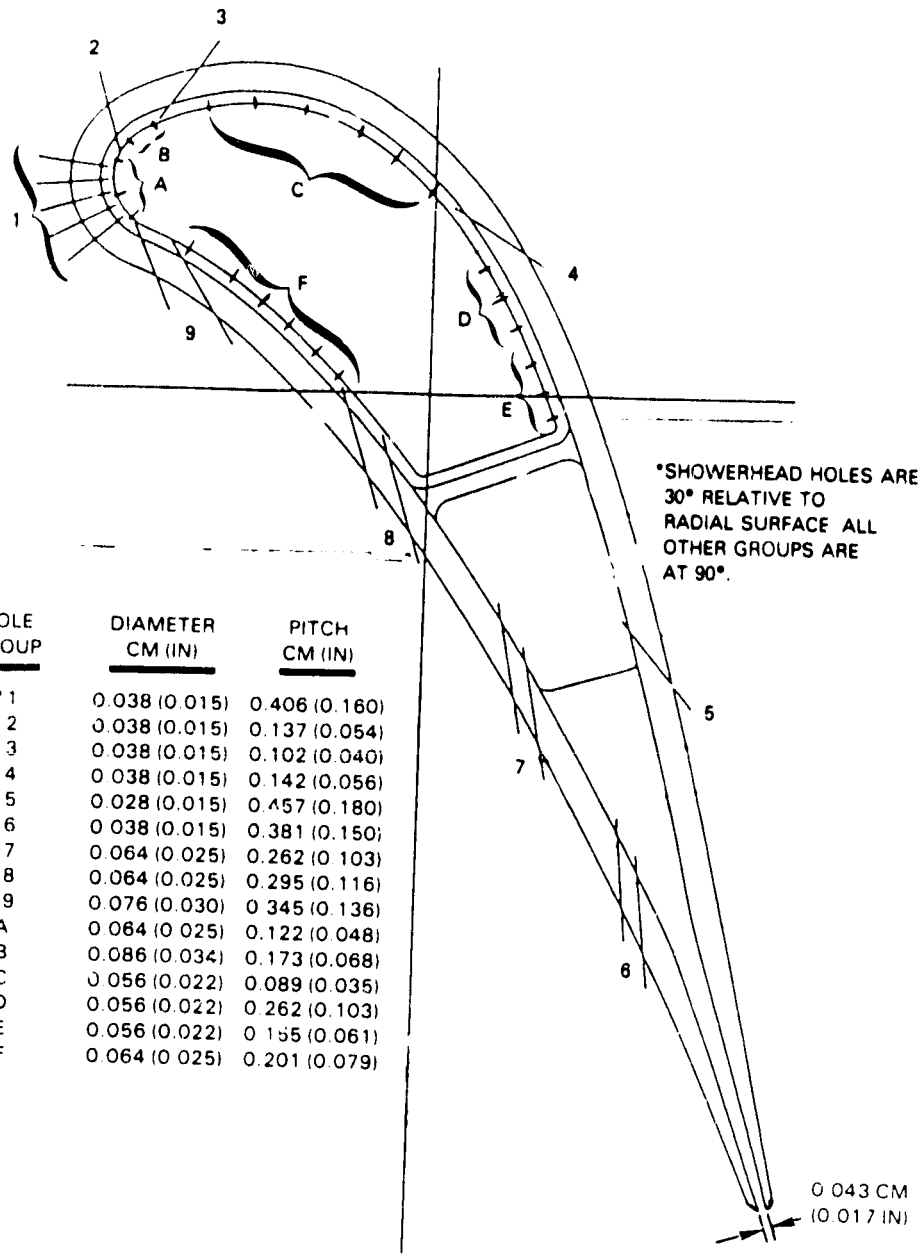

HOLE GROUP	DIAMETER CM (IN)	PITCH CM (IN)
*1	0.038 (0.015)	0.406 (0.160)
2	0.038 (0.015)	0.137 (0.054)
3	0.038 (0.015)	0.102 (0.040)
4	0.038 (0.015)	0.142 (0.056)
5	0.028 (0.015)	0.457 (0.180)
6	0.038 (0.015)	0.381 (0.150)
7	0.064 (0.025)	0.262 (0.103)
8	0.064 (0.025)	0.295 (0.116)
9	0.076 (0.030)	0.345 (0.136)
A	0.064 (0.025)	0.122 (0.048)
B	0.086 (0.034)	0.173 (0.068)
C	0.056 (0.022)	0.089 (0.035)
D	0.056 (0.022)	0.262 (0.103)
E	0.056 (0.022)	0.155 (0.061)
F	0.064 (0.025)	0.201 (0.079)

Figure 5-37 Vane Hole Geometry (1990 Technology)

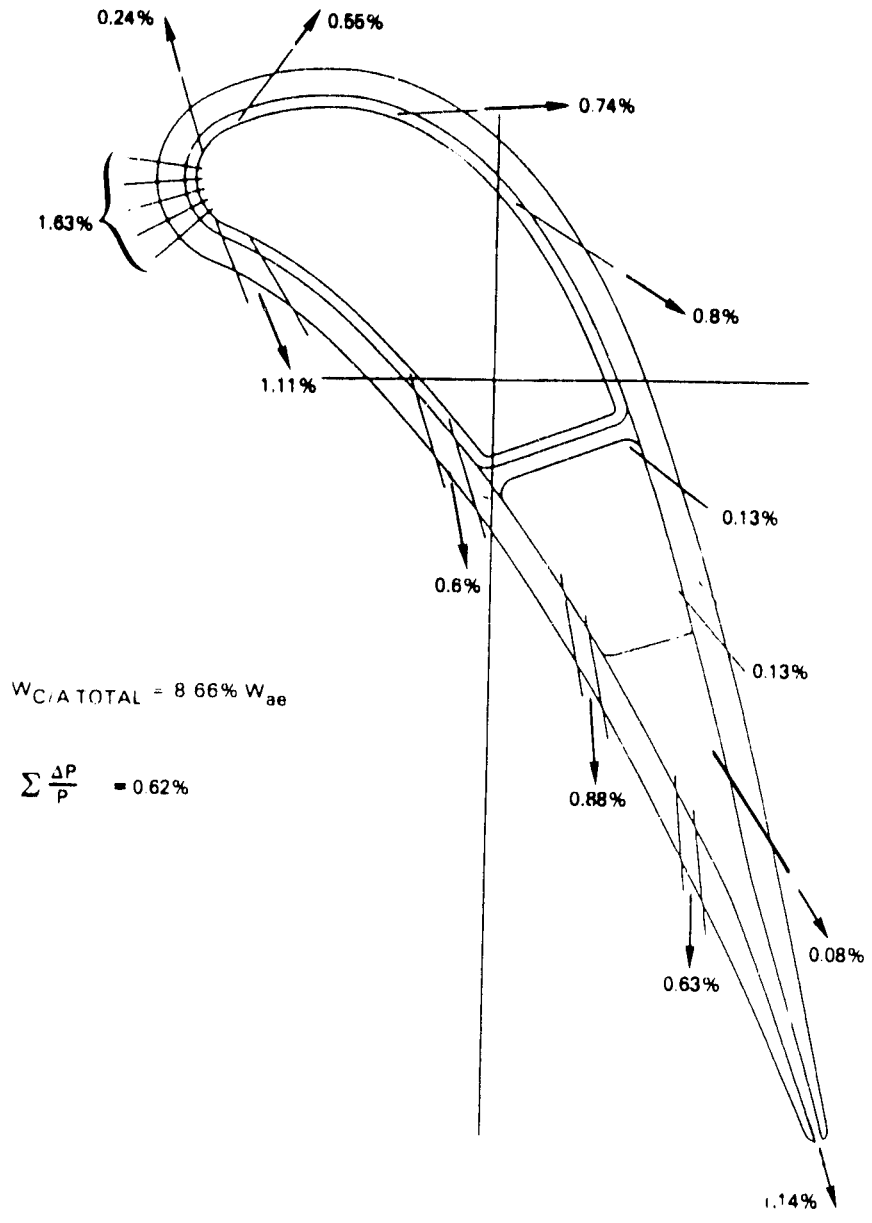

Figure 5-38 Vane Cooling Air Flows (1986 Technology)

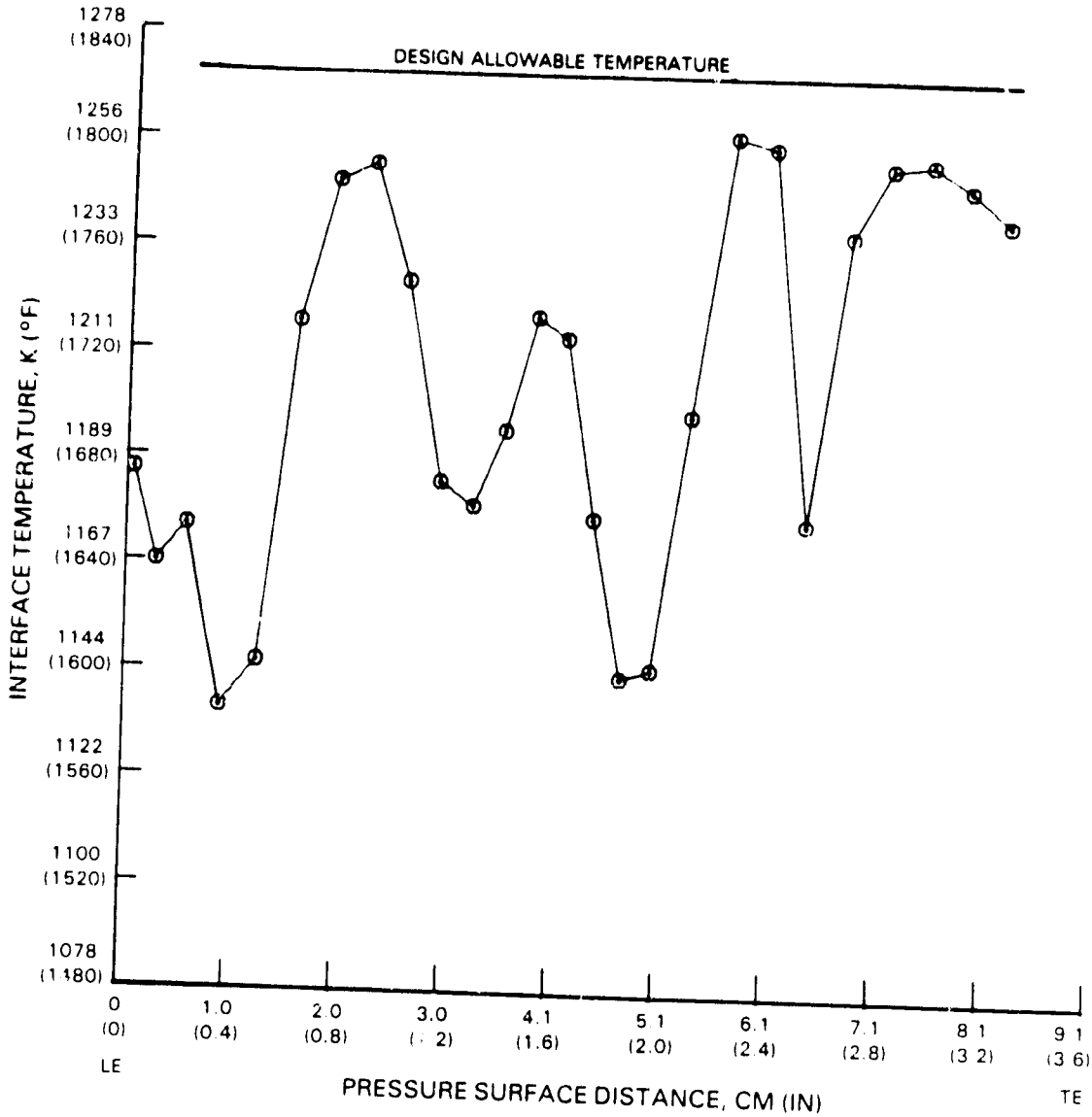

Figure 5-39 Vane Interface Temperature Distribution on Pressure Surface (1986 Technology)

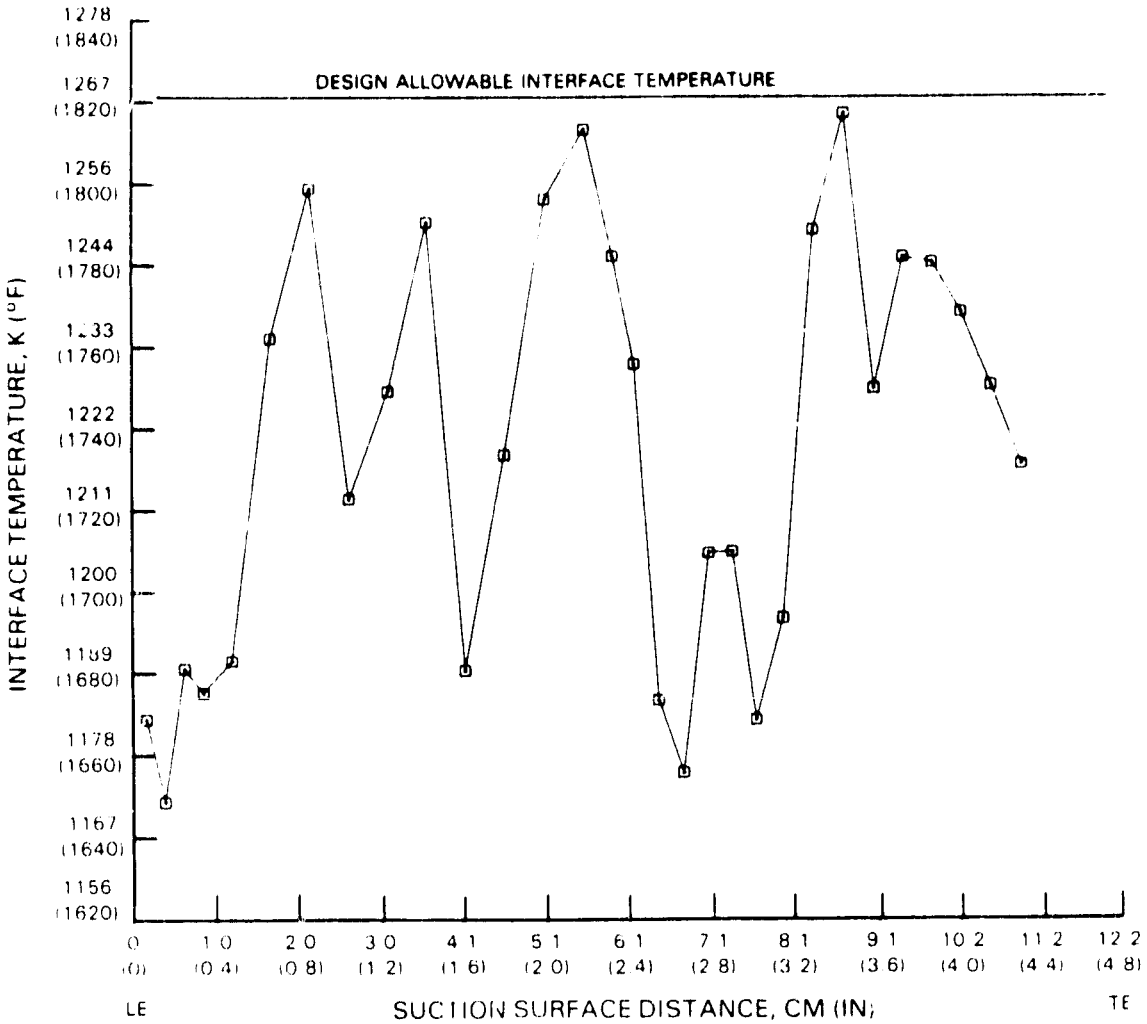

Figure 5-40 Vane Interface Temperature Distribution on Suction Surface (1986 Technology)

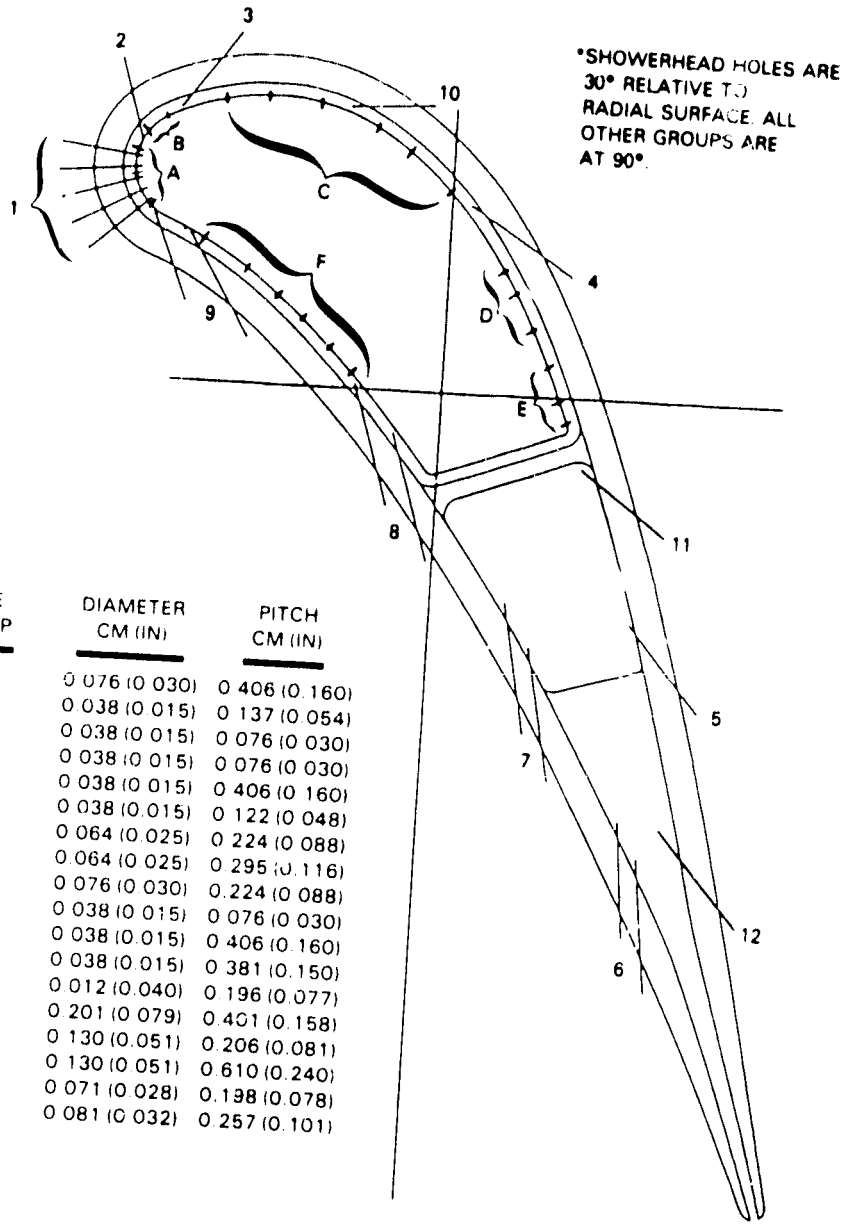

HOLE GROUP	DIAMETER CM (IN)	PITCH CM (IN)
*1	0.076 (0.030)	0.406 (0.160)
2	0.038 (0.015)	0.137 (0.054)
3	0.038 (0.015)	0.076 (0.030)
4	0.038 (0.015)	0.076 (0.030)
5	0.038 (0.015)	0.406 (0.160)
6	0.038 (0.015)	0.122 (0.048)
7	0.064 (0.025)	0.224 (0.088)
8	0.064 (0.025)	0.295 (0.116)
9	0.076 (0.030)	0.224 (0.088)
10	0.038 (0.015)	0.076 (0.030)
11	0.038 (0.015)	0.406 (0.160)
12	0.038 (0.015)	0.381 (0.150)
A	0.012 (0.040)	0.196 (0.077)
B	0.201 (0.079)	0.401 (0.158)
C	0.130 (0.051)	0.206 (0.081)
D	0.130 (0.051)	0.610 (0.240)
E	0.071 (0.028)	0.198 (0.078)
F	0.081 (0.032)	0.257 (0.101)

Figure 5-41 Vane Hole Geometry (1986 Technology)

5.2.5 Blade Durability Design

The VSCE first-stage blade operates at a design AN^2 level approximately 50 percent higher than present state-of-the-art second-stage turbine blades. This high AN^2 (high stress) level, coupled with a hot operating time that is ten times greater than that for a typical subsonic commercial application, results in a cooling requirement that is significantly greater than the present state-of-the-art airfoils.

In order to attain the design life goal of 10,000 hours B-5 UER (i.e., 5 percent of engines will experience unscheduled engine removal) with a minimum cooling flow, both the 1986 and 1990 airfoil designs incorporate advanced single crystal material, a low heat-load pressure wall, stress reducing ribs, augmented internal convection, and advanced state-of-the-art film cooling. The 1990 airfoil only incorporates a 0.025 cm (0.010 in) yttria stabilized zirconia thermal barrier coating in addition to these features.

The blade cooling configuration (Figure 5-42) is a three-feed multipass design with showerhead and pressure and suction side film cooling, internally augmented convection, and a high density pedestal trailing edge design.

Leading edge cooling is accomplished through internal convection and showerhead film. Cooling airflow is passed from the inside diameter of the blade through a leading edge cavity containing internal trip strips. The cooling air is vented to the main stream gas through two rows of showerhead in the leading edge, two rows of film holes on both the pressure and suction surface, and the remaining air to the tip where it is used for cooling the pressure side and the trailing edge tip. A two row showerhead was found to achieve adequate cooling for both the 1986 and 1990 technology levels. The trip strip height and spacing has been established to supply adequate cooling to the mean section, based on state-of-the-art commercial engine design practices. Trip strip geometry has not been optimized to reflect any spanwise cooling variation. Analysis during detailed final design would be used to determine the optimum spanwise spacing.

Midchord cooling is accomplished through a three pass configuration with trip strip augmented convection and external film. Cooling air is fed from a separate midchord feed, flowed radially upward in a rear midchord passage, down the middle region of the airfoil, and then up the last midchord passage where it is vented out through the pressure side and suction side film holes. Utilizing internal convection in conjunction with external film significantly increases the cooling effectiveness of the airfoil. Internally, the full potential of the cooling air is essentially used because the cooling temperature is approaching the wall temperature of the airfoil. Venting spent air over the airfoil reduces the effective gas temperature to the rear portions of the airfoil; since the spent air still has approximately 537 K (1000°F) cooling potential relative to the gas, it can still be used effectively to film cool the blade. Suction side film holes in the blade are shaped similar to the vane holes (Figure 5-33) in order to maximize the film

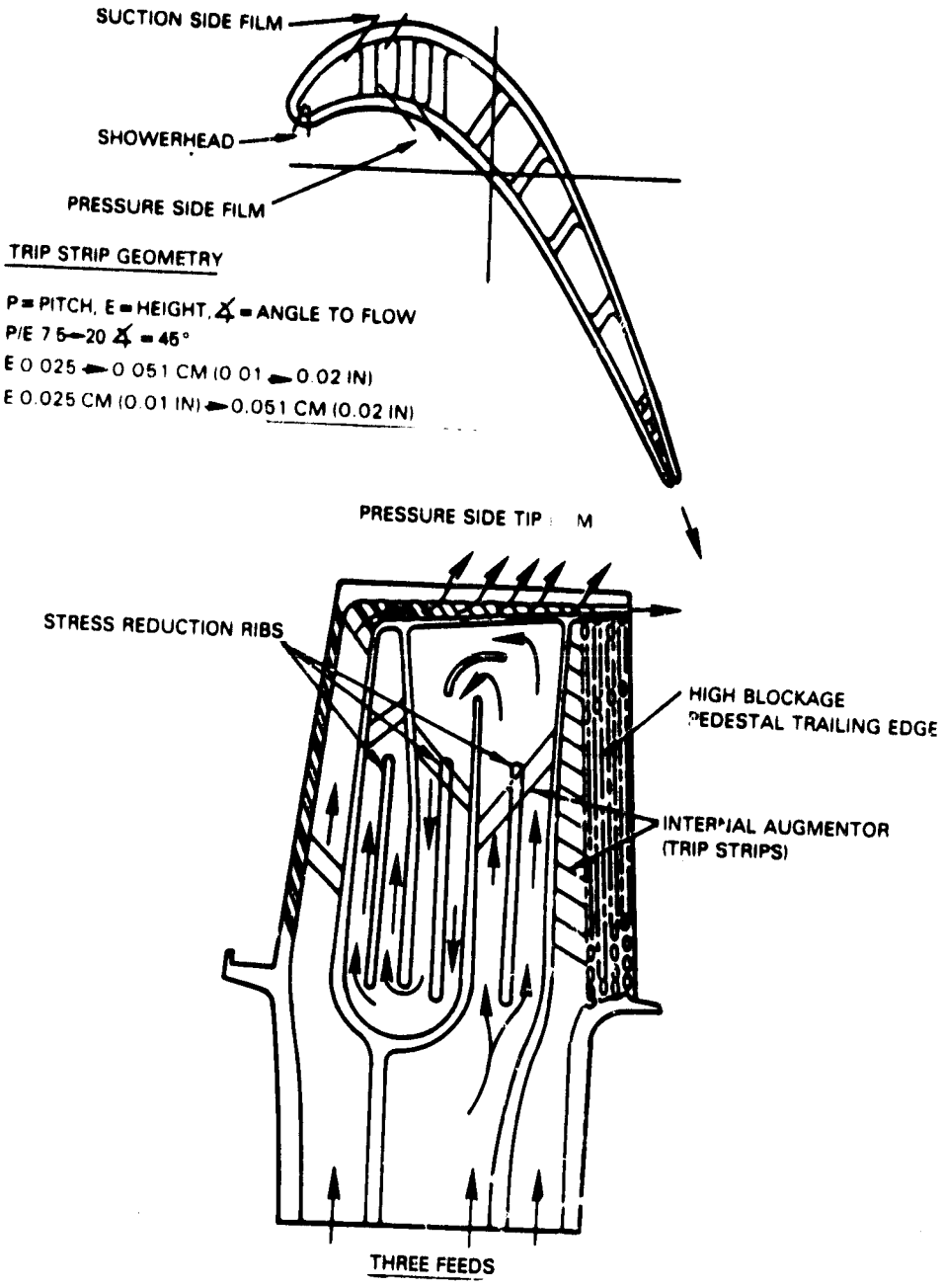

Figure 5-42 Blade Cooling Configuration

effectiveness. The trip strip height and spacing depicted in Figure 5-42 have been established to supply adequate cooling to the mean section and are not optimized to reflect any spanwise cooling variation. Analysis during the detailed final design again will be required to determine the optimum spanwise distribution.

Trailing edge cooling is achieved through a single-pass cavity with trip strips venting to a high density pedestal trailing edge (Figure 5-43). The high density pedestal trailing edge is used to reduce the momentum mixing losses of the airfoil cooling air. The high density pedestals provide increased heat transfer coefficients for a given flow as well as increasing the exit Mach number of the cooling airflow which reduces the momentum mixing losses. Figure 5-44 shows the relationship between trailing edge pedestal density and momentum mixing losses for an initial estimate of 1 percent W_{ae} trailing edge cooling flow. As can be seen from Figure 5-44, the increased density pedestals significantly reduce the cooling losses relative to a typical state-of-the-art pedestal trailing edge. The pedestal density and trailing edge gap of the final design would be optimized, dependent on the cooling airflow requirement of the trailing edge and the overall supply pressure requirement of the blade.

Stress control in the VSCE blade is accomplished through tapering of the airfoil wall thickness and through the use of stress reduction ribs. Wall thicknesses are tapered. At midchord, the wall thickness is 0.203 cm (0.080 in) at the root and 0.088 cm (0.035 in) at the tip. Three stress reduction ribs are added to the midchord cooling passages (Figure 5-42) in order to further reduce the stress of the airfoil. The resulting pull stress distribution of the foil at design speed is shown in Figure 5-45 for both the 1990 design and the 1986 design. Stress levels in the 1990 design are higher due to the added pull load of the thermal barrier coating.

Tapering of the thermal barrier coating to reduce airfoil trailing edge thickness and improve turbine efficiency was not pursued in this blade design. Turbine efficiency could be increased by 0.12 percent with the thermal barrier tapered to the base undercoat (Figure 5-46). However, the resulting metal temperature would be approximately 1244 K (1780°F) which, although acceptable for coating durability, would necessitate a blade coolant flow increase to maintain adequate creep life. Tapering of the thermal barrier coating should be reconsidered as part of a final design in terms of cost, durability and efficiency trade factors.

1990 Technology Blade Design

The 1990 technology blade design requires a 2.77 percent W_{ae} cooling airflow, (Figure 5-47) with 0.96 percent to the leading edge, 0.99 percent to the midchord region, and 0.82 percent to the trailing edge. Creep is the limiting failure mode of the airfoil rather than oxidation or spalling of the thermal barrier coating. Cooling airflows are set to result in uniform creep within the airfoil and thus minimize the required airflow. Detailed creep analysis of the airfoil mean section shows that the limiting location of the 1990 airfoil design is at the trailing edge and the creep distribution at the design creep level as shown in Figure 5-48.

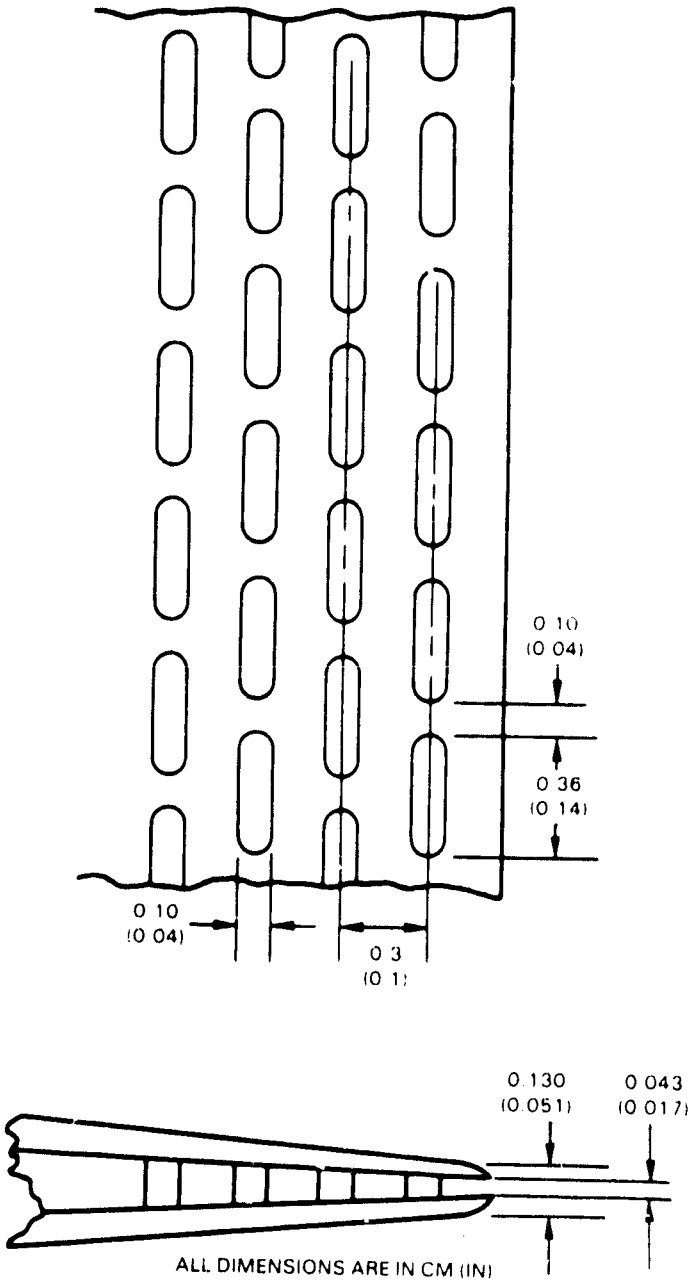

Figure 5-43 Blade Trailing Edge Cooling Configuration (Representative Geometry)

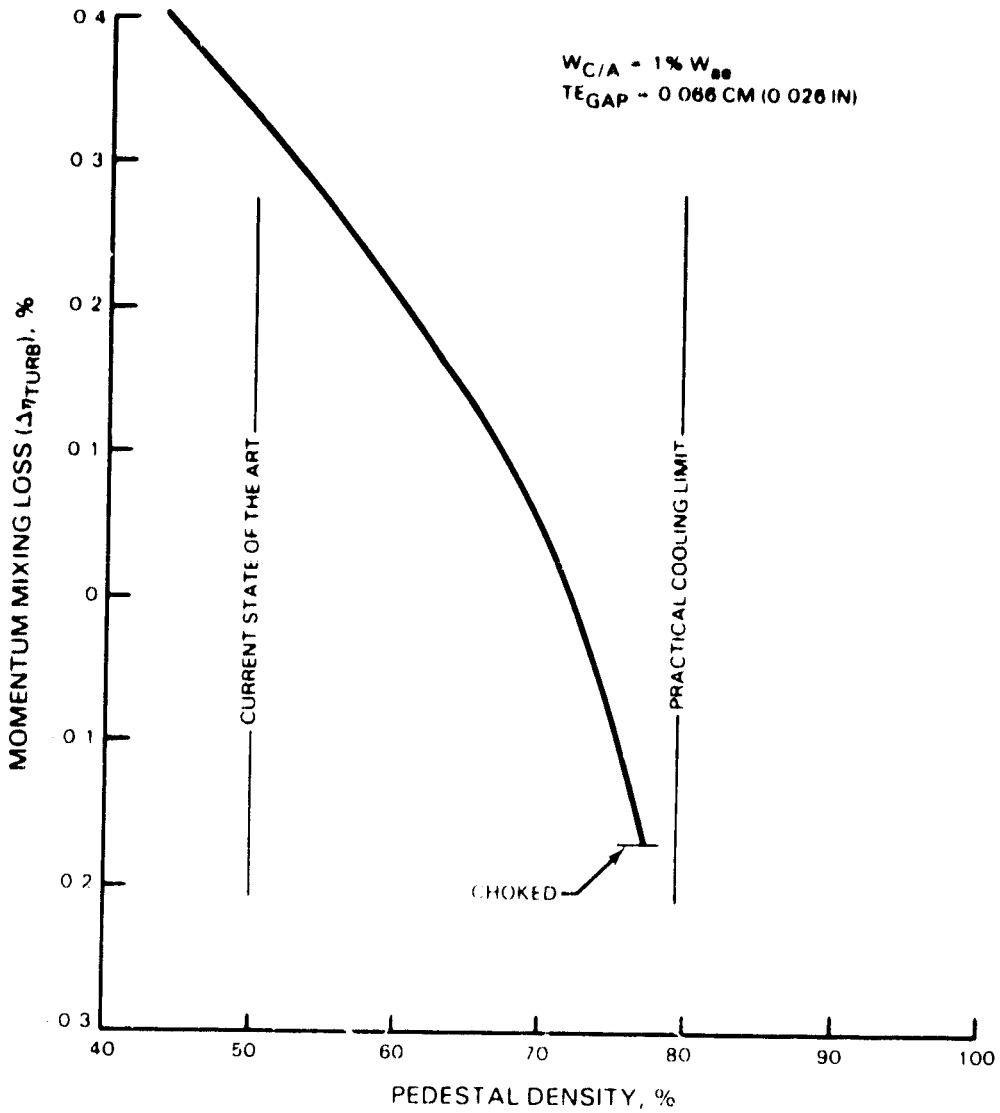

Figure 5-44 Blade Trailing Edge Cooling Losses vs Blockage

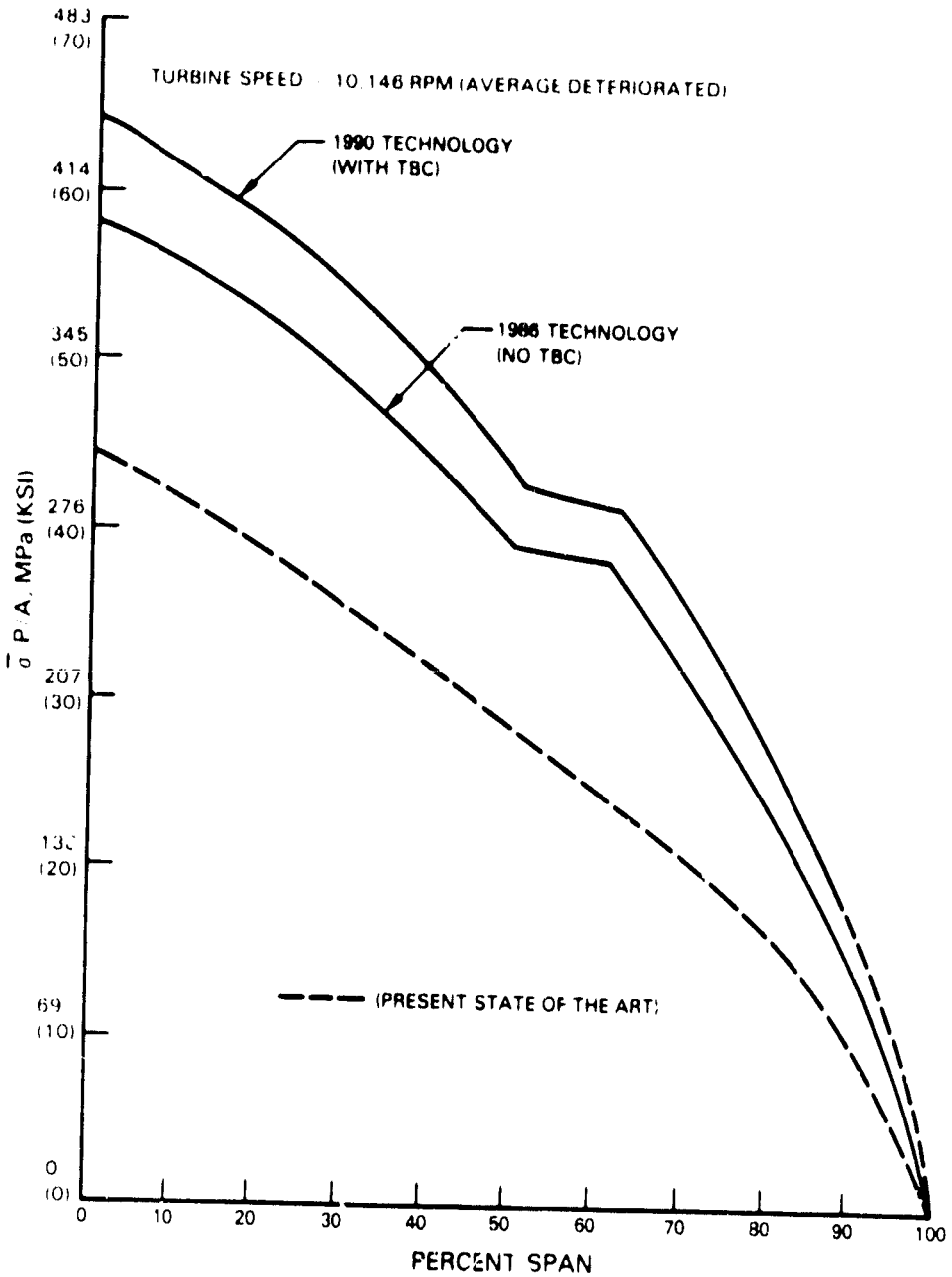

Figure 5-45 Blade Average Pull Stress vs Span for Turbine Speed = 10,146 RPM (Average Deterioration)

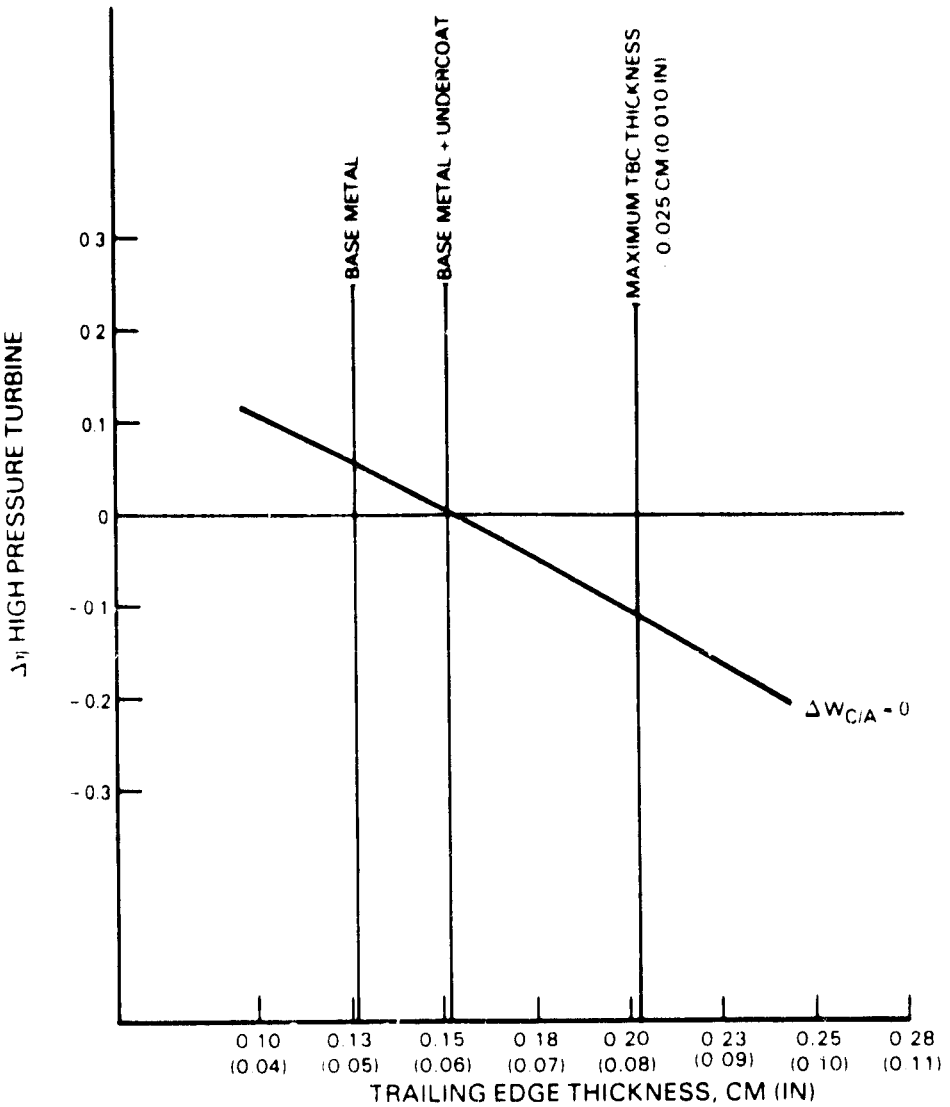

Figure 5-46 First Blade Trailing Edge Thickness Efficiency Sensitivity

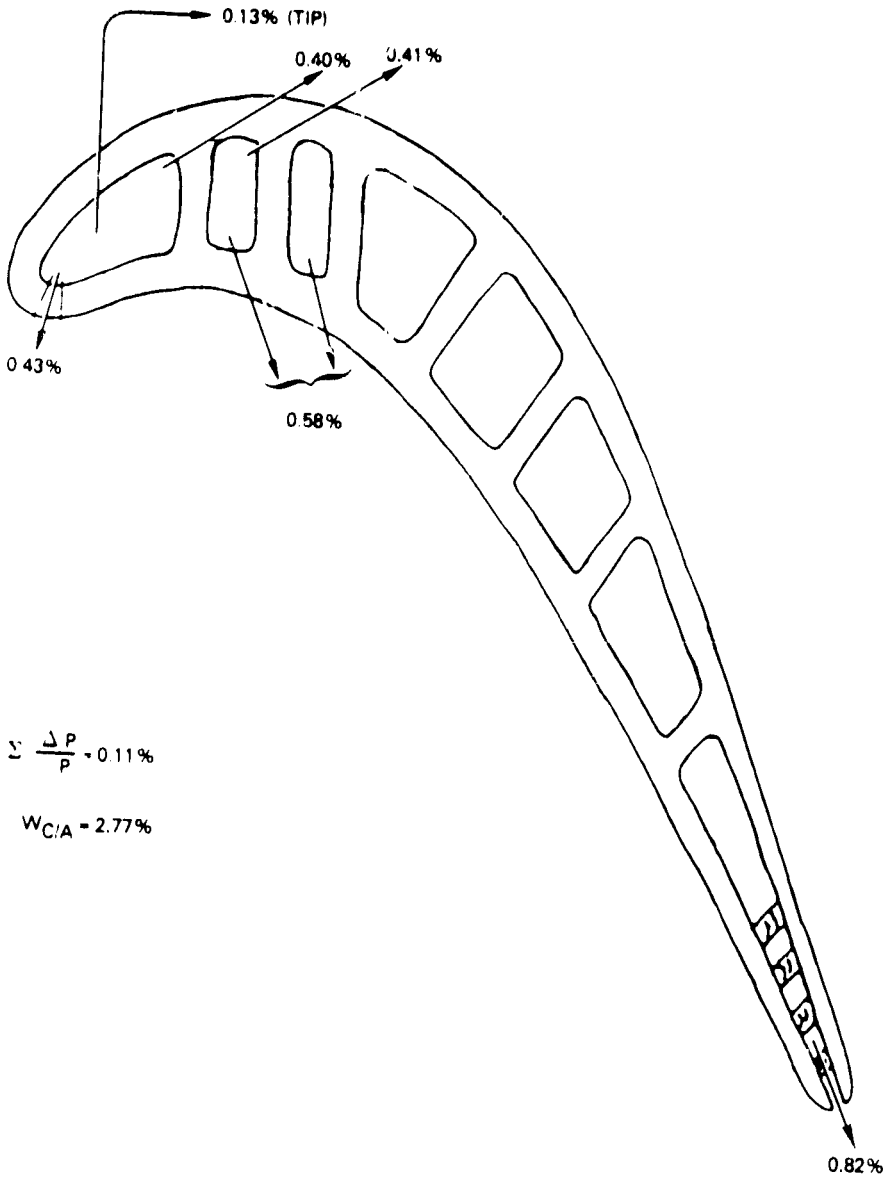

Figure 5-47 1990 Cooling Flow Distribution

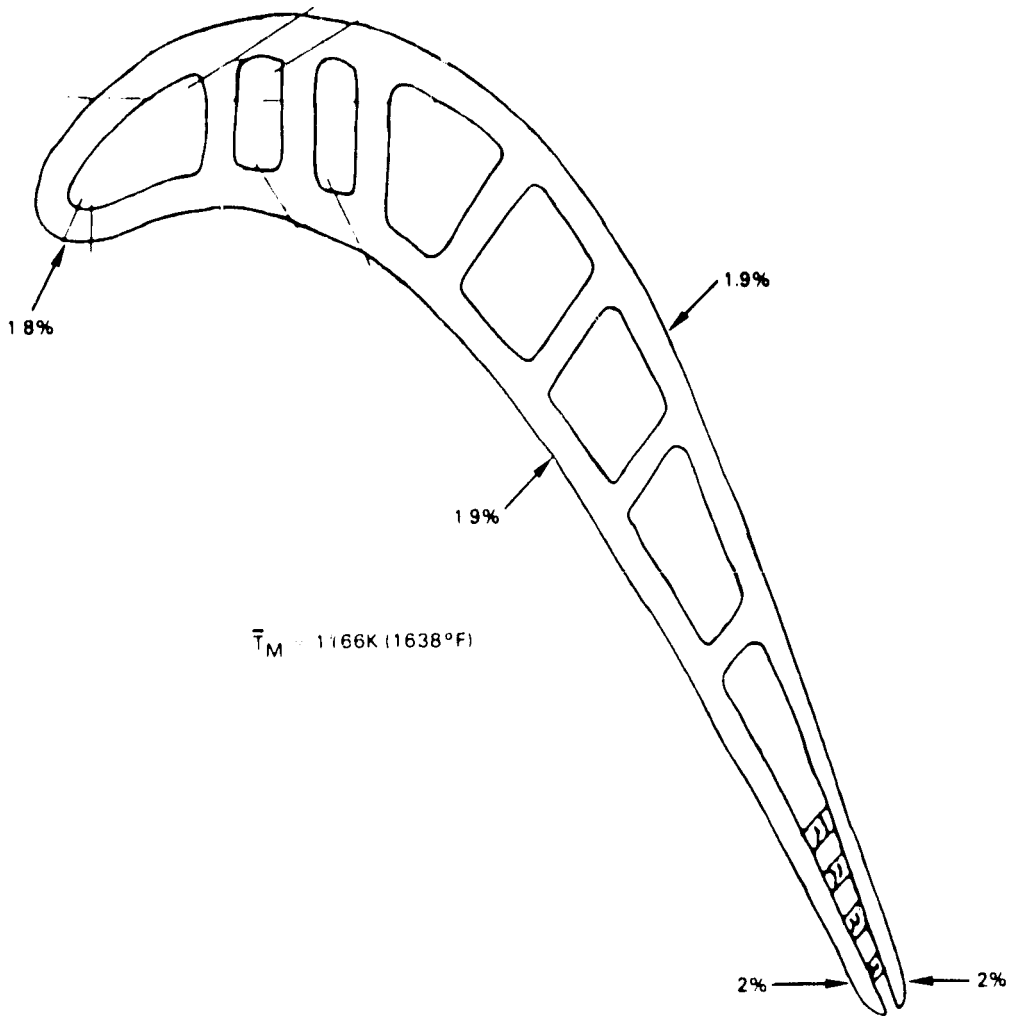

Figure 5-48 Blade Creep at Critical Locations (1990 Technology)

The interface temperatures on both the suction and pressure surfaces (Figures 5-49 and 5-50, respectively) are significantly below the design allowable limit thus providing a margin of safety from coating spalling. Airfoil metal temperatures at midsection are shown in Figure 5-51.

Showerhead holes and film holes are sized to provide adequate cooling while maintaining at least a minimum internal to external pressure ratio of 1.1 to prevent backflow. Final hole sizes for the 1990 blade are shown in Figure 5-52. The resulting supply pressure required for the blade is 68 percent of PT_3 ($P_{supply}/P_3 = 0.68$) (compressor discharge pressure), set by the midchord region (Figure 5-53).

The trailing edge cooling airflow requirement of 0.82 percent W_{ae} results in a design pedestal blockage of 77 percent. The geometry of the trailing edge was chosen to minimize momentum mixing losses by maximizing coolant exit velocities. Pedestal blockage in the trailing edge is maximized with the restriction that the supply pressure requirement of the trailing edge circuit does not exceed the supply pressure requirements of the limiting midchord serpentine as depicted in Figure 5-53. Present airfoils are limited by casting restrictions to 50 percent blockage or a 2 diameter pedestal spacing. Advanced castings can attain greater blockages by utilizing oblong pedestals with a minimum of 0.102 cm (0.040 in) of spanwise opening between adjacent pedestals. As can be seen from Figure 5-53, this represents a significant reduction in cooling loss. A practical limit of 80 percent blockage is set due to a risk of temperature maldistribution in the wake of the last pedestal row.

Final design of the blade would require consideration of spanwise cooling requirements in addition to these requirements at the mean section.

1986 Technology Blade Design

The 1986 technology blade design differs from the 1990 technology design in that it does not utilize thermal barrier coating. Additionally, less advanced burner technology in 1986 and increased first-stage vane and blade flow result in a peak gas temperature of 23.3 K (42°F) hotter than the 1990 technology design. In order to obtain the design life goal of 10,000 hours, B-5 UER (unscheduled engine removal), the 1986 design requires 3.8 percent W_{ae} cooling air, with 1.1 percent at the leading edge, 1.4 percent at the midchord, and 1.3 percent at the trailing edge. The resulting metal temperatures at this mean cross section are shown in Figure 5-54, and the surface metal temperatures are presented in Figures 5-55 and 5-56. Creep in the airfoil is the life limiting failure mode with a creep distribution at failure as shown in Figure 5-57.

Showerhead holes and film holes are sized to provide adequate cooling while again maintaining at least a minimum internal to external pressure ratio of 1.1 to prevent backflow. The cooling airflows and hole geometry for the 1986 blade are shown in Figures 5-58 and 5-59. The resulting supply pressure requirement for the blade is 77 percent P_{T3}. Here, as in the 1990 design, spanwise tailoring of the film has not been considered but should be considered during final detail design analysis.

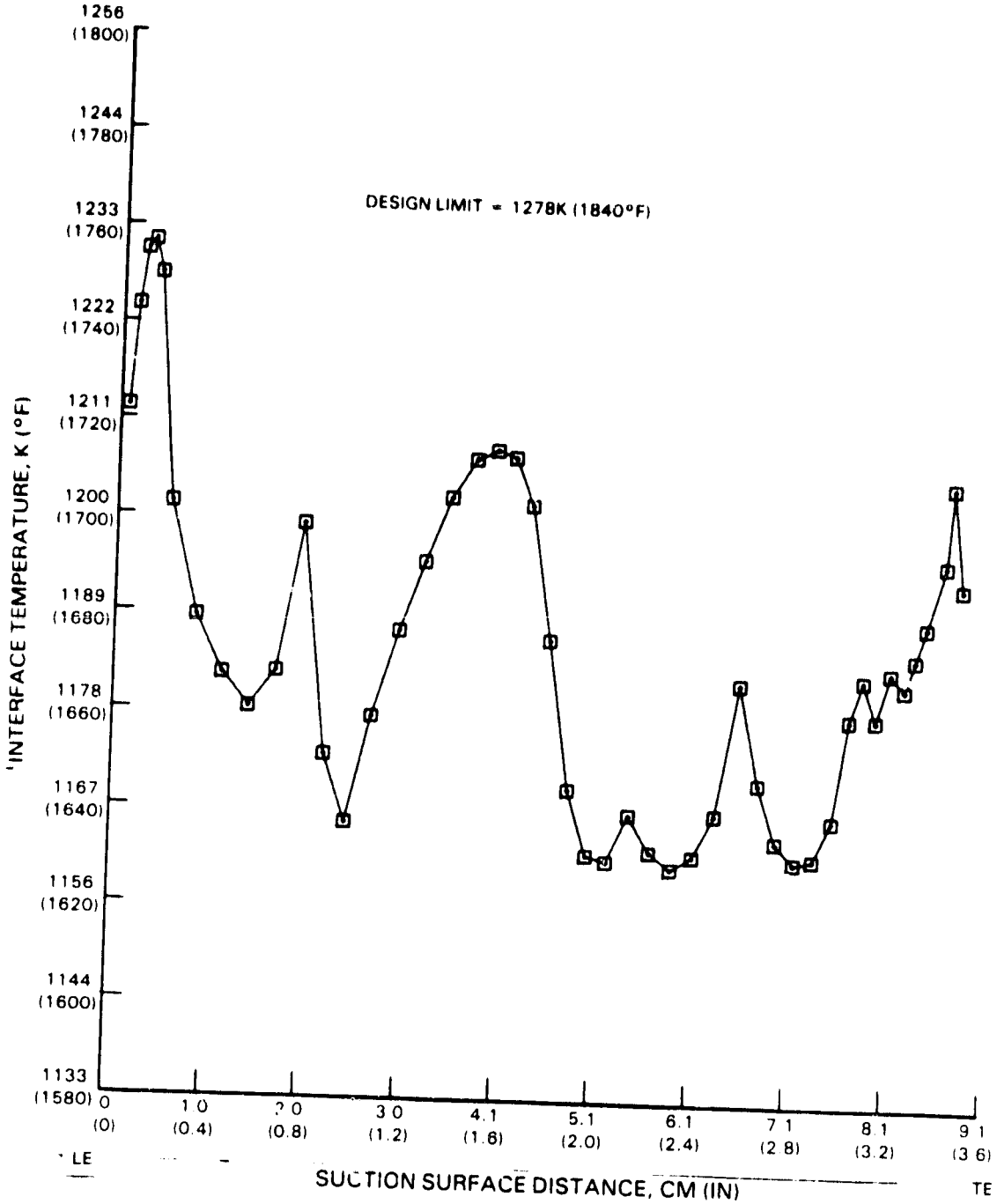

Figure 5-49 Blade Interface Temperature Distribution on Suction Surface (1990 Technology)

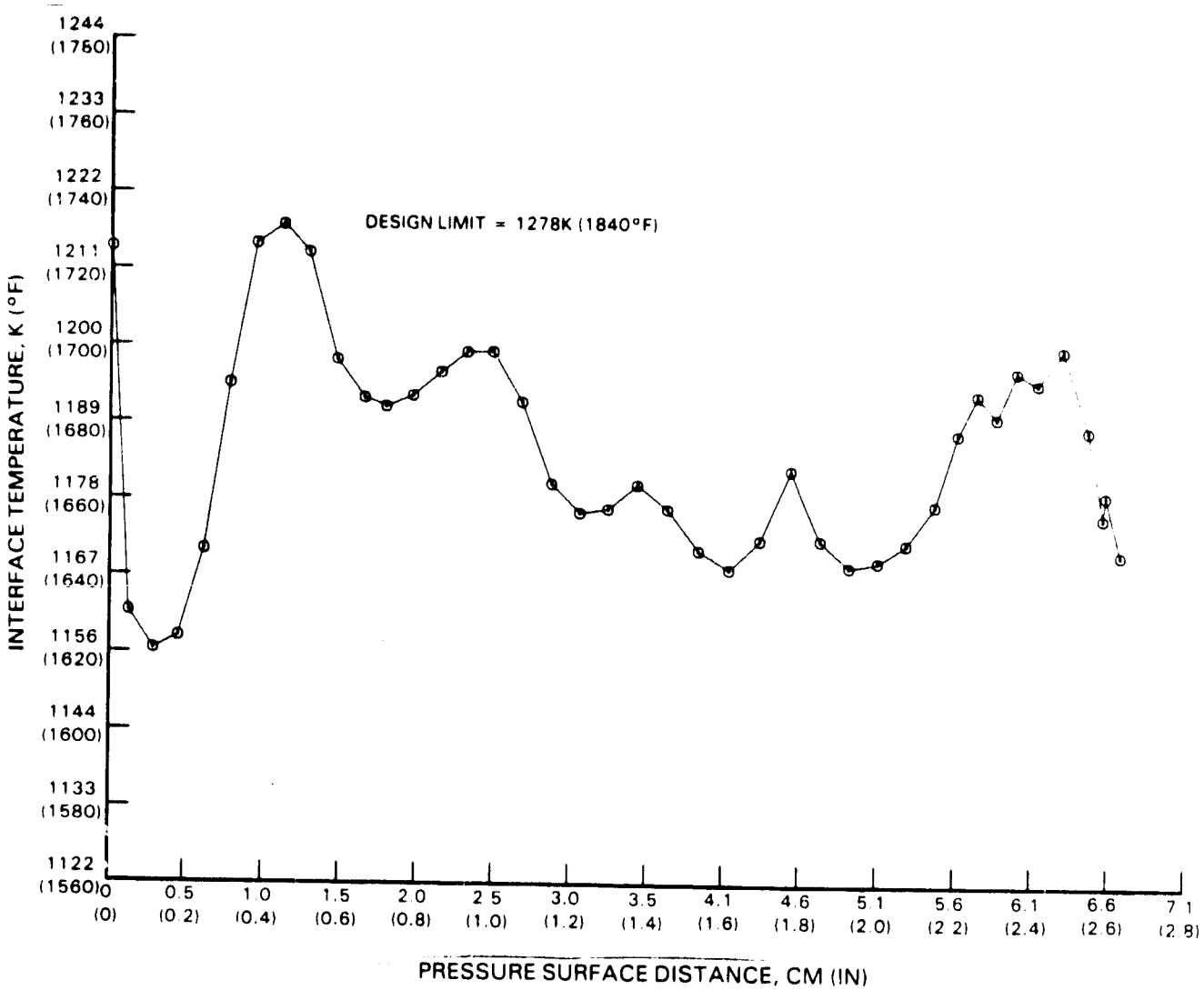

Figure 5-50 Blade Interface Temperature Distribution on Pressure Surface (1990 Technology)

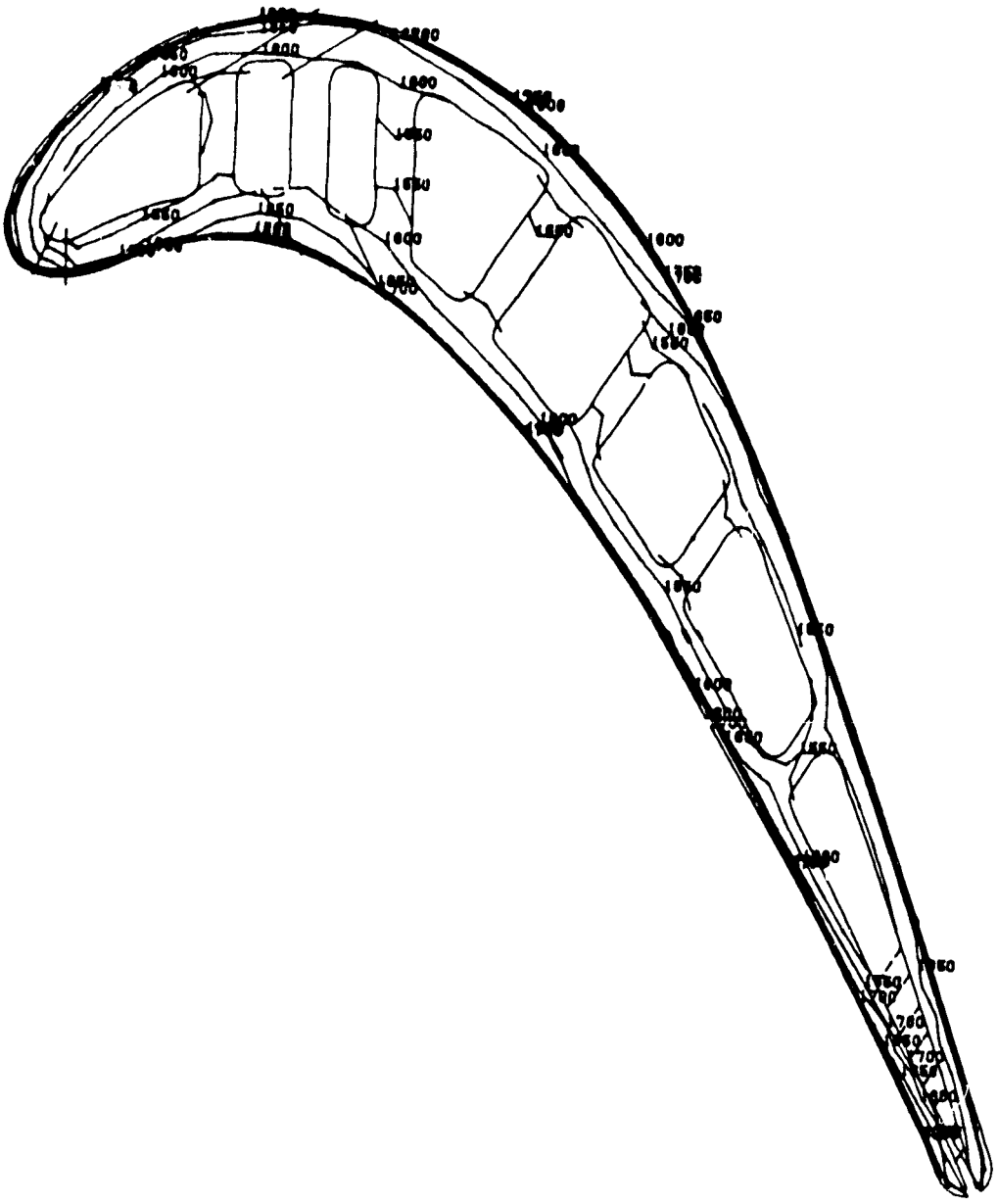

Figure 5-51 Blade Mean Section Isothermals Based on 1990 Technology (All temperatures 1°F are below Design Limit)

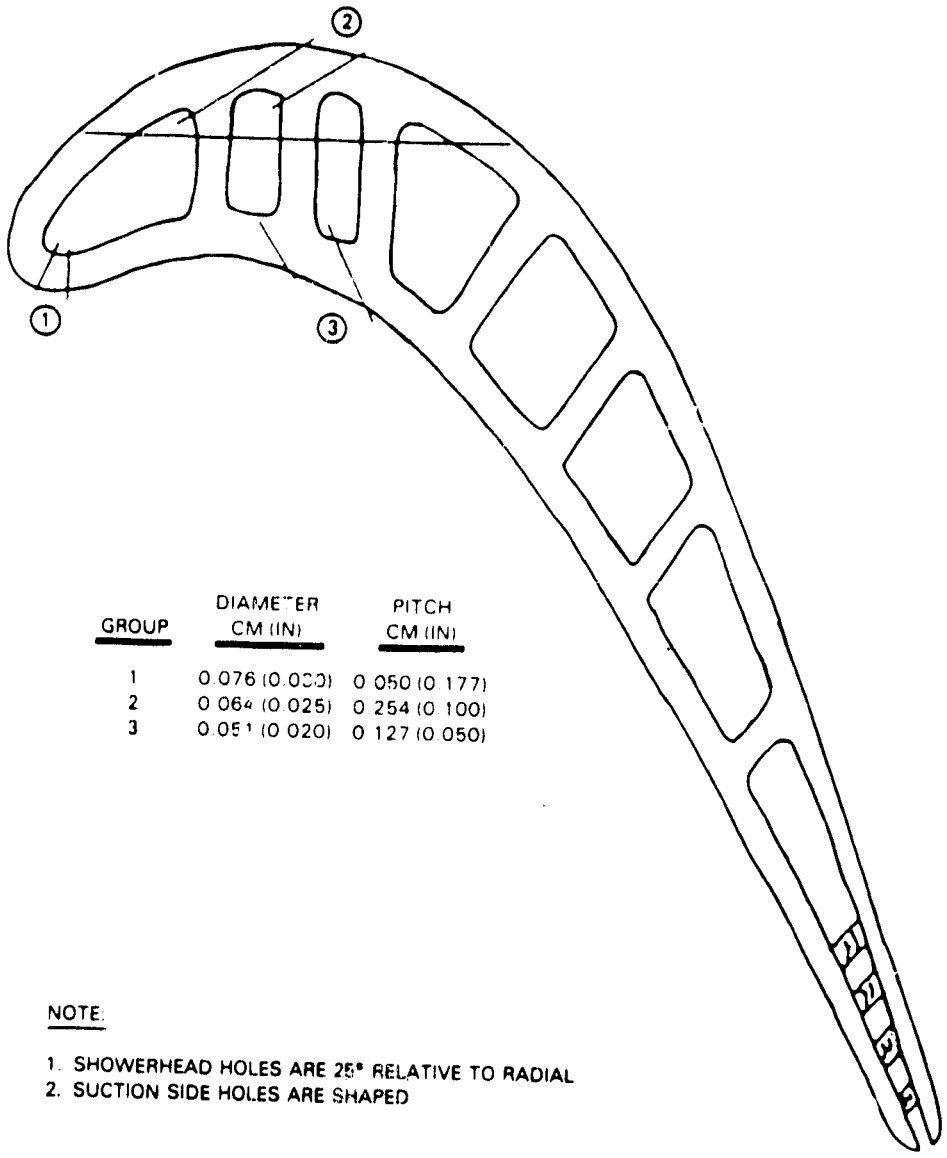

GROUP	DIAMETER CM (IN)	PITCH CM (IN)
1	0.076 (0.030)	0.050 (0.177)
2	0.064 (0.025)	0.254 (0.100)
3	0.051 (0.020)	0.127 (0.050)

NOTE:

1. SHOWERHEAD HOLES ARE 25° RELATIVE TO RADIAL
2. SUCTION SIDE HOLES ARE SHAPED

Figure 5-52 Blade Hole Geometry (1990 Technology)

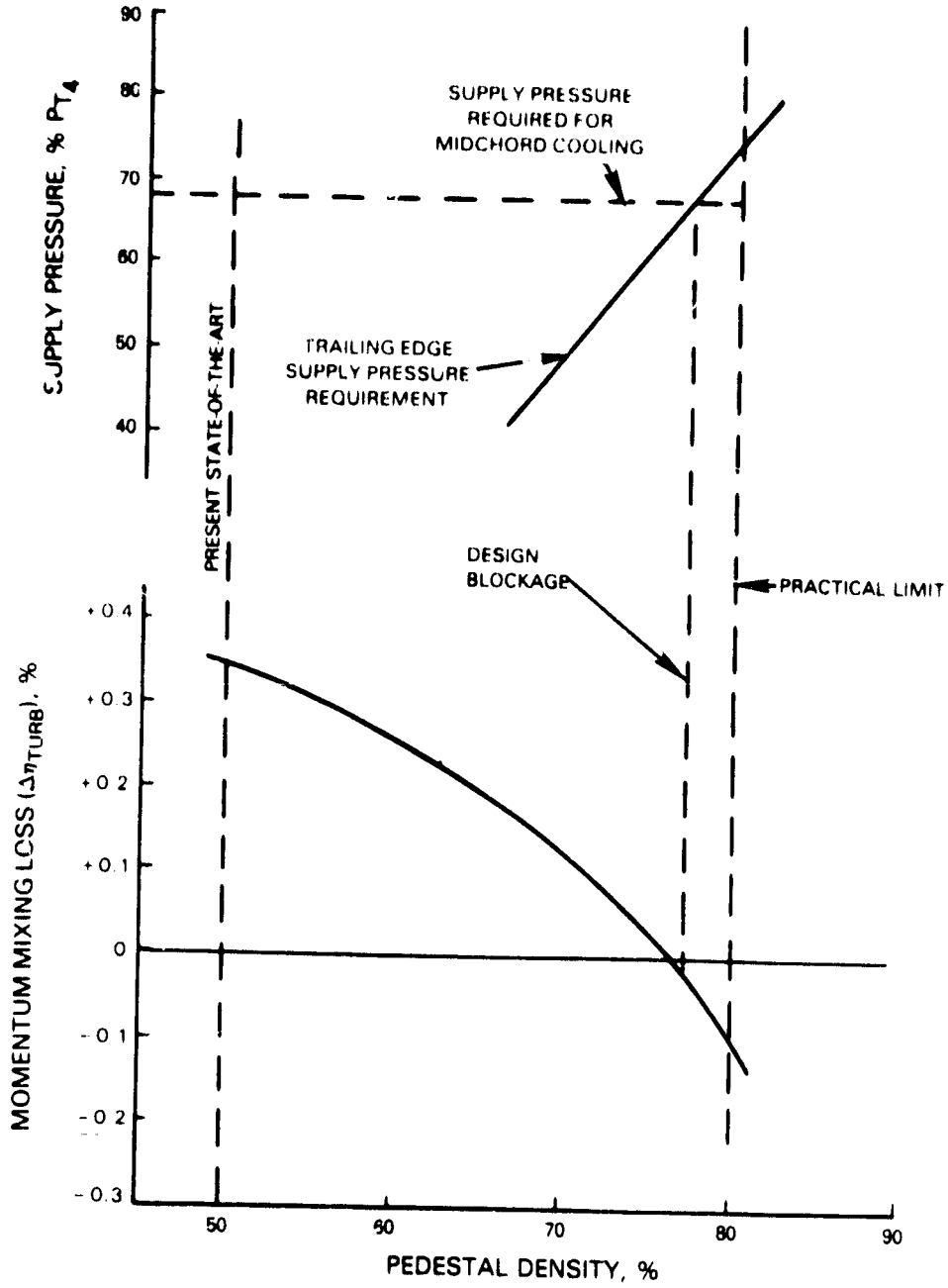

Figure 5-53 Blade Trailing Edge and Midchord Cooling Air Optimization (1990 Technology)

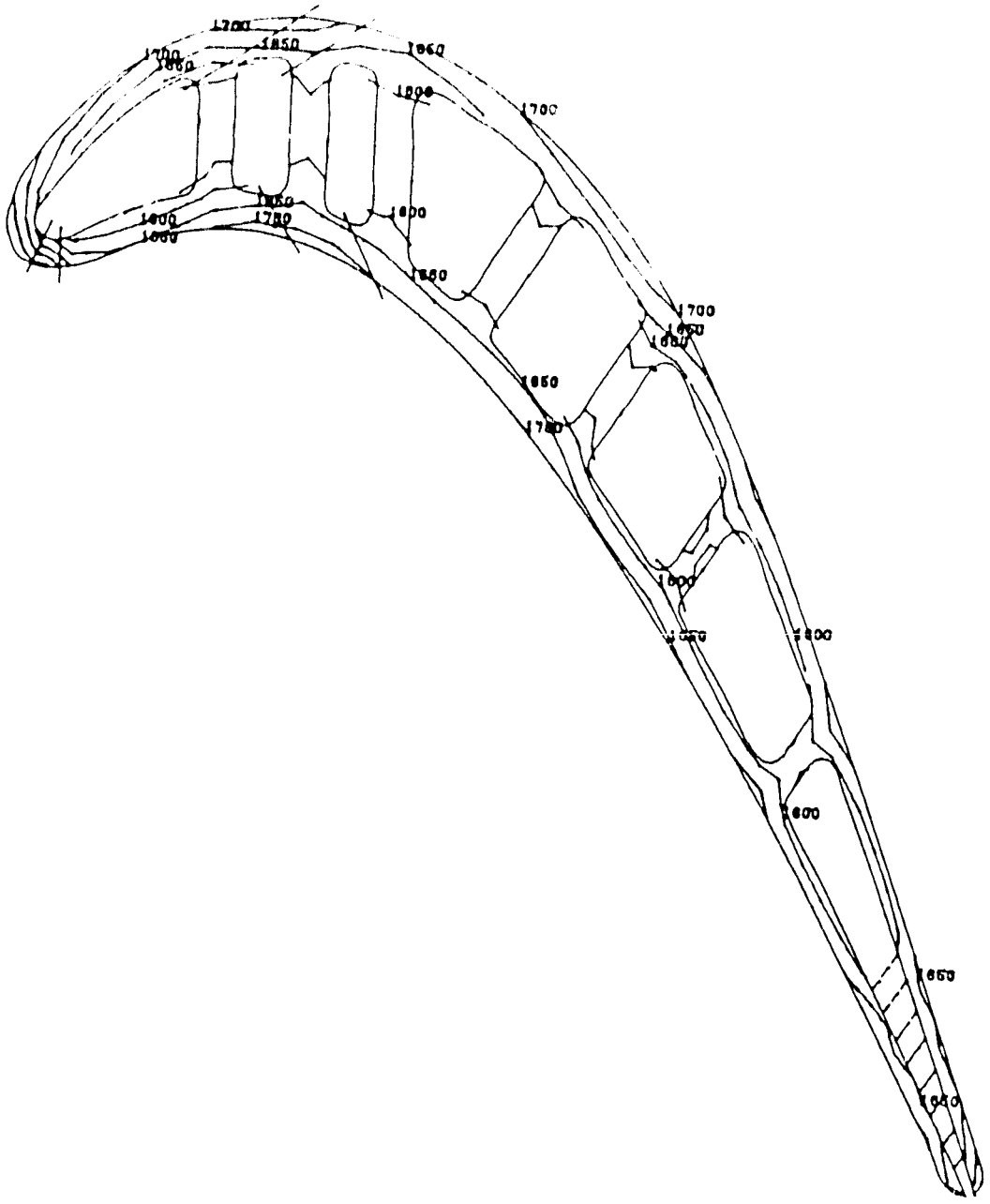

Figure 5-54 Blade Mean Section Isothermals Based on 1986 Technology (All temperatures 1°F are below Design Limit)

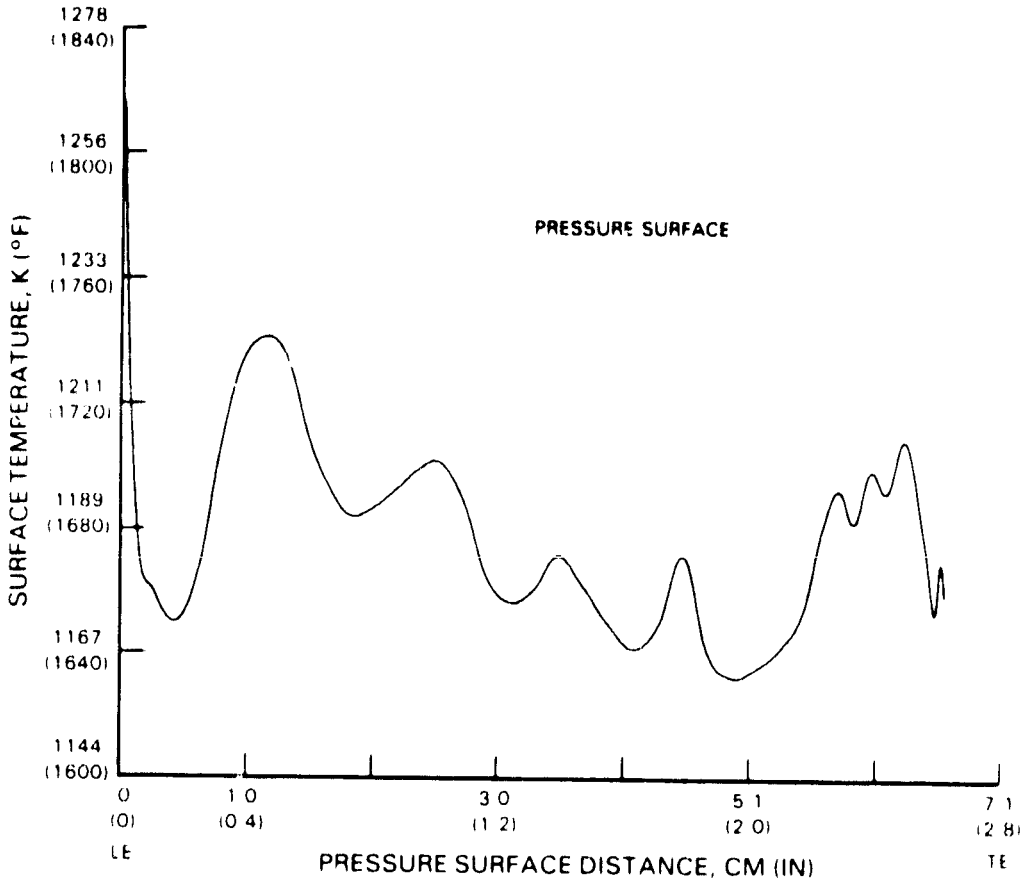

Figure 5-55 Blade Surface Temperature Distribution on Pressure Surface (1986 Technology)

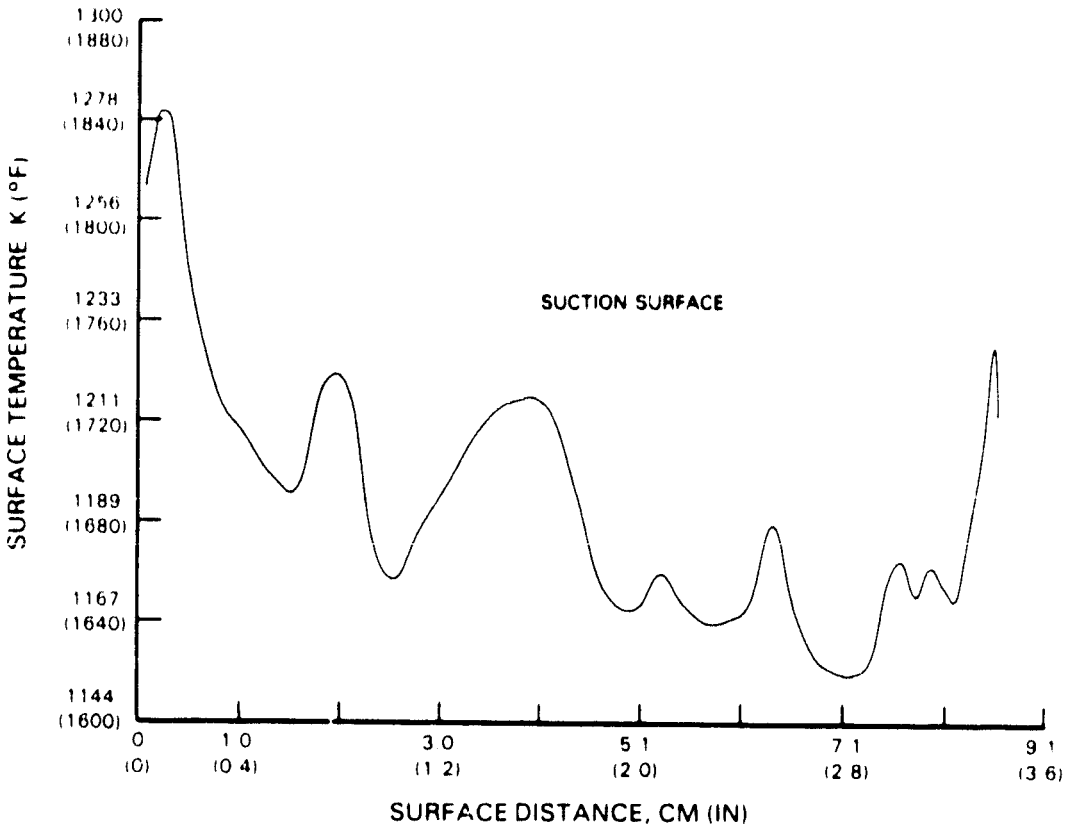

Figure 5-56 Blade Surface Temperature Distribution on Suction Surface (1986 Technology)

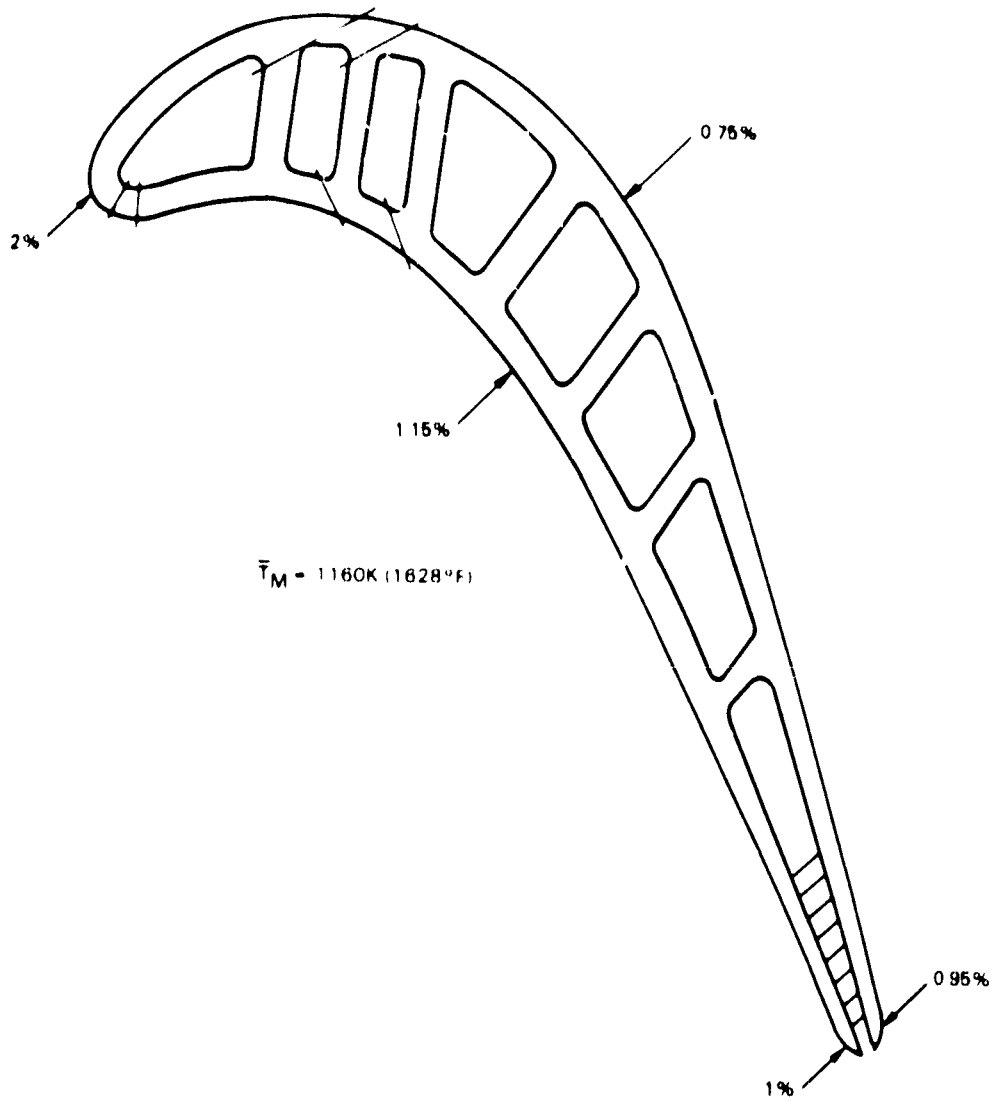

Figure 5-57 Blade Creep at Critical Locations (1986 Technology)

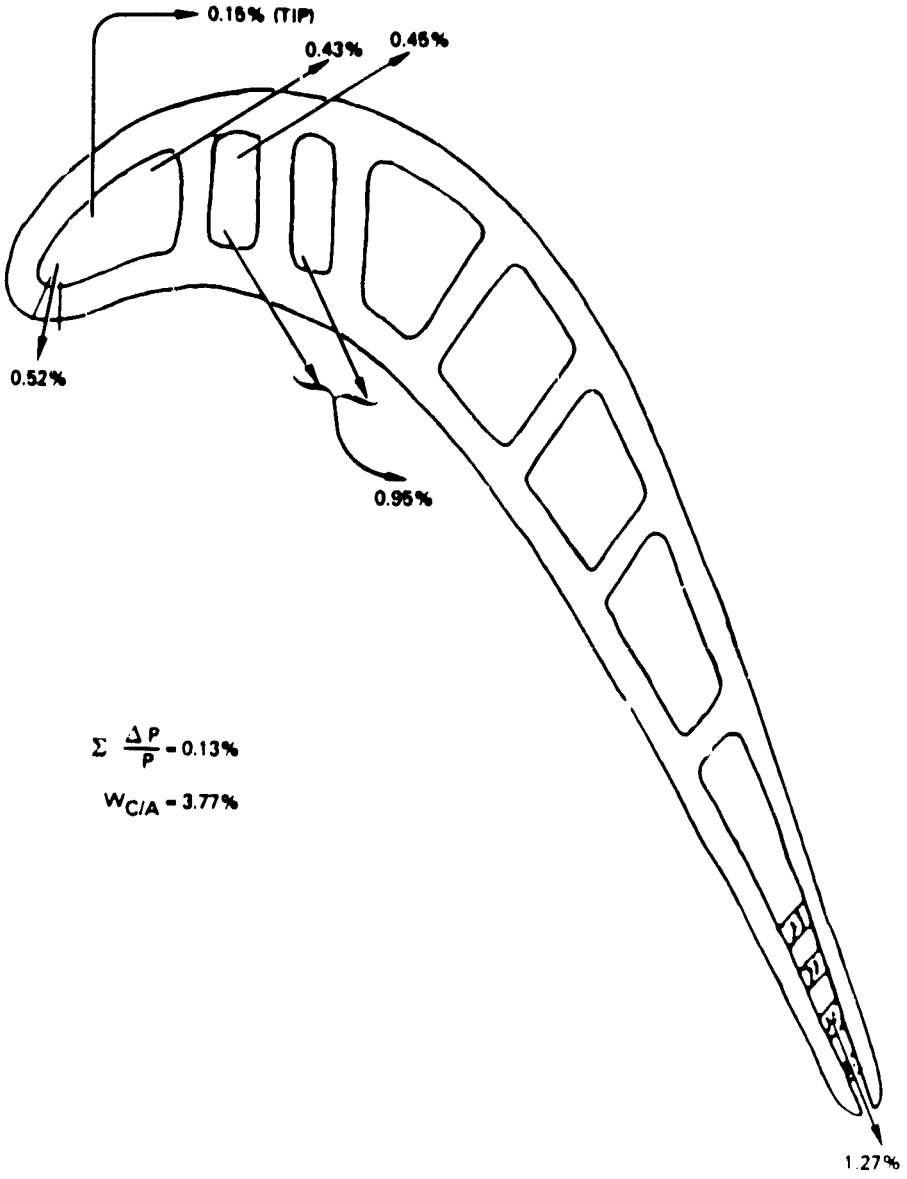

Figure 5-58 Cooling Flow Distribution (1986 Technology)

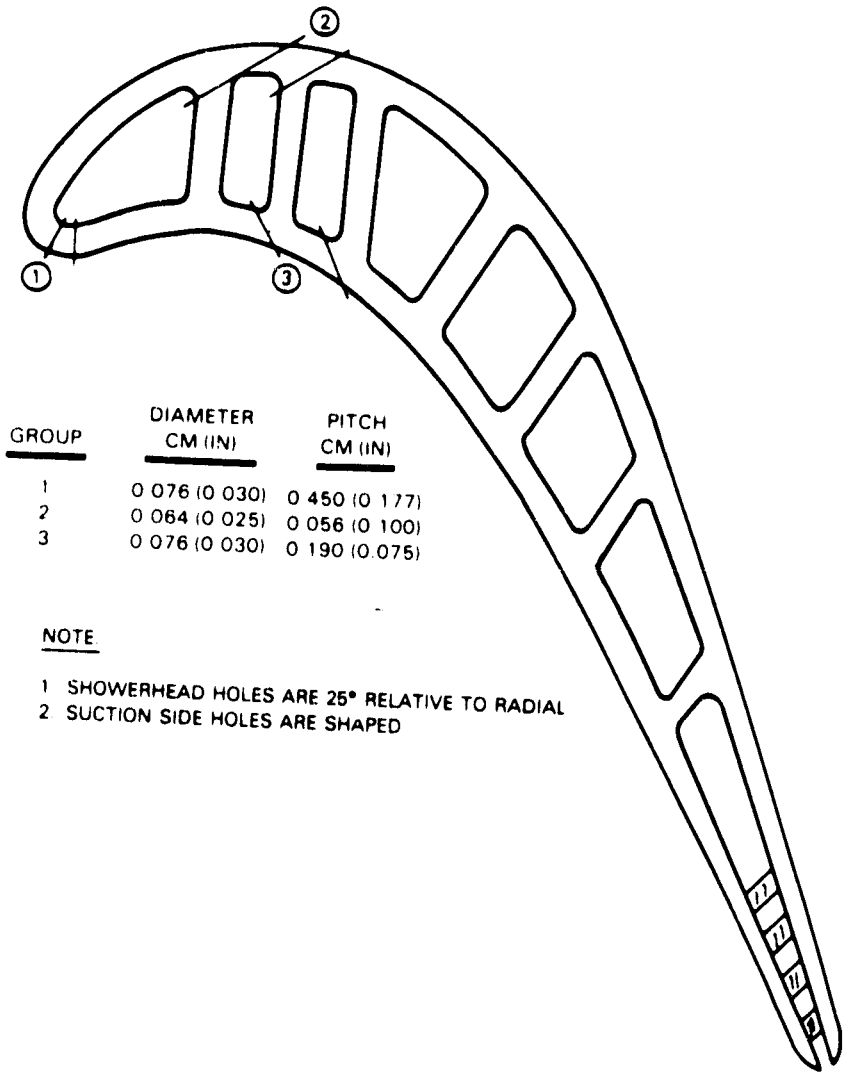

Figure 5-59 Blade Film Hole Geometry (1986 Technology)

SECTION 6.0

BENEFITS EVALUATION

6.1 Benefits for Supersonic Aircraft

The high-pressure turbine for the supersonic cruise aircraft engine represents the incorporation of considerable experience and anticipated technology. The predicted efficiency has exceeded the original most optimistic goals by 0.3 percent to provide a 92.3 percent cooled efficiency. This level was obtained without precoolers and with advanced thermal barrier coating, film cooling, and highly augmented internal cooling. The total cooling air for vane and blade was 5.28 percent of W_{ae} and 2.77 percent of W_{ae}, respectively (Table 6-I). The 1986 design, with less advanced technology, has a lower cooled efficiency of 91.9 percent, and requires 8.66 percent of W_{ae} cooling air for the vane and 3.77 percent W_{ae} cooling air for the blade. Both designs (1990 and 1986) have 10,000 hour lives.

TABLE 6-I

PRELIMINARY DESIGN CONCLUSIONS

Performance Benefit

- o 1990 Design η = 92.3%, 10,000 Hours -- 5.28% W_{ae} Vane
  -- 2.77% W_{ae} Blade
- o 1986 Design η = 91.9%, 10,000 Hours -- 8.66% W_{ae} Vane
  -- 3.77% W_{ae} Blade

6.2 Benefits for Subsonic Aircraft

The advanced technology concepts developed in the high-pressure turbine of the supersonic cruise VSCE also are applicable to other advanced engines. A study based on a commercial subsonic transport engine in the 267,000 N (60,000 lb) thrust class was used to evaluate the overall impact of VSCE technology in subsonic engines. The study engine has a 38:1 overall pressure ratio and a two-stage high-pressure turbine, considered representative of general engine technologies of the 1990's for subsonic aircraft.

The VSCE technologies outlined in Table 6-II, along with the 1983 technologies, were applied to the commercial subsonic transport engine study. The overall benefits of these technologies were determined to be 2.68 percent in high-pressure turbine efficiency and 1.94 percent in thrust specific fuel consumption. Table 6-III shows the detailed breakdown of predicted benefits by individual technology.

TABLE 6-II

1990 TECHNOLOGY FEATURES
COMPARED TO CURRENT SUBSONIC ENGINE

Aerodynamic Technology	1983 (Base)	1990 (Design)
Load Coefficient		+17%
Profile Loss		-10%
End Wall Loss		-15%
Trailing Edge Thickness:		
First Vane	0.198 cm (0.078 in)	0.155 cm (0.061 in)
First Blade	0.198 cm (0.078 in)	0.155 cm (0.061 in)
Second Vane	206 cm (0.081 in)	0.155 cm (0.061 in)
Second Blade	0.183 cm (0.072 in)	0.155 cm (0.061 in)
AN^2	4.2×10^{10}	6.0×10^{10}
Blade Material	PWA 1480	SC3000
Mechanical Technology		
Burner Technology		
TVR (1V/2V)	1.4/1.35	1.25/1.2
Profile Factor (1B/2B)		-4%
Vane Base Material (1V/2V)	PWA 647/PWA 1422	SC1000
Thermal Barrier Coating:		
Vanes	None	0.038 cm (0.015 in) Semi Opaque
Blades	None	0.025 cm (0.010 in) Yttria Stabilized
Improved Cooling		
First Vane		Flared Holes
First Blade		Flared Holes/Low Heat Load
Second Vane/Second Blade		Low Heat Load

TABLE 6-III

1990 TECHNOLOGY - SUBSONIC APPLICATION BENEFITS

	$\Delta W_{C/A}$ (% WAE)	$\Delta \eta_{HPT}$	ΔTSFC
AERODYNAMIC TECHNOLOGY			
• LOAD COEFFICIENT +17% PROFILE LOSS - 10% END WALL LOSS - 15%		+0.550%	-0.310%
• TRAILING EDGE THICKNESS REDUCTION		+0.140%	-0.078%
• AN^2 ($4.2 \times 10^{10} \rightarrow 6 \times 10^{10}$ MAX) – AERO		+1.220%	-0.680%
• AERO COOLING (W/O SC3000/W SC3000)	(+2.24%/+0.38%)	(-0.35%/-0.053%)	(+0.66%/+0.1%)
TOTAL AN^2	(+2.24%/+0.38%)	(+0.87%/+1.17%)	(-0.02%/-0.58%)
• TOTAL AERO TECHNOLOGY (REFLECTS SC3000)	+0.38%	+1.860%	-0.970%
MECHANICAL TECHNOLOGY			
• BURNER TECHNOLOGY	-2.55%	+0.330%	-0.330%
• VANE BASE MATERIAL			
1V (PWA 647 → SC1000)	-1.05%	+0.130%	-0.096%
2V (PWA 1442 → SC1000)	-0.35%	+0.025%	-0.034%
TOTAL BASE MATERIAL	-1.40%	+0.155%	-0.130%
• THERMAL BARRIER COATING			
1V	-2.65%	+0.320%	-0.240%
1B	-0.74%	-0.010%	-0.096%
2V	-0.08%	-0.062%	+0.030%
2B	-0.11%	-0.025%	-0.020%
TOTAL TBC	-3.58%	+0.223%	-0.330%
• IMPROVED COOLING			
1V FLARED HOLES	-0.38%	+0.052%	-0.037%
1B FLARED HOLES/LOW HEAT LOAD	-0.50%	+0.024%	-0.083%
2V LOW HEAT LOAD	-0.07%	+0.005%	-0.007%
2B LOW HEAT LOAD	-0.11%	+0.035%	-0.053%
TOTAL IMPROVED COOLING	-1.06%	+0.116%	-0.180%
• TOTAL MECHANICAL TECHNOLOGY	-8.59%	+0.820%	-0.970%
OVERALL BENEFIT	-8.21%	+2.680%	-1.940%

As shown in Table 6-III, turbine aerodynamic improvements provide 1.86 percent of the efficiency increase and 0.97 percent of the thrust specific fuel consumption decrease, with increased AN^2 contributing a major portion of the benefits. However, the AN^2 benefit obtained from the use of advanced materials is partially offset by the increased coolant flow requirement due to higher AN^2. With current state-of-the-art materials, the proportionately higher coolant flow increases due to higher AN^2 would offset, to a larger degree, the performance gains which would be otherwise achieved.

Figure 6-1 illustrates the net fuel consumption improvement due to AN^2 using current and advanced materials.

Mechanical technologies extension beyond that of the 1983 base further improves engine performance by 0.82 percent and reduces fuel consumption by 0.97 percent. Individual contributions due to burner technology, vane materials, thermal barrier coatings (TBC), and cooling technology are also listed in Table 6-III.

The TBC benefits are greatest where the external airfoil heat loads are highest, generally in upstream airfoils. The net benefits attributed to the TBC are negated by the increased pull loads due to TBC on the blades and a maximum temperature limit of bond coating temperature for coating spalling on blades and vanes. Consequently, no net benefit is realized on the second vane. TBC probably would not be used on such a second vane unless dictated by new thermal problems identified during a final detailed design.

In summary, the advanced technologies utilized for the VSCE supersonic cruise application offer substantial potential for both subsonic and supersonic aircraft engines and warrant pursuing.

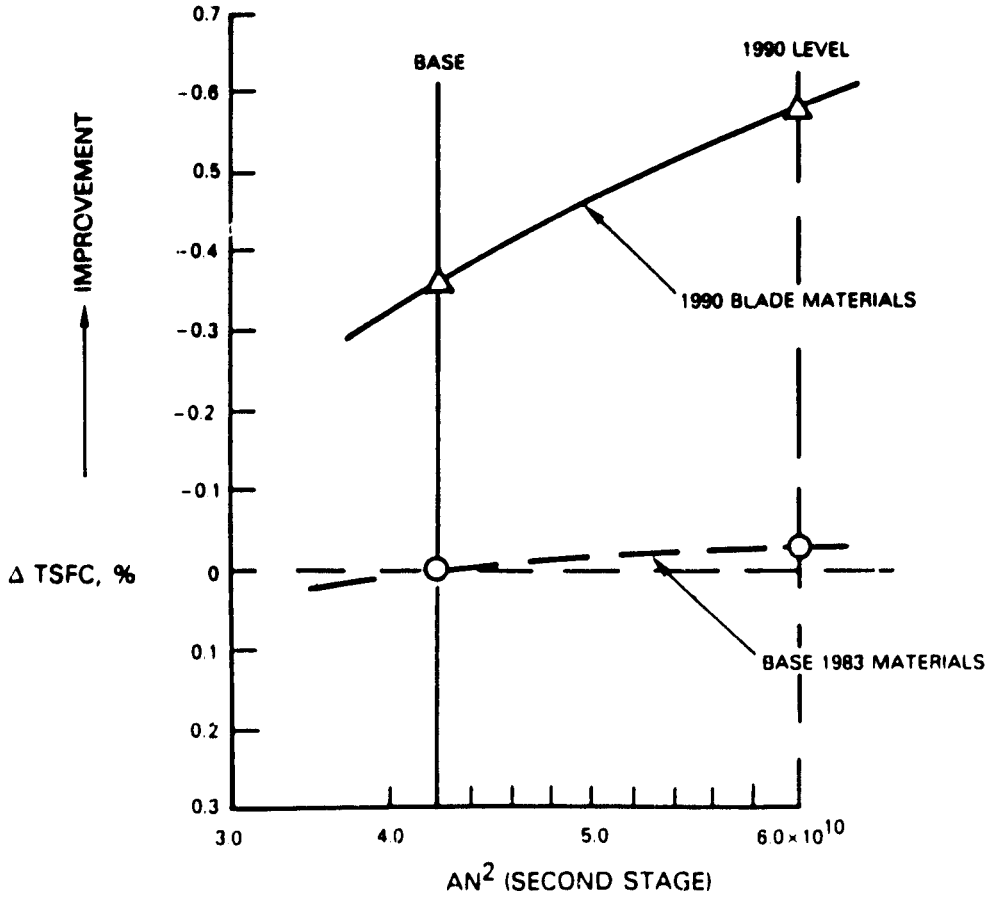

Figure 6-1 ΔTSFC vs AN^2

SECTION 7.0

CONCLUSIONS

The high-pressure turbine preliminary design conducted under this program shows that it is feasible to obtain a 10,000 hour airfoil life and a 92 percent cooled efficiency in the supersonic cruise engine environment. However, incorporation of technology advances relative to the present state-of-the-art turbine practices is critical. The improved technologies include advanced aerodynamics, improved airfoil materials, advanced thermal barrier coatings, new burner technology and improved cooling/casting methods.

These advanced technologies also have a significant payoff in subsonic engines, offering almost a 2 percent improvement of fuel consumption. A breakdown of the improvements by individual technology is summarized in Table 7-I below.

TABLE 7-I

CONCLUSIONS

Program	Thrust Specific Fuel Consumption
AN^2	-0.58%
Airfoil Aerodynamics	-0.31%
Thermal Barrier	-0.33%
Improved Cooling	-0.18%
Vane Material	-0.13%
Trailing Edge	-0.08%
Burner Technology	-0.33%
	-1.94%

In order to make possible an advanced supersonic transport engine by the 1990s or to achieve the 2 percent fuel consumption reduction in subsonic engines, it is imperative that technology development programs be initiated now. These programs would allow several years of research and development of these new technologies.

Specific programs should be directed at manufacturability of airfoils containing advanced cooling concepts. These airfoil manufacturability efforts should investigate methods of casting complex internal cooling concepts, controlling wall thicknesses, forming diffuser shaped holes in thermal barrier coatings, and reducing the thickness of cooling passages for trailing edges of airfoils.

SECTION 8.0

RECOMMENDATIONS

The preliminary design of the high-pressure turbine for the second generation supersonic cruise aircraft engine has reinforced the conclusion of previous studies that high-pressure turbine technology is crucial.

This preliminary design study was confined to the high-pressure turbine. A detail design should be started to examine more completely the interactions with other components. A large benefit has been obtained by increasing the turbine annulus area and reducing its speed. Preliminary examination indicates these modifications to be acceptable but, their impact should be pursued to the level of emphasis in a detailed design.

In addition, a level of manufacturing technology was assumed which is beyond the current state-of-the-art. Ongoing technology programs will provide some of these advances, but specific programs must be conducted for reducing trailing edge thickness, controlling wall thicknesses, casting internal complex cooling surfaces, and producing shaped holes through thermal barrier systems.

The application of this technology to subsonic commercial engines demonstrated this technology to be germane to all advanced engine designs. The initiation of the technology programs for high stress turbines (AN^2), advanced airfoil aerodynamics, thermal barrier systems, improved airfoil cooling techniques, and burner technology in a timely fashion will produce broad benefits in all future engine applications.

APPENDIX - HIGH TURBINE AIRFOIL COORDINATES

A. BASE BLADE

X cm	Y TOP cm	ELLIPSE cm	Y BOT cm	ELLIPSE cm
0.0	1.72266	1.67835	1.49864	1.67835
0.01824	1.75546	1.75106	1.51464	1.62571
0.03648	1.78513	1.78498	1.52998	1.61186
0.05472	1.81214		1.54463	1.60506
0.07296	1.83686		1.55860	1.60220
0.09120	1.85956		1.57186	1.60207
0.10944	1.88045		1.58442	1.60404
0.12768	1.89971		1.59625	1.60776
0.14592	1.91749		1.60736	1.61300
0.16416	1.93390		1.61772	1.61962
0.18240	1.94905		1.62734	1.62751
0.22800	1.98195		1.64806	
0.27360	2.00851		1.66396	
0.31920	2.02949		1.67494	
0.36480	2.04544		1.68095	
0.41040	2.05675		1.68195	
0 45600	2.06372		1.67794	
0.50160	2.06659		1.66894	
0.54720	2.06552		1.65500	
0.59280	2.06061		1.63619	
0.63840	2.05192		1.61262	
0.68400	2.03949		1.58440	
0.72960	2.02329		1.55168	
0.77520	2.00327		1.51462	
0.82080	1.97932		1.47338	
0.86640	1.95129		1.42813	
0.91200	1.91896		1.37907	
0.95760	1.88204		1.32637	
1.00320	1.84014		1.[illegible]23	
1.04880	1.79274		1.21083	
1.09440	1.73912		1.14834	
1.14000	1.67829		1.08296	
1.18560	1.60926		1.01484	
1.23120	1.53133		0.94415	
1.27680	1.44440		0.87105	
1.32240	1.34895		0.79569	
1.36800	1.24593		0.71820	
1.41360	1.13640		0.63873	
1.45920	1.02177		0.55739	
1.50480	0.90283		0.47431	
1.55040	0.78052		0.38959	
1.59600	0.65554		0.30333	
1.64160	0.52842		0.21563	
1.65984	0.47707		0.18017	
1.67808	0.42548		0.14450	
1.69632	0.37365		0.10863	
1.71456	0.32161		0.07255	
1.73280	0.26938		0.03628	
1.75104	0.21697		-0.00018	
1.76928	0.16439		-0.03682	-0.02795
1.78752	0.11165		-0.07365	-0.03444
1.80576	0.05878		-0.11065	-0.03043
1.82400	0.00576	-0.00000	-0.14783	-0.00000

HIGH TURBINE AIRFOIL COORDINATES

B. LOW HEAT LOAD BLADE

X cm	Y TOP cm	Y BOT cm
0.017210	1.626726	1.626726
0.018240	1.625578	1.750953
0.036480	1.611741	1.784879
0.054720	1.604946	1.812143
0.072960	1.602092	1.836859
0.091200	1.601968	1.85955
0.109440	1.603953	1.880446
0.127680	1.607686	1.899707
0.145920	1.612938	1.917486
0.164160	1.619562	1.933902
0.182400	1.627467	1.948053
0.228000	1.648063	1.977949
0.273600	1.663960	2.001514
0.319200	1.674945	2.018494
0.364800	1.680954	2.03143
0.410400	1.681954	2.03603
0.456000	1.677[illegible]3	2.03926
0.501600	1.668 1	2.03906
0.547200	1.654997	2.03483
0.592800	1.636189	2.02719
0.638400	1.612616	2.01668
0.684000	1.587000	2.00382
0.729600	1.555000	1.98546
0.775200	1.525000	1.96338
0.820800	1.48000	1.93082
0.866400	1.44000	1.90898
0.912000	1.3900	1.87079
0.957600	1.32000	1.83161
1.003200	1.255	1.78632
1.048800	1.178259	1.73329
1.094399	1.101506	1.67327
1.139999	1.024752	1.61500
1.185599	0.947998	1.54648
1.231200	0.871244	1.47212
1.276800	0.794490	1.39165
1.322400	0.717736	1.30480
1.368000	0.64098	1.21128
1.413600	0.564229	1.11195
1.459200	0.487475	1.00570
1.504800	0.410721	0.89338
1.550400	0.333967	0.77584
1.596000	0.257213	0.65391
1.641600	0.180459	0.52843
1.659840	0.149757	0.47743
1.678080	0.119056	0.42605
1.696320	0.088354	0.37431
1.714560	0.057653	0.32226
1.732800	0.02692	0.26994
1.751040	-0.004000	0.21740
1.769279	-0.027954	0.16466
1.787519	-0.034443	0.11179
1.805759	-0.030428	0.05881
1.824000	0.0	0.0

HIGH TURBINE AIRFOIL COORDINATES

C. VANE COORDINATES

X cm	Y TOP cm	ELLIPSE cm	Y BOT cm	ELLIPSE cm
0.0	3.63289	3.50924	3.27173	3.50924
0.02097	3.64927	3.59959	3.27763	3.42101
0.04194	3.66514	3.63608	3.28222	3.38668
0.06291	3.68050	3.66323	3.28548	3.36168
0.08388	3.69509	3.68535	3.28741	3.34171
0.10485	3.70917	3.70412	3.28800	3.32509
0.12582	3.72248	3.72041	3.28726	3.31094
0.14679	3.73528	3.73474	3.28519	3.29875
0.16776	3.74731	3.74746	3.28179	3.28819
0.18873	3.75883		3.27706	3.27900
0.20970	3.76933		3.27102	3.27103
0.26212	3.79313		3.25022	
0.31455	3.81233		3.22148	
0.36697	3.82718		3.18507	
0.41940	3.83716		3.14132	
0.47182	3.84228		3.09060	
0.52425	3.84254		3.03333	
0.57667	3.83742		2.96991	
0.62910	3.82692		2.90080	
0.68152	3.81080		2.82637	
0.73395	3.78853		2.74707	
0.78637	3.76062		2.66326	
0.83880	3.72758		2.57533	
0.89122	3.68587		2.48359	
0.94365	3.63826		2.38041	
0.99607	3.58373		2.29003	
1.04850	3.52205		2.18876	
1.10092	3.45292		2.08482	
1.15335	3.37563		1.97847	
1.20577	3.29048		1.86987	
1.25820	3.19662		1.75925	
1.31062	3.09387		1.64676	
1.36305	2.98179		1.53253	
1.41547	2.85993		1.41672	
1.46790	2.72780		1.29948	
1.52032	2.58478		1.18088	
1.57275	2.43025		1.06106	
1.62517	2.26345		0.94011	
1.67760	2.08346		0.81808	
1.73002	1.88934		0.69507	
1.78245	1.67995		0.57117	
1.83487	1.45391		0.44643	
1.88730	1.20955		0.32089	
1.90827	1.10627		0.27047	
1.92924	0.99962		0.21994	
1.95021	0.88942		0.16930	
1.97118	0.77552		0.11855	
1.99215	0.65776		0.06769	
2.01312	0.53588		0.01674	
2.03409	0.40970		-0.03432	-0.02643
2.05506	0.27897		-0.08547	-0.03668
2.07603	0.14339		-0.13671	-0.03336
2.09700	0.00268	-0.00001	-0.18804	-0.00001

D. BASE BLADE PRESSURE SIDE VELOCITY DISTRIBUTION

M	X(M) (ft)	UG(M) (ft/sec)
1	0.002	63.891
2	0.003	73.100
3	0.004	89.276
4	0.005	102.929
5	0.006	115.409
6	0.007	126.276
7	0.008	130.052
8	0.009	132.908
9	0.011	134.715
10	0.012	132.243
11	0.014	128.267
12	0.016	126.843
13	0.019	124.557
14	0.022	121.562
15	0.024	119.945
16	0.027	118.318
17	0.029	116.667
18	0.033	114.554
19	0.037	111.986
20	0.041	121.965
21	0.045	130.811
22	0.049	148.578
23	0.053	164.145
24	0.063	200.964
25	0.073	250.848
26	0.085	316.365
27	0.097	382.240
28	0.110	470.497
29	0.123	580.601
30	0.138	701.853
31	0.153	870.954
32	0.168	1011.181
33	0.184	1280.219
34	0.201	1463.714
35	0.216	1811.865
36	0.219	1951.336

E. BASE BLADE SUCTION SIDE VELOCITY DISTRIBUTION

	(ft)	(ft/sec)
M	X(M)	UG(M)
1	0.002	162.649
2	0.003	296.729
3	0.003	387.353
4	0.004	460.701
5	0.005	553.795
6	0.005	633.918
7	0.006	705.517
8	0.007	810.263
9	0.007	904.005
10	0.008	998.170
11	0.009	1095.296
12	0.011	1146.320
13	0.012	1204.897
14	0.013	1233.503
15	0.014	1261.779
16	0.015	1280.740
17	0.017	1299.498
18	0.019	1306.007
19	0.020	1312.450
20	0.022	1323.662
21	0.024	1334.762
22	0.026	1362.094
23	0.029	1359.050
24	0.031	1433.990
25	0.033	1478.214
26	0.038	1534.930
27	0.042	1590.368
28	0.046	1672.381
29	0.050	1751.749
30	0.054	1786.951
31	0.058	1821.843
32	0.066	1900.508
33	0.073	1940.419
34	0.081	1993.985
35	0.089	2046.681
36	0.098	2126.5[illegible]
37	0.107	2226.3[illegible]
38	0.118	2347.7
39	0.130	2461.628
40	0.144	2523.232
41	0.161	2502.937
42	0.180	2402.061
43	0.201	2274.600
44	0.223	2178.647
45	0.245	2117.965
46	0.268	2065.768
47	0.276	2110.272

F. LOW HEAT LOAD BLADE PRESSURE SIDE VELOCITY DISTRIBUTION

(ft)	(ft/sec)
X(M)	UG(M)
0.002	42.964
0.004	57.480
0.005	69.715
0.006	79.488
0.007	88.724
0.008	96.593
0.010	100.063
0.012	102.929
0.014	106.192
0.016	109.347
0.019	103.879
0.021	98.592
0.024	92.477
0.028	95.082
0.031	97.100
0.035	102.879
0.039	110.230
0.044	127.803
0.048	142.902
0.057	160.545
0.068	192.796
0.080	260.965
0.094	347.664
0.109	486.295
0.125	627.717
0.140	768.857
0.155	963.480
0.171	1108.487
0.186	1372.400
0.201	1506.020
0.208	1631.931

G. LOW HEAT LOAD BLADE SUCTION SIDE VELOCITY DISTRIBUTION

	(ft)	(ft/sec)
M	X(M)	UG(M)
1	0.002	34.146
2	0.003	83.656
3	0.004	113.283
4	0.004	134.631
5	0.005	156.550
6	0.006	233.517
7	0.007	291.068
8	0.007	338.951
9	0.008	468.891
10	0.009	570.720
11	0.010	696.503
12	0.011	804.174
13	0.013	996.586
14	0.014	1088.149
15	0.015	1173.832
16	0.016	1227.019
17	0.017	1273.484
18	0.019	1326.875
19	0.021	1344.460
20	0.022	1361.085
21	0.024	1366.364
22	0.026	1370.790
23	0.027	1379.611
24	0.029	1388.395
25	0.032	1417.031
26	0.034	1444.979
27	0.036	1504.155
28	0.038	1561.920
29	0.043	1629.819
30	0.047	1696.197
31	0.051	1777.418
32	0.055	1856.939
33	0.059	1858.680
34	0.063	1860.420
35	0.070	1883.917
36	0.073	1898.126
37	0.086	2001.010
38	0.094	2073.163
39	0.102	2236.695
40	0.112	2261.839
41	0.123	2302.090
42	0.136	2344.329
43	0.150	2373.916
44	0.166	2471.532
45	0.184	2478.127
46	0.204	2444.615
47	0.226	2270.402
48	0.250	2141.797
49	0.274	2030.454
50	0.285	2129.866

List of Symbols and Abbreviations

A	area
avg	average
BCA	best cruise altitude
c	heat exchanger
CO	carbon monoxide
Cx	axial flow velocity
Dia	diameter
EPA	Environmental Protection Agency
EPAP	Environmental Protection Agency Parameter
f	film effectiveness
Fn	net thrust
h	specific work
ID	inner diameter
IFE	Inverted Flow Engine
LBE	Low Bypass Engine
LE	leading edge
M	Mach number
N	mechanical speed, rpm
NASA	National Aeronautics and Space Administration
NO_x	oxides of nitrogen
OD	outer diameter
P	pressure
P_s	static pressure
P_t	total pressure
PR	pressure ratio
P&W	Pratt & Whitney
rpm	revolutions per minute
SC	single crystal
SCAR	Supersonic Cruise Aircraft Research
S/H	showerhead
T	temperature
T_{amb}	ambient temperature
TBC	thermal barrier coating
T_c	cooling temperature
TE	trailing edge
T_g	gas temperature
T_m	metal temperature
TOBI	tangential on-board injection
TSFC	thrust specific fuel consumption
TVR	temperature variance ratio, pattern factor
U	tangential wheel speed
UER	unscheduled engine removal
V	velocity
VCE	Variable Cycle Engine
VSCE	Variable Stream Control Engine
Wac	total cooling airflow
Wae	total engine airflow

Δ	difference
η	efficiency
Θ	overall cooling effectiveness
β	heat load parameter
σ	stress

REFERENCES

1. Hunt R.B., et al: "Noise and Economic Study for Supersonic Cruise Airplane Research - Phase III", P&WA Final Report, NASA CR-165612, March 1982

2. Howlett, R.A., Hunt R.B.,:"VSCE Technology Definition Study", P&WA Final Report, NASA CR-159730, Aug 1979

3. Hunt R.B., et al: "Noise and Economic Study for Supersonic Cruise Airplane Research", P&WA Final Report, NASA CR-165423, June 1981

4. Howlett, R.A., et al: "Advanced Supersonic Propulsion Study - Phase III", P&WA Final Report, NASA CR-135148, December 1976

5. Nicholson, T.H. et al, "Heat Transfer Optimized Turbine Rotor Blades - An Experimental Study Using Transient Techniques." ASME 82-GT-304